PB-232 287

FLAME CHARACTERIZATION PROBES

R. C. Kesselring, et al

Rockwell International Corporation

Prepared for:

Environmental Protection Agency

March 1974

DISTRIBUTED BY:

NTIS

National Technical Information Service
U. S. DEPARTMENT OF COMMERCE
5285 Port Royal Road, Springfield Va. 22151

EPA-650/2-74-023

FLAME CHARACTERIZATION PROBES

by

R. C. Kesselring

Rocketdyne Division
Rockwell International Corporation
6633 Canoga Avenue
Canoga Park, California 91304

and

K. M. Gorji, W. S. Young
W. E. Rodgers, and E. L. Knuth

School of Engineering and Applied Science
University of California
Los Angeles, California 90024

Contract No. 68-02-0628
ROAP No. 21ADG-51
Program Element No. 1AB014

EPA Project Officer: William B. Kuykendal

Control Systems Laboratory
National Environmental Research Center
Research Triangle Park, North Carolina 27711

Prepared for

OFFICE OF RESEARCH AND DEVELOPMENT
U.S. ENVIRONMENTAL PROTECTION AGENCY
WASHINGTON, D.C. 20460

March 1974

1a

This report has been reviewed by the Environmental Protection Agency and approved for publication. Approval does not signify that the contents necessarily reflect the views and policies of the Agency, nor does mention of trade names or commercial products constitute endorsement or recommendation for use.

PB 232 287

TECHNICAL REPORT DATA
(Please read Instructions on the reverse before completing)

1. REPORT NO.
EPA-650/2-74-023

2.

3. RECIPIENT'S ACCESSION NO.

4. TITLE AND SUBTITLE
Flame Characterization Probes

5. REPORT DATE
March 1974

6. PERFORMING ORGANIZATION CODE

7. AUTHOR(S) R. C. Kesselring (Rocketdyne), and K. M Gorji, W. S. Young, W. E. Rodgers, and E. L. Knuth (UCLA)

8. PERFORMING ORGANIZATION REPORT NO.

9. PERFORMING ORGANIZATION NAME AND ADDRESS
Rocketdyne Division, Rockwell International Corp.
6633 Canoga Avenue
Canoga Park, California 91304

10. PROGRAM ELEMENT NO.
1AB014; ROAP 21ADG-51

11. CONTRACT/GRANT NO.
68-02-0628

12. SPONSORING AGENCY NAME AND ADDRESS
EPA, Office of Research and Development
NERC-RTP, Control Systems Laboratory
Research Triangle Park, North Carolina 27711

13. TYPE OF REPORT AND PERIOD COVERED
Final

14. SPONSORING AGENCY CODE

15. SUPPLEMENTARY NOTES

16. ABSTRACT The report gives results of work dealing with the problem of extracting temperature, species concentration, and velocity data from flames. A literature review was conducted to determine the state-of-the-art for making the following measurements in a particulate-laden flame environment: flame temperature--1100 to 2500°C; stable chemical species--NO, H2, O2, CO, SO2, CO2, N2, NO2, and Ar; unstable chemical species--O, N, OH, H, and other flame intermediates; and velocity--magnitude and direction. Based on results of the literature review, three separate probes were designed and fabricated to make these measurements. In order to measure the unstable species and also to provide a calibration reference for the stables species and temperature, a molecular beam mass spectrometer equipped with a time-of-flight chopper was used.

Reproduced by
NATIONAL TECHNICAL
INFORMATION SERVICE
U S Department of Commerce
Springfield VA 22151

17. KEY WORDS AND DOCUMENT ANALYSIS

a. DESCRIPTORS	b. IDENTIFIERS/OPEN ENDED TERMS	c. COSATI Field/Group
Air Pollution Flames Measurement Probes Mass Spectrometers Molecular Beams		13B 21B 14B

18. DISTRIBUTION STATEMENT Unlimited	19. SECURITY CLASS *(This Report)* Unclassified	21. NO. OF PAGES 186
	20. SECURITY CLASS *(This page)* Unclassified	22. PRICE $12.50

EPA Form 2220-1 (9-73)

ABSTRACT

Experimental methods for use in characterizing the "dirty flame" environments that result from the burning of coal and/or residual oil were sought. A search of the combustion literature was made to determine the applicability of the existing techniques that have been more commonly applied to the characterization of less formidable flame environments.

Techniques were selected for the measurement of temperature, chemical species (stable and unstable) and velocity (magnitude and direction) in high temperature "dirty flames": (1) the pneumatic venturi pyrometer for temperature measurement, (2) the 5-hole pitot probe for velocity measurement, (3) a quick-quench species probe for measurement of stable species, and (4) molecular-beam mass spectrometry for determination of unstable species.

Probe designs, based on the selected techniques, were developed that would allow: (1) long probe life, (2) low response time, (3) high spatial resolution, and (4) minimal flowfield disturbance.

After fabrication of the three probes, and after calibration of the velocity probe, the operational aspects of the probes were evaluated in a pre-mixed gas flame (at Rocketdyne). Satisfactory operation was indicated for all probes.

Subsequently, the temperature and species probes were removed to UCLA for comparative tests with UCLA's molecular-beam mass spectrometer technique in a pre-mixed gas flame. Again, satisfactory agreement was indicated. The molecular-beam mass-spectrometric technique was also employed to obtain unstable species concentrations in the same flame.

Evaluation of the probes suitability for use in a residual oil flame was initially intended, but was not accomplished within the resources available for the program.

This report was submitted in fulfillment of Contract No. 68-02-0628 by Rocketdyne Division, Rockwell International, Canoga Park, California, under the sponsorship of the Environmental Protection Agency. Work was completed as of 1 October 1973.

CONTENTS

	Page
Abstract	iii
List of Figures	vi
Acknowledgements	viii
Introduction and Summary	1
Evaluation of Available Experimental Techniques	6
Temperature Measurement	7
Species Measurement	12
Velocity Measurement	16
Selection of Measurement Techniques	19
Probe Design and Fabrication	26
Heat Transfer and Pressure Drop Requirements	26
Velocity Probe	33
Species Probe	33
Temperature Probe	45
Velocity Probe Calibration	56
Calibration Measurements	56
Construction of Calibration Charts	64
Use of Calibration Charts	68
Probe Checkout and Evaluation at Rocketdyne	69
Temperature Probe	69
Velocity Probe	74
Species Probe	76

CONTENTS (Continued)

Page

Molecular-Beam Mass Spectroscopy at UCLA 78

- Experimental Apparatus 78
- Experimental Measurements and Data Reduction 83
- Experimental Results 88

Verification Testing of Rocketdyne Probes 99

Conclusions 103

References 104

Appendix A

Flame Measurement Techniques Appearing in the Literature 106

Appendix B

Review of Selected Literature on Flame Characterization by Molecular-Beam Sampling 137

Appendix C

Tabulation of Data Obtained With UCLA Molecular-Beam Mass-Spectrometer Sampling System 159

Appendix D

Theoretical Maximum Flame Temperature and Species Composition of Methane - Air Mixtures at Various Equivalence Ratios 175

Appendix E

Factors for the Conversion of Units to the Metric System 176

FIGURES

No.		Page
1	Program Flow Diagram	3
2	Schematic Diagram of Molecular-Beam Sampling System	14
3	Mass Flowrate of Combustion Gas Through a Probe as a Function of Probe ID and Gas Velocity	28
4	Mass Flowrate of Probe Cooling Water as a Function of Combustion Gas Flowrate Through Probe, Probe OD and Combustion Gas ΔT	29
5	Probe Length Required as a Function of Combustion Gas Flowrate Through Probe, Probe ID, and Final (Cooled) Combustion Gas Temperature	32
6	Velocity Probe - Detail Design Drawing	35
7	Five-Hole Pitot-Type Velocity Probe	37
8	Conceptual Design of Quick Quench Sampling Probe	39
9	Hot-Gas Sampling Probe Assembly	43
10	Rework of Hot-Gas Sampling Probe	46
11	Quick Quench Species Probe	47
12	Pneumatic Venturi Pyrometer - Initial Conceptual Layout Drawing	48
13	Temperature Probe (Pneumatic Venturi Pyrometer)--Final Detail Design Drawing	51
14	Pneumatic Venturi Temperature Probe	54
15	Temperature Probe - End View of Upstream Venturi	55
16	Typical Velocity Calibration Curves	57
17	Velocity Probe Calibration Rig	58
18	Velocity Probe Calibration Orientation	59
19	Velocity Probe Calibration Chart for Yaw (α) and Pitch (β)	60
20	Velocity Probe Calibration Chart for Velocity Magnitude	63
21	Relation Between Angles for Velocity Determination in Five-Hole Pitot Probe	64

FIGURES (Continued)

No.		Page
22	Velocity Probe Calibration Chart for Determination of Angle of Flow	66
23	Velocity Probe Calibration Chart for Determination of Velocity Magnitude	67
24	Gas Burner Design	70
25	Temperature Probe/Gas Burner Schematic	71
26	Evaluation of Temperature Probe in Premixed Gas Flame	73
27	Velocity Probe/Gas Burner Schematic	75
28	Species Probe/Gas Burner Schematic	77
29	The Mass Spectrometer is Used to Analyze the Chemical Composition	80
30	Flame Sampling System	82
31	Dual-Disk TOF Chopper	82
32	Average Molecular Weight of Combustion Gases vs Equivalence Ratio for Methane-Air Flames	89
33	Beam Signals for H, OH, and O Radicals vs Equivalence Ratio at D = 2.00 Inches	91
34	Mole Fraction of Direct-Sampled CO_2 and CO, Recycled CO_2 and CO, vs Equivalence Ratio at D = 2.00 Inches	92
35	Mole Fraction of Direct-Sampled NO and H_2 and Recycled NO vs Equivalence Ratio for D = 2.00 Inches	93
36	Beam Signals for Direct-Sampled O_2 and H_2O and Recycled O_2 and H_2O vs Equivalence Ratio for D = 2.00 Inches	94
37	TOF and Thermocouple Measured Flame Temperatures vs Equivalence Ratio	98

ACKNOWLEDGEMENTS

A portion of the research was subcontracted to the University of California at Los Angeles under Rocketdyne Purchase Order No. R24PXZ3156678.

The Rocketdyne Program Manager was L. P. Combs and Dr. R. C. Kesselring was Rocketdyne's principal investigator. Professor E. L. Knuth was responsible for the unstable species effort and the overall molecular-beam mass spectrometry work performed at UCLA.

W. E. Rodgers was responsible for the modifications made to the UCLA molecular-beam mass spectrometer system and K. M. Gorji and Dr. W. S. Young conducted the molecular-beam tests and performed the data analysis.

This report has been assigned Rocketdyne Report No. R-9411.

INTRODUCTION AND SUMMARY

The objective of this program was the design, development, demonstration, and delivery of probes that may be used to measure temperatures, chemical species, and velocities in flames with emphasis on developing operational capability of the probes in the "dirty flame" environments characteristic of burning coal and residual oil.

The major design problems that were necessary to consider relate to the environments in which the probes must operate. The media are potentially quite dirty, consisting of as many as three phases (solid, liquid, and gas) of material that is capable of condensing and forming dirty, tenacious coatings that can harden to change probe geometry or to catalyze unwanted chemical reactions. The combustion media are quite hot, requiring cooling for most materials, and the combustion chambers are designed such that access to them with probes is physically difficult. Also, the combustion media are chemically reactive; a factor that can change the composition of samples gases if not quickly quenched or alter temperature readings by physical sensors if allowed to react catalytically on surfaces.

A prime concern with any probe is that the presence of the probe itself does not disturb the medium sufficiently to affect the measurement significantly. Potential disturbing effects include distortion of pressure or velocity profiles, chemical effects such as flameholding by the probe itself, excessive heat losses to or from the probe, or excessive removal of combustion gas. Most such effects are minimized by using probes that are physically small. Therefore, an important objective of this program was to minimize probe size while avoiding the plugging and contamination characteristic of dirty combustion environment.

Another factor of concern for temperature, velocity, or species concentration probes is the time response of the probe. The combustors of interest typically exhibit fluctuations with time, so that all of the quantities of interest vary with time. Resolution of the time variance of these quantities requires fast-response probes, and fast-response recording. Generally, fast response is associated with small probe and/or system size, although other factors such as convective heat transfer to thermocouples can enter into consideration.

To accomplish the objectives, the program was divided into two tasks as shown in Fig. 1. During Task I, the literature concerning flame measurement techniques was reviewed thoroughly, including flame characterization by molecular-beam sampling. Based on results from this review, promising measurements techniques were selected. The selected techniques were used as the basis for design of individual temperature, velocity, and stable species probes, which were developed subsequently in Task II.

A 5-hole pitot probe technique was used in the velocity probe. A quick-quench concept was used in the species probe in which cooled sample gas is pumped back to the probe entrance and mixed with the hot gas sample to cool the sample and rapidly quench the reactions, preventing further NO reaction. A pneumatic venturi pyrometer was used as the temperature probe. An alternate method, suction pyrometry, was considered carefully but it was concluded to possess little chance of immediate success in the measurement of temperatures in excess of 3200 F. The pneumatic venturi pyrometer, if provided with adequate cooling, has no upper temperature limit.

All probes fabricated during this contract were designed to meet length, cooling water flow, and pressure drop requirements that permit them to be adapted easily for future use in EPA experimental installations, if so desired.

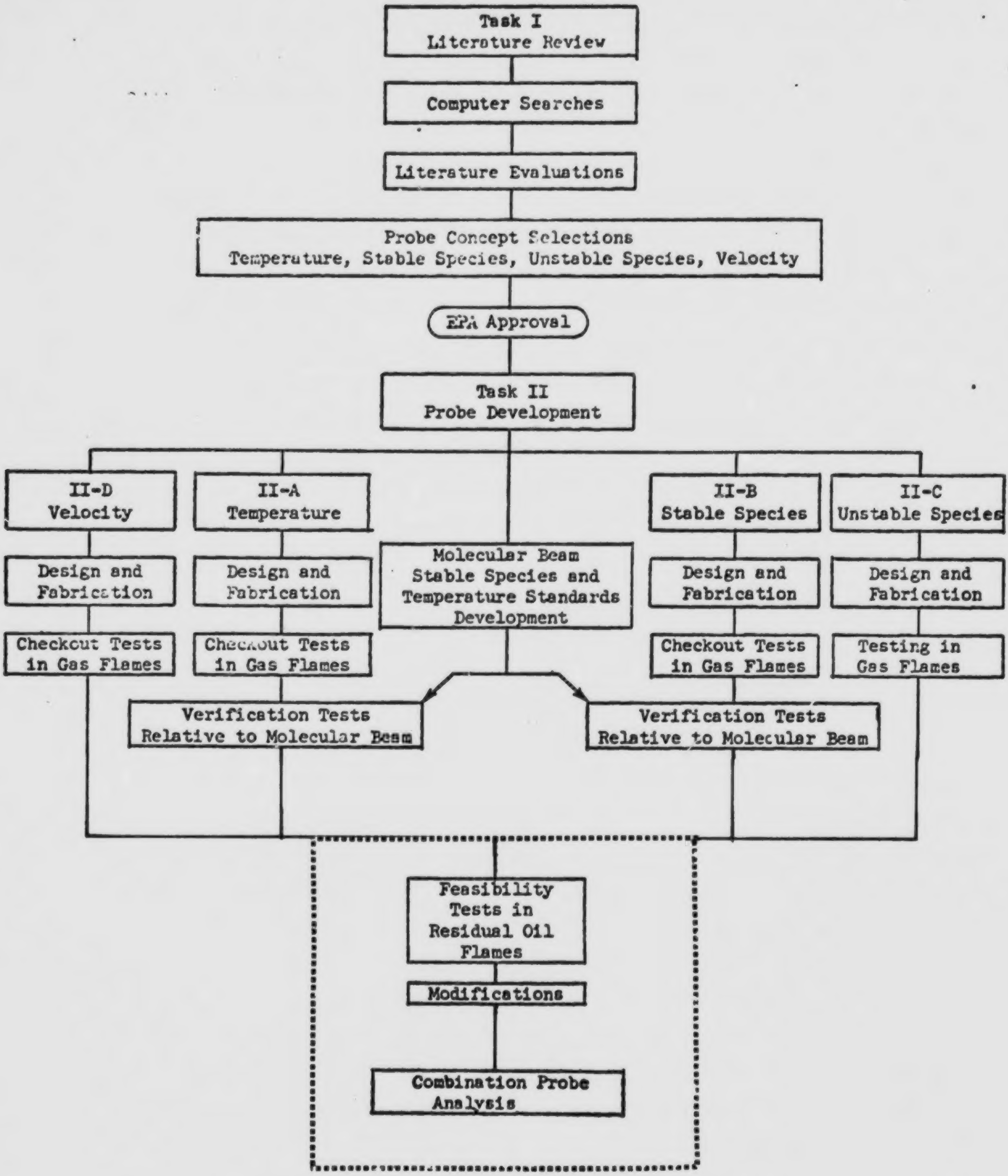
Task I
Literature Review
Computer Searches
Literature Evaluations
Probe Concept Selections
Temperature, Stable Species, Unstable Species, Velocity
EPA Approval
Task II
Probe Development
II-D
Velocity
II-A
Temperature
II-B
Stable Species
II-C
Unstable Species
Design and Fabrication
Design and Fabrication
Design and Fabrication
Design and Fabrication
Molecular Beam
Stable Species and Temperature Standards Development
Checkout Tests in Gas Flames
Checkout Tests in Gas Flames
Checkout Tests in Gas Flames
Testing in Gas Flames
Verification Tests Relative to Molecular Beam
Verification Tests Relative to Molecular Beam
Feasibility Tests in Residual Oil Flames
Modifications
Combination Probe Analysis

Figure 1. Program flow diagram

For determination of unstable species in a pre-mixed gas flame, a UCLA molecular-beam mass-spectrometer system was modified and upgraded. A liquid-nitrogen cryo-surface was added to the detection chamber to reduce the background noise in the mass-spectrometer output. To facilitate measurements of low-concentration species, a logarithmic amplifier was designed and constructed. Handling of the signal component owing to metastable molecules (not filtered out by the mass spectrometer) was facilitated through the use of a base-line compensator. For the determination of the effects of vibrational-temperature changes on mass-spectrometer fragmentation patterns, a heated effusive source was constructed, and the mass spectrometer was calibrated for beam-gas vibrational temperatures up to 900 C. For flame temperature measurements, a dual-disk time-of-flight chopper was installed in the collimating chamber.

In addition, a methane-air burner was designed and built at UCLA in which flat vertical-flow flames were produced over a porous alumina disk used as a flame holder. The inlet to the molecular-beam mass-spectrometer system and the burner shroud were adapted for sampling from this burner.

The UCLA molecular-beam mass-spectrometer system was used to directly sample pre-mixed methane/air flame. With this technique, quantitative measurements of CO_2, CO, H_2, and NO concentrations, qualitative measurements of O_2, H_2O, OH, O, and H concentrations, and quantitative measurements of flame temperatures were shown to be feasible.

The individual probes fabricated during the program were checked out and calibrated in a series of tests. Calibration testing of the 5-hole velocity probe was performed at Rocketdyne in a cold-flow apparatus. Calibration curves were constructed for the probe to allow determination of velocity direction and magnitude. A second gas burner, equivalent to the UCLA gas burner, was assembled at Rocketdyne and used to preliminarily evaluate the temperature, velocity, and species probes in a pre-mixed methane-air flame. Satisfactory operation of the probes was demonstrated.

After preliminary evaluation in a gas flame at Rocketdyne, the species and temperature probes were removed to UCLA for calibration by comparison of the temperature and composition of gases drawn through the probe with those obtained with the molecular beam/mass spectrometer (MBMS) technique. Simultaneous measurements with the Rocketdyne temperature probe and the time-of-flight MBMS technique were accomplished. Good agreement between the two temperature techniques was found at stoichiometric conditions but not quite as good as off-stoichiometric conditions; somewhat higher temperatures being indicated by the time-of-flight MBMS technique than by the probe. Comparison tests at UCLA of the Rocketdyne species probe with the MBMS technique were accomplished consecutively, not simultaneously, because the UCLA mass spectrometer was used for the analysis of the composition of the samples obtained with both techniques. The species probe was found to eliminate the radicals H, OH, and O (anticipated), increase the measured concentrations of CO_2, CO, and O_2 (not anticipated), decrease the measured concentrations of NO (not surprising), and sharply decrease the measured concentrations of H_2O (anticipated). It is not known whether the elimination of cooled combustion gas recycle in the Rocketdyne species probe would improve, worsen, or leave unchanged, the comparative results between the species probe and the MBMS technique. The results of the species comparison tests thus indicate that further investigations may be merited dependent upon the accuracy desired in the measurement of the particular species.

Feasibility testing of the probes in a residual oil flame, as well as the analysis of a combination probe design, was originally planned after completion of the probe verification tests with the MBMS technique (shown by the dotted boxes in Fig. 1), but was not performed.

EVALUATION OF AVAILABLE EXPERIMENTAL TECHNIQUES

The most significant factors that must be considered in the development of probes for characterization of oil or coal flames are related to the flame environment. Depending on the particular fuel selected, the type of burner used and the position within an oil or coal flame, the flame conditions may be difficult to probe and sample, because they present a two- or even three-phase flow of very hot, turbulent, and chemically reactive gases. At any particular location, the local gases can, by turbulent fluctuations, change rapidly and frequently from reductive to oxidative and vice versa. Solids, liquids, and condensables in the combustion gases can combine to form very tenacious, unpredictable coatings on unprotected surfaces. The formation of such coatings on probes inserted in a flame for the purpose of measuring flame characteristics can easily alter probe geometries and, thereby, functions. In addition, these coatings may serve to catalyze unpredictable and undesirable chemical reactions. Because the combustion media are so chemically reactive, the composition of sampled gases may change appreciably if the sample is not quenched quickly. Temperature readings may also change appreciably if catalytic reactions are allowed to occur on the surfaces of physical sensors.

Initial effort on this program was a study and assessment of existing techniques for flame characterization. Literature searches were made to obtain available information and aid selection of suitable techniques. Measurement techniques reported in the literature, including those concerning molecular beam mass spectrometric techniques are described in

Appendixes A and B. An evaluation of those techniques that might be considered applicable to measurements in the dirty flame environments characteristic of coal or residual oil flames are further discussed below.

TEMPERATURE MEASUREMENT

Suction Pyrometry

The suction pyrometer technique involves the aspiration of sample gas at high speed past a noble-metal thermocouple enclosed in multiple shields in order to maximize convective heat transfer, while minimizing radiative heat transfer, to the thermocouple.

The aspirated thermocouple probe (suction pyrometer) is a reasonable technique for measurements of flame temperatures. High aspiration rates can effectively reduce errors caused by radiation and surface catalysis. However, a temperature limit exists above which the radiation shield materials fail and preclude probe use. Also, impingement of liquid (oil) droplets on the thermocouple represents a problem because of the possible cooling effects resulting from vaporization and endothermic decomposition of the oil. The suction pyrometer may not be acceptable in the presence of large particles because of possible sensor damage by repeated high-velocity particle collisions caused by high-aspiration rates.

To minimize temperature errors caused by droplet impingement, it is desirable to orient suction pyrometers so that the likelihood of droplet impingement is minimal. As the gas is aspirated past the thermocouple, it is possible to cause the gas to turn a corner (or even to swirl) to help separate droplets from the gas, which ultimately contacts the temperature-sensing element. In addition to decreasing the possibility of droplet impingement on the couple, such action also decreases the rate at which the flow passages in the radiation shields become plugged (Ref. 1).

Pneumatic Venturi Pyrometer

Another attractive temperature measurement technique is the pneumatic venturi pyrometer. This instrument involves the aspiration of sample gas through two venturi nozzles in series with cooling of the gas between nozzles. Application of the continuity equation to the continuously flowing gas stream allows analytical determination of the hot sample gas temperature from measured values of:

1. The cold sample gas temperature (at downstream nozzle)
2. The pressure drops across the upstream and downstream nozzles
3. An instrument constant (see Appendix A).

The temperature limit of the venturi pyrometer is only a function of the materials of construction used, probe design and the probe cooling provided. This technique is particularly attractive for high-temperature application and involves shorter response times (i.e., seconds) than experienced with suction pyrometers (i.e., minutes) (see Appendix A). However, under the dirty flow conditions, characteristic of oil and coal combustors, solid deposits in the venturi nozzles can cause rapid change in the value of the instrument constant, K, because of changes in nozzle throat areas and discharge coefficients. For application in a "dirty" flame, it is advisable to calibrate such a device in position before and after each measurement. Pressure drops across the throats of each of the two nozzles serve to define the area and discharge coefficients of the contaminated nozzles. Such calibration would also serve as an indication of when the probe should be removed from the flame for thorough cleaning.

An additional factor that may influence the operation of a pneumatic probe is the probability of two-phase flow in the probe nozzles (especially for positions in a flame close to an oil burner's spray nozzle or a pulverized coal injection and ignition site). The influence of small amounts of liquid or solid particles may influence the gas flow through a venturi nozzle in several ways, dependent on the size and concentration of the particles. Possibly the largest effect is the momentum transfer and gas pressure change resulting from droplet disintegration. Aerodynamic forces to which the liquid droplets are exposed in an accelerating gas stream, e.g., in a probe nozzle, tend to cause breaking of large droplets into many small droplets, the sizes of which are difficult to predict even if the sizes of the large droplets entering the nozzle were known. The net result is that it is difficult to correct the nozzle pressure drops for the effects of two-phase flow in the presence of liquid droplets. Near the injection site in an oil burning combustor, where oil droplets constitute only about 6 percent of the total mass flow, inaccuracy in two-phase flow effects could lead to temperature errors of as much as a few percent for pneumatic probes. However, near the injection site, temperatures are usually low, and methods other than pneumatic probes should be satisfactory for measuring those temperatures. In relatively clean zones (not close to oil or coal injection sites), where condensed or solid phases amount to less than 1 or 2 percent of the mass flow, errors in temperature measurements caused by two-phase flow effects should be less than 1 percent.

Velocity of Sound Probes

Temperature determination from velocity of sound measurements is a technique usable in the presence of a dirty flame. Measurement of sound velocity in combustion gases results in the determination of a value for $(\gamma T/M)^{1/2}$. The ratio γ/M is nearly constant, and its estimation permits determination of the combustion gas temperature. Velocity of sound measurements can be made either by noting the time of passage of a sound wave past two detectors, or by observation of the physical size of specially induced standing sound wave patterns. In both of these cases, on the order of 5 to 10 cm of sound wave path length is required to obtain a precise sound wave determination. This path length requirement infers very poor spatial resolution on the part of the sound velocity temperature measurement technique. For 10^9 Btu/hr combustors, the

5- to 10-cm spatial resolution may be adequate, but for 10^5 Btu/hr combustors, it is definitely not adequate. Sound velocity techniques thus appear unacceptable for use in "dirty" flame combustor environments on the basis of spatial resolution.

Optical Pyrometry

This technique involves the measurement of the brightness of a flame (whose temperature is to be determined) by comparison with the brightness of an object of known temperature. The measured brightness of the flame is then related to gas temperature. If the object used for comparison is a sodium ion and the brightness of the D-line is used as the standard, the technique is known as the sodium line reversal method.

The two major drawbacks to optical pyrometry are poor spatial resolution and a relatively high lower temperature limit (see Appendix A). To measure local temperatures optically with acceptable spatial resolution, it is necessary for the combustion gas to be optically dense at the wavelength(s) of interest, and to use a probe that localizes the source of light to the spatial point of interest. Such a probe can consist of a rod of high-quality glass that easily transmits the Na-D line, coupled with appropriate Na-D line narrow band filters. The glass rod should be continuously cooled, possibly by containment inside a tube having an inert gas purge. To make a temperature measurement, the purge must be interrupted, or preferably changed instantaneously to aspiration of combustion gas, to bring hot gas very close to the end of the glass rod probe. To avoid overheating the glass rod, the period of combustion gas aspiration and hence the period of measurement must be severely limited. The end of the glass rod should be cleaned once every few measurements. If the Na-D line is used, together with appropriate narrow-band filters, it may be possible to use a commonly available sensing device, such as a CdS cell. Disadvantages of the suggested optical technique include the requirement for development and calibration. Also, this or any related optical technique is not capable of better than 1 or 2 percent accuracy at most in a high-response system. Additionally, depending upon the fuel being used, it may be necessary to seed the combustion system with small amounts of sodium. An obvious disadvantage of this optical probe technique is its lower temperature limit of 2500 F (caused by weak emission below this point).

Molecular Beam

Translational temperatures in gas flames can be determined directly from measurement of molecular speeds. This is accomplished by means of a molecular-beam sampling apparatus in conjunction with a time-of-flight apparatus. The molecular-beam sampling apparatus causes gas withdrawn from a combustion process to undergo a very rapid expansion to supersonic velocities. The molecules that remain on or near the axis of this expanding flow are naturally those molecules whose velocity was directed in the axial direction at the end of transition from continuum to free molecular flow. By intermittently chopping the molecular beam and measuring the time required for a chopped portion of the beam to arrive at a detector site, the velocity of the axially-directed molecules in the beam can be determined. This hydrodynamic velocity (V) is a direct indication of the stagnation temperature (T) of the source gas and the mainstream gas temperature can be calculated from the expression

$$T = \frac{\gamma-1}{2} \frac{mV^{2*}}{\gamma R}$$

The molecular beam method offers the advantage of temperature measurements without the need of blackbody or any other sort of temperature calibration. The calibration required is one of time (used in molecular velocity determination) that can be performed very accurately. The molecular beam technique also offers excellent response, well under one millisecond. However, the molecular beam probe is generally associated with relatively large probes (90-degree cone typical) that might disturb flow patterns. Unfortunately, the molecular beam technique is not recommended for use in "dirty flame" environments because of almost certain plugging of the tiny sampling orifice by oil droplets or solid particles. With the exception of the plugging and probe-size aspects, the molecular beam technique is a superior method and this technique can be used to calibrate any other technique selected for use in the flame field.

---

*See page 87 for a more detailed description of the calculation procedure.

Evaluation

From this survey of possible methods for measuring flame temperatures, both the suction pyrometer technique and the pneumatic venturi pyrometer technique were selected for further consideration. The final selection between these two techniques is discussed in a later section of this report.

SPECIES MEASUREMENT

Sampling Probes

Continuous operation of a species sampling probe in the thermal environments characteristic of heating units or utility boilers is not difficult because of the relatively low pressures and velocities. Low-pressure water cooling is usually adequate for probe survival. However, it is necessary in designing sampling probes to allow for thermal expansion of exterior probe surfaces, to ensure that the probe remains intact without any cracks, breaks, or distortions caused by repetitive heating and cooling. The various features of species sampling probes are discussed in Appendix A.

Conventional water-cooled (convective-quench) species probes have been used quite successfully in obtaining samples from distillate oil flames (e.g., Ref. 2). However, to ensure that no further reaction occurs in the probe itself, a "quick quench" of the sampled gas is desired. In addition, operation of a species sampling probe in a dirty, condensation-and-deposition-prone medium invites plugging and formation of coatings on both the interior and the exterior surfaces. For a conventional (i.e., small sized, near-atmospheric pressure) water-cooled probe, the formation of some exterior and some interior coatings is almost unavoidable. Formation of deposits on the exterior of the probe does not inhibit use of the probe, and it is of little concern. Plugging and formation of deposits on the interior of a cooled probe can be minimized by providing a boundary layer of clean gas near the interior probe surfaces, particularly at the narrowest restriction where plugging is most apt to occur. Not only would this clean gas injection serve to quench the sample gas rapidly, but it would also provide a clean gas internal boundary layer to inhibit condensation of oils and sticking of small carbonaceous particles near the probe inlet. This design would not totally inhibit deposition within the probe, but it would minimize the deposition and also keep any deposits that do form relatively cool by direct contact with the cold, clean gas from the injection sites. Keeping the deposits cool (which cannot be well accomplished by heat transfer through the probe wall because of thickness, poor contact with the wall, and low-thermal conductivity of the depositions themselves) is important to prevent hot deposits from catalyzing further chemical reaction of the sampled gases. The quench gas could be either an inert gas or cooled, recycled sample gas. Use of the sample gas itself for quenching would ostensibly simplify chemical analysis procedures, but response times could be quite long. On the other hand, inert quench gas could be provided at high flowrates, limited only by total volumetric sample rate and probe pressure limitations. Using externally supplied inert quench gas, quenching times would be limited only by the time required for mixing the inert gas with the sample gas and could conceivably be as low as a few microseconds.

Molecular Beam/Mass Spectrometer

The molecular beam technique involves the extremely rapid expansion of a small sample of combustion gas from the combustion zone through a small pinhole orifice and into a high-vacuum-source chamber (see Fig. 2 and Appendix A).

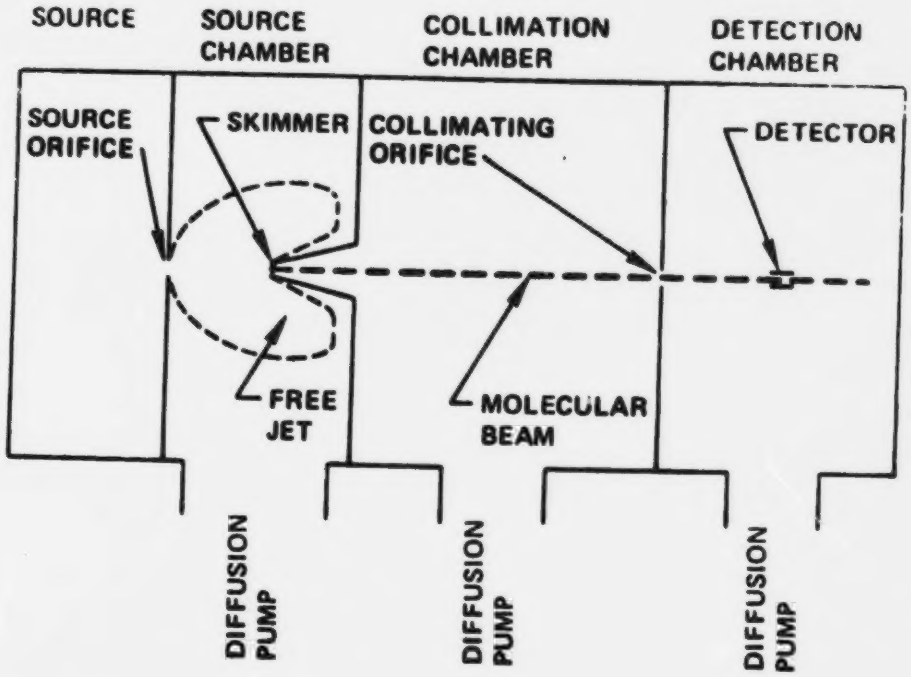
SOURCE
SOURCE CHAMBER
COLLIMATION CHAMBER
DETECTION CHAMBER
SOURCE ORIFICE
SKIMMER
COLLIMATING ORIFICE
DETECTOR
FREE JET
MOLECULAR BEAM
DIFFUSION PUMP
DIFFUSION PUMP
DIFFUSION PUMP

Figure 2. Schematic diagram of molecular-beam sampling system

The aerodynamic expansion is continued until free molecular flow is achieved, and a portion of the expanded jet is skimmed and collimated to form a molecular beam that may be analyzed using a mass spectrometer as the detector.

Through the rapid quench times of the molecular beam are highly desirable and perhaps necessary for quenching fast reactions such as those involved in NO formation, there are also disadvantages. The pinhole sample port for a molecular beam is generally quite small, on the order of a few tenths of a millimeter. The pinhole is made small to minimize the quench time, but it cannot be so small that it samples only gases from boundary layers on the end of the sampler. Plugging of the pinhole by liquid or solid particulates in an oil or coal flame is almost a certainty. An additional disadvantage of the molecular-beam sample apparatus is the angle of the Prandtl-Meyer expansion and the high-vacuum requirements that make the apparatus somewhat bulky for sampling the interior portions of an easily disturbed combustion process.

Spectroscopy

Spectroscopy, the science of measuring and correlating spectral light emission and absorption characteristics, can be used to identify various chemical elements within a flame. The techniques employed are discussed in Appendix A.

While spectroscopy is a superior method for measuring chemical species in uniform flowfields, its application to non-uniform flowfields requires the use of a very complex system that enables the attainment of large matrices of data. For particle-containing flow streams (such as the combustion zones of oil and coal burners) spectroscopic techniques do not appear appropriate because the particulates could provide an overwhelming continuum background signal and could also interfere with absorption measurements by scattering light from the external excitation source. For clear exhausts much effort would be required to identify useful lines and to determine their absorption coefficients.

Evaluation

Use of a quick-quench probe for determination of stable chemical species was concluded to be the technique best suited for application in the "dirty flame" environments of interest. The even faster quenching molecular-beam apparatus was considered to be the best method for determining unstable species, and for certain unstable species it is the only known practical method at present. Additionally, since the molecular-beam technique can also be used to obtain stable species concentrations it can be used as a check against the stable species sampling probe in other than "dirty flame" environments. Similarly, since the molecular-beam technique can be used to determine temperature, it can also be used as a reference from which to calibrate and/or evaluate the temperature measurement technique selected for use.

VELOCITY MEASUREMENT

Magnitude

Pitot Probes-These commonly-used devices permit determination of a flowing stream's dynamic pressure, which is a direct measure of its velocity, by use of a differential pressure measurement between a total-pressure (impact) tap and a static-pressure tap. Pitot probes have been successfully used in distillate oil flames (see Appendix A) and plugging of the impact probe tap can be avoided through the use of a purge system. Plugging of pitot probes is less a problem than plugging of certain types of temperature and species probes, because there is no aspiration of sample gas through the pitot probe. Modification of pitot probes for application in dense two-phase (liquid-gas) flowfields has also been accomplished (see Appendix A).

Hot-Wire Anemometry-A hot-wire anemometer consists essentially of a fine, electrically-heated wire inserted in a fluid stream. A change in velocity of the fluid stream affects the rate of heat flow from wire to fluid and thus, tends to heat or cool the wire. This, in turn, alters the resistance of the wire and produces a measurable effect in the electrical heating circuit. Hot-wire techniques are not applicable for use in flowfields where droplet ignition is occurring or where droplets or solid particles impacting on the hot-wire could grossly alter the wire's thermal balance or even damage it.

Mechanical Anemometry-Mechanical anemometry involves determination of velocities by the capability of the gas flow to cause movement of small windmill-type structures. Their use in combustion zones presents many problems (see Appendix A), not the least of which are excessive probe size cooling and selection of materials of construction.

Pulsed Tracer-Pulsed tracer techniques (see Appendix A) possess the advantage of permitting velocity to be measured without a knowledge of gas density. Such techniques are also feasible in gas flows containing solids or liquid droplets. A major disadvantage is that velocity magnitude cannot be determined without knowledge of velocity direction. This disadvantage may be overcome if tracers are followed photographically, but for "dirty flame" environments this presents perhaps even a greater disadvantage.

Direction

Tracers-Tracer techniques may also be used to determine velocity direction. However, as stated above, the use of this technique in a "dirty flame" combustion environment adds complexities to the technique, which preclude its selection.

Multiple-Port Impact Probe-Multiple-port impact (pitot-type) probes are reliable methods for the determination of flow direction. One type of device employs pairs of individual probes that are gimbaled in a three-dimensional field in order to balance the pressure readings and determine the flow direction (see Appendix A). Another type of multi-port probe is the hemispherically-shaped pitot probe having multiple taps on the single probe head. This latter probe avoids the use of a gimbaling apparatus. Flow direction is determined by measurement of the pressure distribution over the probe head and locating the stagnation point, and thus velocity direction. Careful calibration of each particular probe is required. Such calibration can easily be accomplished in a non-reactive flowfield.

Evaluation

A 5-hole hemispherical pitot probe appears to offer a relatively easy means of determining both velocity magnitude and direction without the problem of gimbaling the probe in the flame. This technique has been employed at the International Flame Research Foundation (Ref. 1) in dirty flame environments with apparent success.

SELECTION OF MEASUREMENT TECHNIQUES

The preponderance of information concerning measurement techniques in "dirty flame" environments originates from work done at the International Flame Research Foundation (IFRF) in IJmuiden, Holland. Only two references based on IJmuiden work were available at the program outset (Ref. 1 and 3) and they were found to be most informative. However, the technical details concerning various measurement techniques were not adequately discussed in all cases.

Based on the evaluation of the literature references obtainable at the program outset, a tentative selection was made of the measurement techniques to be employed in this program (the selections to remain tentative until the conclusion of verbal communication with EPA and IFRF personnel). The tentatively selected measurement techniques were:

Flame Temperature - Pneumatic Venturi Pyrometry or Suction Pyrometry
Stable Chemical Species - Gas Quench Probe
Unstable Chemical Species - Molecular-Beam Spectroscopy
Velocity - Multi-port Impact Probe

Emphasis was placed on the selection of a temperature measurement technique for use in residual oil flames. Two methods were considered, the suction pyrometer technique and the pneumatic venturi pyrometer technique (Ref. 1). The suction pyrometer technique involves the aspiration of the sample gas at high speed past a noble metal thermocouple enclosed in multiple shields in order to maximize convective heat transfer, while minimizing radiative heat transfer, to the thermocouple. The pneumatic venturi pyrometer involves drawing the sample gas through two nozzles with cooling of the gas between nozzles. The gas temperature at the downstream (cold) nozzle is easily monitored by a conventional thermocouple or other device. From the continuity equation, the upstream (hot) gas temperature is calculated from the measured downstream (cold) gas temperature, the respective pressure drops across the two nozzles, and an instrument constant, K, as follows:

$$T_{\text{hot gas}} = K \frac{\Delta P_{\text{hot}}}{\Delta P_{\text{cold}}} T_{\text{cold gas}}$$

Before communication with the IFRF, a very recent book was received (Ref. 4) that presents "in readily accessible form" the results of 24 years of cooperative research by the IFRF. The book supplied answers to a number of questions but, for the most part, appeared too general and lacked presentation of data comparing measurements obtained with both the suction pyrometer and the pneumatic venturi pyrometer. Without actually stating so, Ref. 1 implied that the suction pyrometer has been selected as the standard temperature measurement technique at IFRF for all types of flames. The pneumatic pyrometer was regarded as less accurate than the suction pyrometer and "only of interest for measurements in gases where the temperature is very high or heavily laden with dust."

Both the suction pyrometer technique and the pneumatic venturi technique were discussed with Dr. Michael Heap of the IFRF (Ref. 5). Dr. Heap, who has considerable personal experience with suction pyrometry, stated emphatically that he preferred the suction pyrometer over the pneumatic venturi, which he personally has never used, in residual oil or pulverized coal flames. He gave three main reasons for this preference:

1. The suction pyrometer, unlike the pneumatic venturi, requires no instrument calibration.

2. Greater ease of operation is experienced with the suction pyrometer because sets of radiation shields may be quickly replaced if plugged while, with the pneumatic venturi, chemical cleaning may be required to remove sticky tar-like oil deposits from the hot throat.
3. The suction pyrometer can give accurate measurements in any flowfield while work of about 5 years ago at the IFRF indicated that measurements with the pneumatic venturi are velocity sensitive and that there are circumstances in swirling flows where the pneumatic venturi is useless.

Work at the IFRF had centered predominantly around gas, residual oil and pulverized coal flames. Heap (Ref. 5) stated that when blockage is experienced with a suction pyrometer in a pulverized coal flame, a total of three sheaths (the outer radiation shield, the inside radiation shield and the alumina sheath over the thermocouple) quite often fuse together necessitating replacement of the entire set. With oil flames, soot (if produced) often blocks the suction lines. In the oily part of the flame, oil may block the suction lines as well. Heap further stated that, with the suction pyrometer, measurements in oil flames are easier than in coal flames. The suction pyrometer has a temperature limit of about 1700 C (3550 R) imposed by problems with thermal shock on the shield at higher temperatures. The only advantages of the pneumatic venturi are, in Heap's opinion, the higher permissible operating temperature, and perhaps, its ease of prolonged use in dry, dusty atmospheres (such as fly ash).

Concerning the thermal mapping of an individual flame with a suction pyrometer, Heap stated that, where the flame occupies 1/3 or more of the volume of a furnace, approximately 90 percent of the temperature mapping could be accomplished with one or two sets of shields. However, to map the entire flame, 40 sets of shields may be required for coal flames (perhaps less for residual oil). Even so, Heap considers himself fortunate to obtain valid measurements in coal and oil flames closer than

20 to 30 cm (8 to 12 inches) from the burners and believes some regions are beyond measurement under certain circumstances.

The pneumatic venturi technique appears to have been used only for sonic gas flows in the U.S.A. (Ref. 6 and 7), but its use in industrial furnaces has been reported (Ref. 8 and 9) by the British Coal Utilization Research Association (BCURA). Reference 9 describes its use in water-tube boilers with gas, oil, and pulverized fuel flames and shows favorable comparisons in certain uses with the suction pyrometer. The advantages of the pneumatic venturi pyrometer, especially when compared to the suction pyrometer, are reported as being:

1. Equally accurate at all temperatures
2. Rapid response
3. Slower blockage tendency
4. More easily cleaned
5. Higher operating temperature.

The measurement sensitivity of the pneumatic venturi with respect to the external velocity flowfield appeared to have been solved (Ref. 8 and 6) by the substitution of a piezometer ring, with six equally spaced pressure taps, for the single pressure tap.

Thus, the suction pyrometer technique is apparently preferred by researchers at the IFRF (Ref. 5) while the pneumatic venturi pyrometer is apparently preferred by researchers at BCURA (Ref. 8 and 9). In an attempt to resolve the somewhat contradictory advantages claimed for the two instruments, the United States representative of the Land Instrument Co. (which manufactures, in England, both a suction pyrometer and a pneumatic venturi pyrometer) was contacted (Ref. 10). While no current use of the venturi pyrometer in this country was known to him, a recent report of experimental studies on the venturi pyrometer was forwarded to Rocketdyne. This 1969 report (Ref. 11), which was the basis for Heap's (Ref. 5) statements, points out the sacrifice in accuracy occasioned by a lack of knowledge of the discharge coefficient of the upstream venturi nozzle under actual "hot flow" conditions as compared to "cold flow" conditions. The need to correct temperature measurements obtained in flow of considerable approach velocity is also emphasized*. These elaborate corrections are a function of the suction velocity, approach velocity and the direction of flow approach. It is concluded in Ref. 11 that "practical advantages claimed for the VPP-probe (venturi pyrometer) for use in dirty gases (Ref. 7), namely blockage and soot deposits easy to remove and growing only slowly, are not attractive when time-consuming and delicate correction procedures are to be adopted in order to get reliable results." Also, "from the present experience, a VPP-probe cannot compete with a suction pyrometer with regard to measuring accuracy, reliability and ease of operation for temperature measurements in furnaces. Its usefulness is limited to applications where very high gas temperatures have to be measured, or where short response times are required."

While no United States use of the pneumatic venturi in oil or coal combustion atmospheres was located, a suction pyrometer has been used by Howard and Essenhigh to study the pyrolysis of pulverized coal particles in pulverized fuel flames (Ref. 12). Suction pyrometer temperatures as high as 1793 K were recorded. The suction pyrometer temperatures were taken as particle temperatures. Although such a measurement should indicate a temperature somewhere between that of the particles and that of the gas, Ref. 12 reports calculations that indicate a negligible temperature difference between the two phases for particles smaller than about 200 microns. No difficulty in pyrometer use was reported (Ref. 12).

Based upon the evaluation of the literature, it was concluded that, for residual oil flames, the venturi pyrometer is a higher risk technique than the suction pyrometer. However, the suction pyrometer, as it currently exists, is limited to operation below 1700 C (3090 F) because of thermal stresses in the radiation shields. Conversely, the temperature limit of the venturi pyrometer is only a function of the cooling provided. Since operation in a temperature range near 3600 F is desired with the probe, two alternatives were considered: (1) increasing the operating temperature limit of the suction pyrometer through use of new shield materials or attachment methods, and (2) designing the "best possible" venturi pyrometer.

---

*Interestingly, it is mentioned that "the influence of approach flow can be reduced by using a suitable design of the hot-nozzle profile, placing the upstream pressure tappings somewhat inside the nozzle." The placement of the upstream tap is the only apparently significant difference in design between the pneumatic venturi pyrometer types used by researchers at the IFRF and at BCURA.

At a meeting at Rocketdyne on 30 January 1974, Dr. Heap related his recent experiences at the IFRF, IJmuiden, in which an attempt was made to upgrade the suction pyrometer for use at higher temperatures (hopefully approaching 2000 C). The previously used radiation shields made of Sillimanite (60-80% Al_2O_3 + S_iO_2) were replaced with more expensive shields made of recrystallized alumina for these tests. Although recrystallized alumina is reported to be stable to 1900 C (3452 F), sagging of the sheath was encountered repeatedly during operation at indicated temperatures of about 1780 C (3200 F). In addition, rapid oxidation of the thermocouple material itself was a serious problem. Attempts were made to provide a protective layer of inert gas between the thermocouple and the thermocouple sheath. It was concluded that a serious materials problem exists when attempting to operate a suction pyrometer above 1800 C. A number of European investigators are attempting to overcome this problem.

If a suction pyrometer capable of operation at no more than 1700 C (3060 F) is desired, the most logical course of action would be to use IJmuiden's design. However, a temperature probe capable of operation at 3600 F or more was desired. Consequently, the pneumatic venturi pyrometer concept was selected for use in this program.

The tentative selections of techniques for measuring flame species and velocity were also discussed with Dr. Heap. Upon completion of these discussions, the tentative choices were agreed upon as the techniques to be applied in the Probe Development stage of the program.

PROBE DESIGN AND FABRICATION

HEAT TRANSFER AND PRESSURE DROP REQUIREMENTS

In order to design a probe for a particular flame application, the expected heat load to the probe must be known or estimated. The probe may then be designed to avoid its thermal destruction in the intended application. In addition, probe cooling requirements must be such that unrealistic coolant pressure drops are not required.

All probes fabricated during this program were designed to operate in a 3600 F residual oil flame. The expected local heat flux and total heat load to the probe caused by radiation (both from the hot combustion gases and refractory furnace walls) and convection from the combustion gases were calculated from conventional correlations. Assuming probe operation in a cylindrical, refractory-lined, 30-in. diameter stainless-steel combustor, expected temperatures of the refractory combustor liner and of the combustor inner wall were calculated using correlations for gaseous radiation, developed by H. C. Hottel, together with the separated flow convection relations of Sparrow and of Zemanick. The resultant heat load to the outer surface of a probe inserted in the 3600 F flame was calculated to be 210,000 Btu/hr ft^2. This value was assumed to be characteristic of the environment of any probe developed during this program and was used to achieve a realistic combination of probe temperature, cooling water ΔT, and cooling water pressure drop in the final probe design.

To aid in heat transfer analyses, probe requirements for cooling water flow and cooling length were calculated and plotted. The curves shown in Fig. 3 , which were calculated from the continuity equation, were used to obtain the mass flowrate of combustion gas through a probe as a function of probe ID and gas velocity through the probe. Figure 4 was developed for use in estimating the cooling water requirement for an individual probe. The curves in this figure were calculated from a heat balance on the cooling water, i.e.,

$$(\dot{W}\ C_p\ \Delta T)_{H_2O} = q_{\underset{\text{probe OD}}{\text{rad}}} + (\dot{W}\ C_p\ \Delta T)_{gas} \tag{1}$$

A value of ΔT_{H_2O} = 120 F was assumed* in the development of Fig. 4 as was a probe immersion length in the flame of 36 inches. The curves shown in Fig. 4 are nearly independent of combustion gas temperature drop over a range of 2600 to 3100 F.

The use of Fig. 4 is recommended for the purpose of estimating the minimum amount of water ($\dot{W}_{H_2O}$) required to cool a probe once its inside and outside diameters, and the suction rate of gas through the probe ($\dot{W}_{gas}$), are known. By using greater than this minimum amount of cooling water, the temperature rise of the water could be decreased from the value of 120 F assumed in Fig. 4 . Since the radiation heat transfer term on the right hand side of Eq. 1 is much greater than the capacitance term $(\dot{W}\ C_p\ \Delta T)_{gas}$, the W C_p ΔT term may be assumed negligible in order to obtain a quick estimate of the cooling water temperature rise (ΔT) for any

---

*It is desirable to avoid picking up sufficient heat in the cooling water to result in two-phase flow or steam at the cooling water exit. By holding ΔT_{H_2O} to a maximum of 120 F, and assuming an inlet water temperature of 70 F, the maximum outlet water temperature of 190 F would preclude two-phase flow.

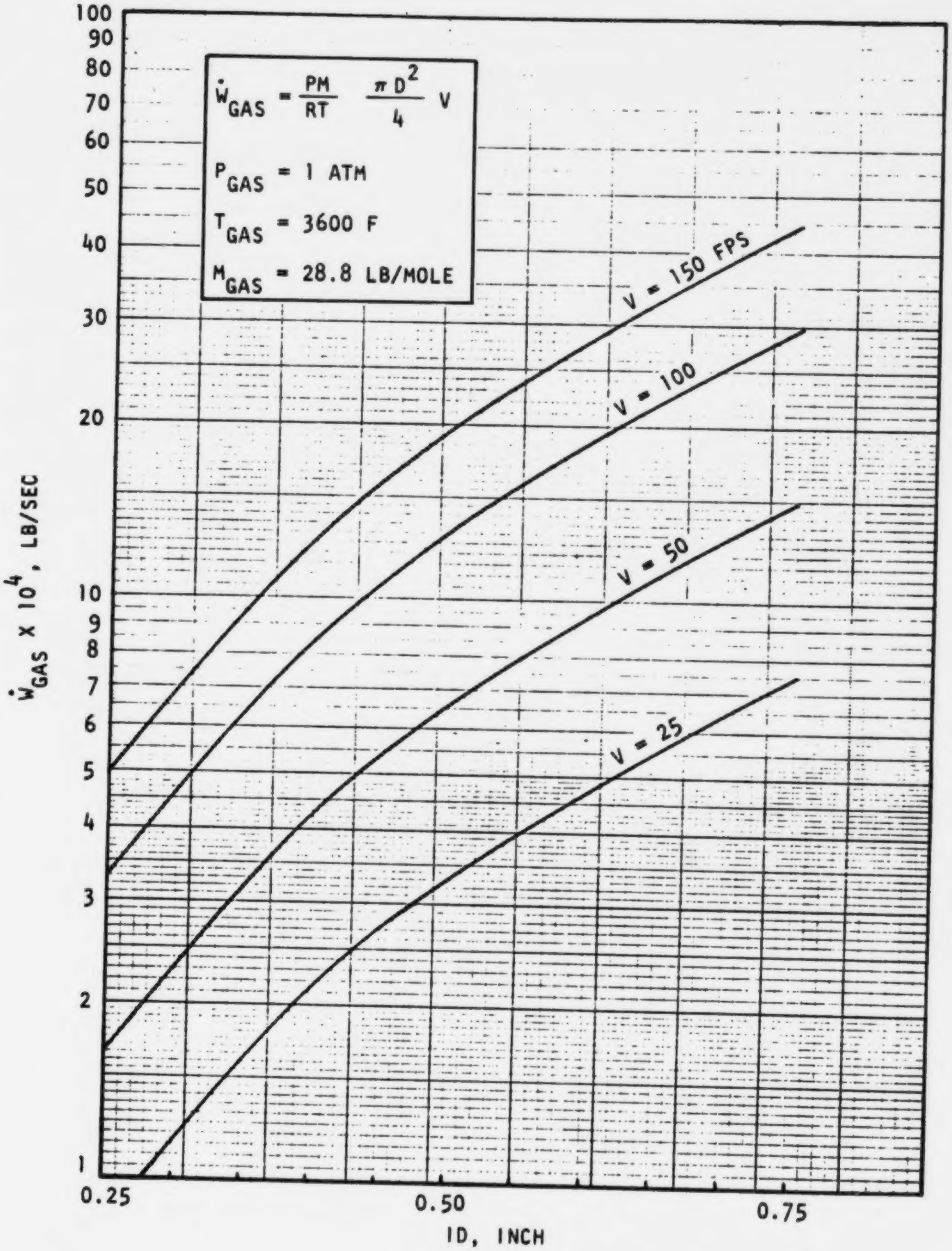

Figure 3. Mass flowrate of combustion gas through a probe as a function of probe ID and gas velocity

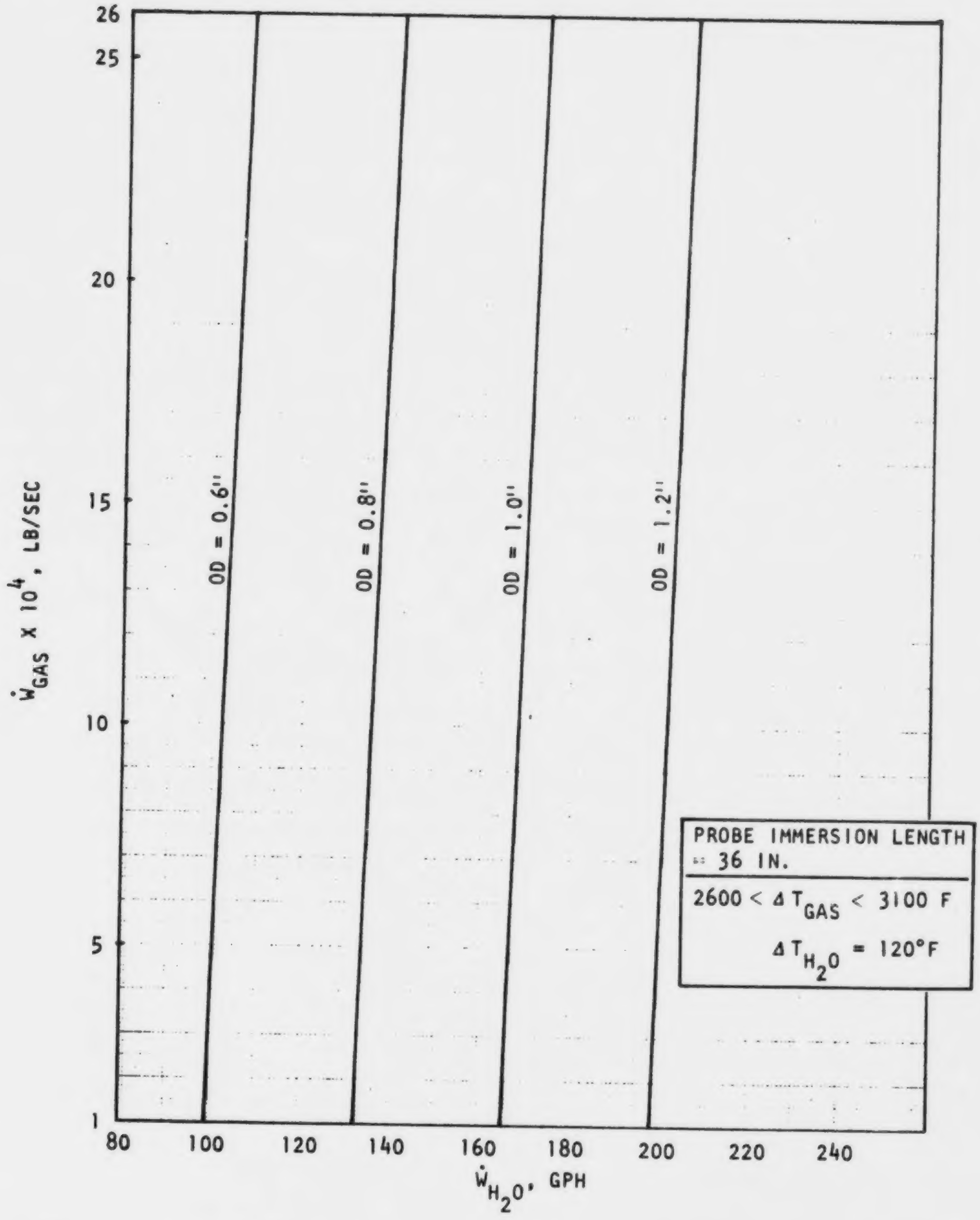

Figure 4. Mass flowrate of probe cooling water as a function of combustion gas flowrate through probe, probe OD and combustion gas ΔT

outside probe diameter, immersion length, and cooling water flowrate as follows:

From Eq. 1:

$$\Delta T_{H_2O} = \frac{\dfrac{q_{rad}}{\text{probe OD}}}{(\dot{W}\ C_p)_{H_2O}} \qquad (2)$$

but $q_{rad} = 210{,}000$ B/hr ft^2 = $210{,}000\ \pi\ D_o L_i$ B/hr
$C_{p_{H_2O}} = 1$ B/lb F

Therefore

$$\Delta T_{H_2O} = \frac{210{,}000\ \pi\ D_o\ L_i}{(\dot{W}\ C_p)_{H_2O}}$$

or

$$T_{H_2O} = 549\ \frac{D_o\ L_i}{\dot{W}_{H_2O}}$$

where

ΔT_{H_2O} = cooling water temperature drop, F
D_o = probe outside diameter, inches
L_i = probe immersion length, inches
$\dot{W}_{H_2O}$ = cooling water flowrate, gph

The probe length required to cool the 3600 F combustion gas to a temperature, T_{cg}, by conduction/convection heat exchange with the cooling water, i.e.,

$$(\dot{W}\ C_p\ \Delta T)_{gas} = hA\ \Delta T_{LM}$$

can be estimated through the use of Fig. 5 . Figure 5 shows the required probe length as a function of cool gas temperature, gas flowrate, and inside probe diameter.

The cooling water pressure drop resulting from flow through the probe was estimated using the expression

$$\Delta P_{H_2O} = 1.965 \times 10^{-7} \frac{L_t \dot{W}_{H_2O}^{2} pf}{A^3}$$

where

ΔP_{H_2O} = cooling water pressure drop, psi

L_t = total length of probe, inches

$\dot{W}_{H_2O}$ = cooling water flowrate, gph

p = wetted perimeter, inches

A = cross-sec area, in.^{2}

f = dimensionless friction factor = $(0.00140 + 0.125/Re^{0.32})$

Re = Reynold's number = $3.515 \times 10^2 \dot{W}_{H_2O}/P$

All probes fabricated during this program satisfy length and cooling water flow and pressure drop requirements that should permit them to be adapted easily for use in EPA experimental installations if so desired. It is necessary, nonetheless, to use Fig. 3 through 5 in conjunction with the intended actual suction velocity and immersion depth in order to ensure that:

1. An adequate quantity of cooling water is used
2. The probe length provided is sufficient to cool the combustion gas to an acceptable value.

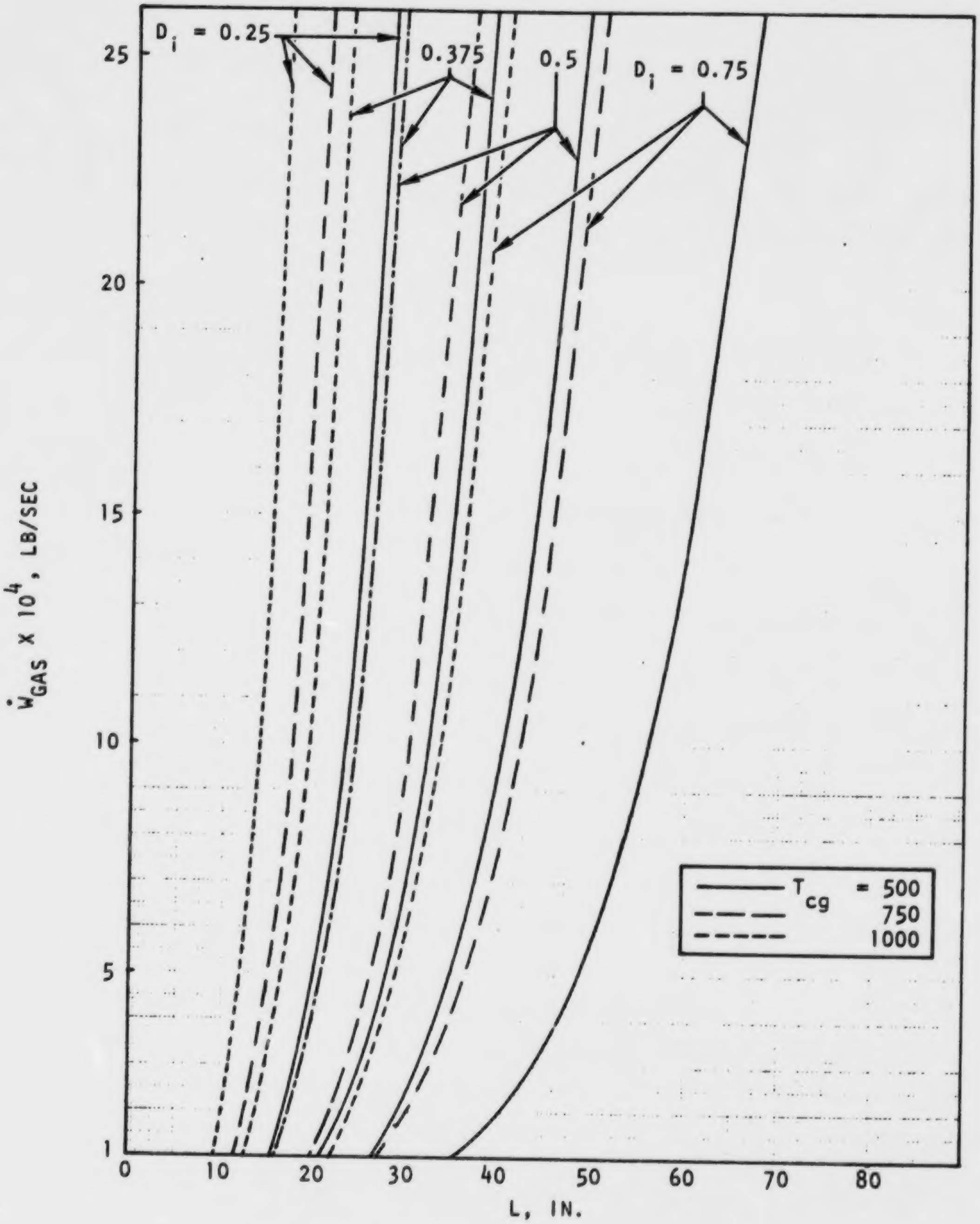

Figure 5 . Probe length required as a function of combustion gas flowrate through probe, probe ID, and final (cooled) combustion gas temperature

The use of Eq. 4 to calculate coolant water pressure drop enables one to determine if sufficient source pressure exists to allow the desired flowrate of cooling water.

VELOCITY PROBE

The 5-hole pitot probe concept was selected for the velocity measurement probe. Each probe must be calibrated so that both the magnitude and direction of the velocity can be determined from measurement of three differential pressures without rotation or gimbaling of the probe in a flame. A hemispherically-shaped, stainless-steel head of approximately 12 mm diameter that contains five drilled holes of approximately 1.5 mm diameter was chosen for the design, shown in Fig. 6 . The four holes surrounding the central hole are oriented at a 45-degree angle to the probe axis. Except for the stainless-steel probe head, the probe is water cooled. The purpose of the uncooled stainless-steel probe head is to minimize deposition of oil and tar within the pressure measurement passages. The uncooled probe head was designed to function at temperatures sufficiently high to burn those particles that deposit on the head, thereby eliminating blockage in oil jets in the region between the flame front and the burner exit (Ref. 4). Nevertheless, the probe head was designed to limit the probe tip temperature to 1800 F. For the heat transfer calculations, the probe length immersed in the 3600 F flame was assumed to be 36 inches. Assuming a 120 F rise in cooling water temperature, a cooling water pressure drop of less than 30 psi was calculated for the concentric tube probe design of Fig. 6 , where water flows toward the tip through the inner tube and returns through the annulus. Figure 7 is a photograph of the velocity probe after fabrication.

SPECIES PROBE

A quick-quench probe concept was chosen for extraction of gases to be analyzed for stable species. The design, shown in Fig. 8 , features a channel design concept in which the basic element of the probe is an

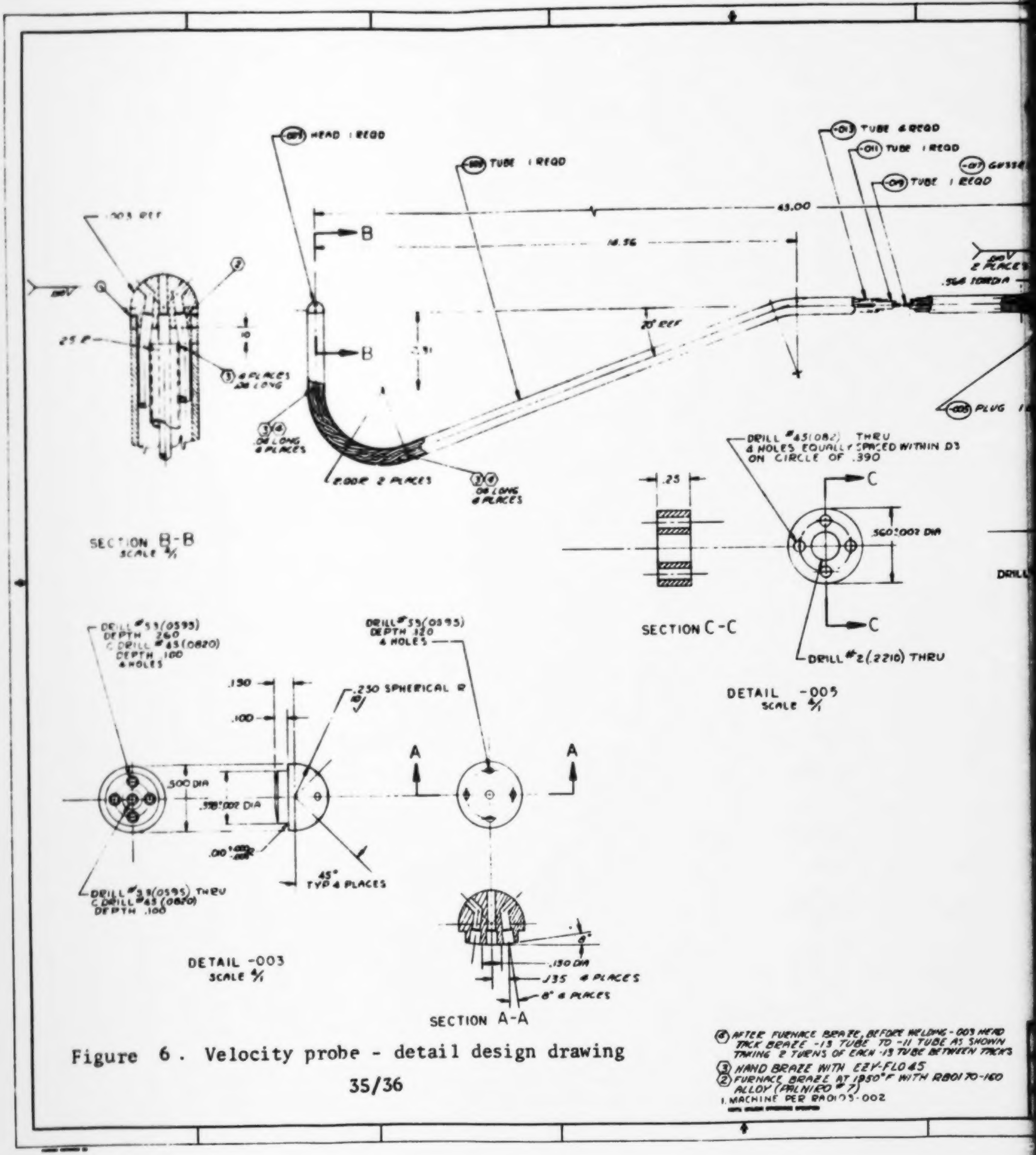
-003 HEAD 1 REQD
-009 TUBE 1 REQD
-013 TUBE 4 REQD
-011 TUBE 1 REQD
-017 GUSSE
-015 TUBE 1 REQD
.003 REF
43.00
16.56
20° REF
2.91
.564 TORDIA
2 PLACES
-005 PLUG
.25 R
4 PLACES .08 LONG
.08 LONG 4 PLACES
2.00R 2 PLACES
SECTION B-B SCALE 4/1
DRILL #43(.082) THRU 4 HOLES EQUALLY SPACED WITHIN .03 ON CIRCLE OF .390
.25
.560±.002 DIA
SECTION C-C
DRILL #2(.2210) THRU
DETAIL -005 SCALE 4/1
DRILL #53(.0595) DEPTH .260 C DRILL #43(.0820) DEPTH .100 4 HOLES
DRILL #53(.0595) DEPTH .120 4 HOLES
.150
.100
.250 SPHERICAL R
.500 DIA
.350±.002 DIA
.010
45° TYP 4 PLACES
DRILL #53(.0595) THRU C DRILL #43(.0820) DEPTH .100
DETAIL -003 SCALE 4/1
A
A
.130 DIA
.135 4 PLACES
8° 4 PLACES
SECTION A-A
④ AFTER FURNACE BRAZE, BEFORE WELDING -003 HEAD TACK BRAZE -13 TUBE TO -11 TUBE AS SHOWN TAKING 2 TURNS OF EACH -13 TUBE BETWEEN TACKS
③ HAND BRAZE WITH EZY-FLO 45
② FURNACE BRAZE AT 1950°F WITH RB0170-160 ALLOY (PALNIRO #7)
1. MACHINE PER RA0103-002

Figure 6. Velocity probe - detail design drawing

A

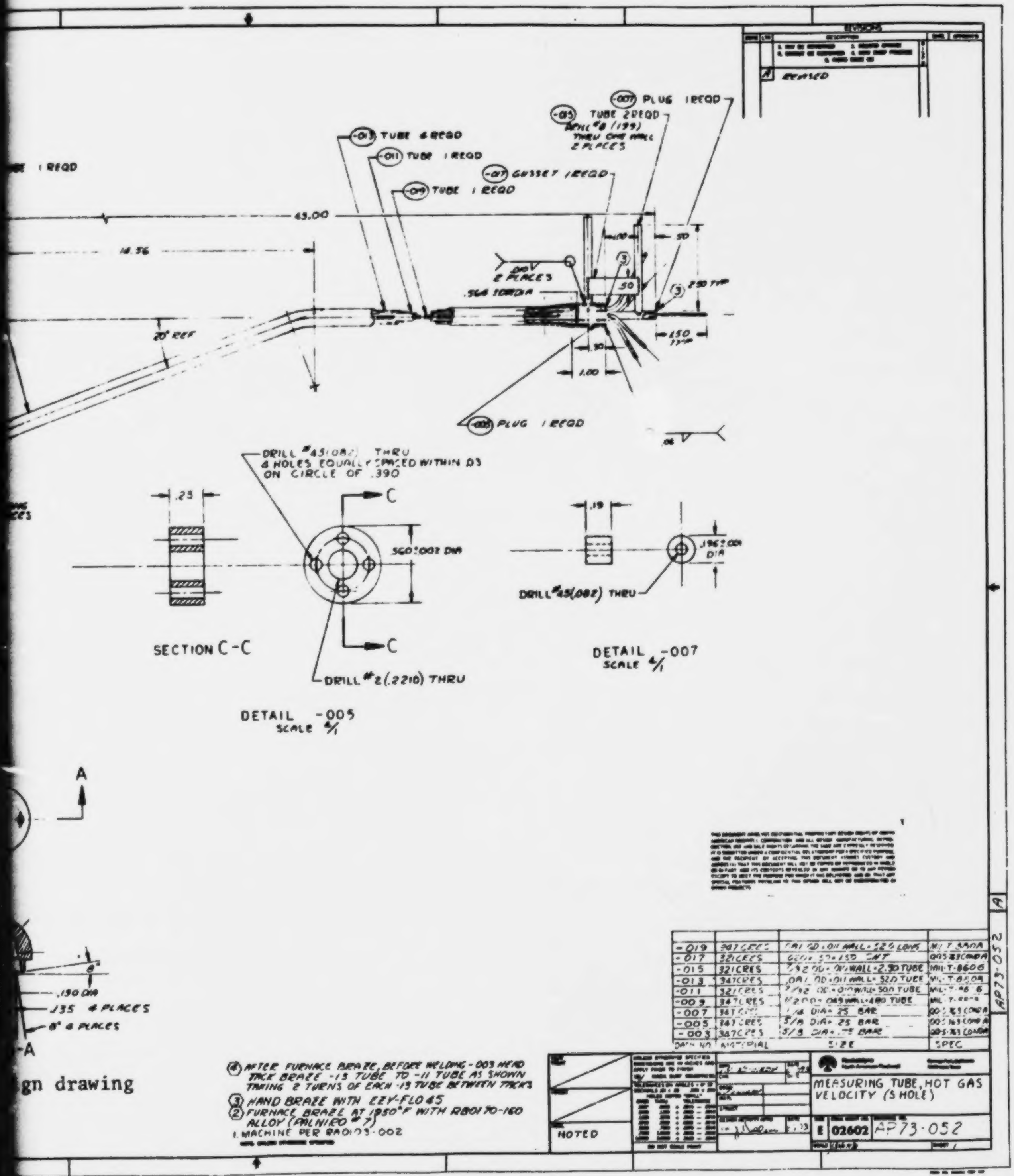
REVISIONS
A REVISED
-007 PLUG 1 REQD
-015 TUBE 2 REQD
DRILL #8 (.199) THRU ONE WALL 2 PLACES
-013 TUBE 6 REQD
-011 TUBE 1 REQD
-017 GUSSET 1 REQD
-019 TUBE 1 REQD
1 REQD
63.00
14.56
.010 2 PLACES
.564 ±.010 DIA
.50
.50
③
③
.250 TYP
.110
20° REF
.150 TYP
.90
1.00
-005 PLUG 1 REQD
.06
DRILL #45(.082) THRU
4 HOLES EQUALLY SPACED WITHIN .03
ON CIRCLE OF .390
.25
C
C
.560±.002 DIA
SECTION C-C
DRILL #2 (.2210) THRU
DETAIL -005
SCALE 4/1
.19
.196±.001 DIA
DRILL #45(.082) THRU
DETAIL -007
SCALE 4/1
A
8°
.130 DIA
.135 4 PLACES
8° 4 PLACES
-A
A
AP73-052

-019	347CRES	.041 OD × .011 WALL × 32.0 LONG	MIL-T-8808
-017	321CRES	.020 × .32 × .150 SHT	00533 COND A
-015	321CRES	7/32 OD × .010 WALL × 2.30 TUBE	MIL-T-8606
-013	347CRES	.041 OD × .011 WALL × 32.0 TUBE	MIL-T-8808
-011	321CRES	7/32 OD × .010 WALL × .500 TUBE	MIL-T-8606
-009	347CRES	1/2 OD × .049 WALL × .480 TUBE	MIL-T-8808
-007	347CRES	1/16 DIA × .25 BAR	00563 COND A
-005	347CRES	5/8 DIA × .25 BAR	00563 COND A
-003	347CRES	5/8 DIA × .75 BAR	00563 COND A
DASH NO	MATERIAL	SIZE	SPEC

④ AFTER FURNACE BRAZE, BEFORE WELDING -003 HEAD TACK BRAZE -13 TUBE TO -11 TUBE AS SHOWN TAKING 2 TURNS OF EACH -13 TUBE BETWEEN TACKS

③ HAND BRAZE WITH EZY-FLO 45

② FURNACE BRAZE AT 1950°F WITH RB0170-160 ALLOY (PALNIRO #7)

1. MACHINE PER RA0103-002

NOTED

MEASURING TUBE, HOT GAS VELOCITY (5 HOLE)

E 02602 AP73-052

SHEET 1

ign drawing

B

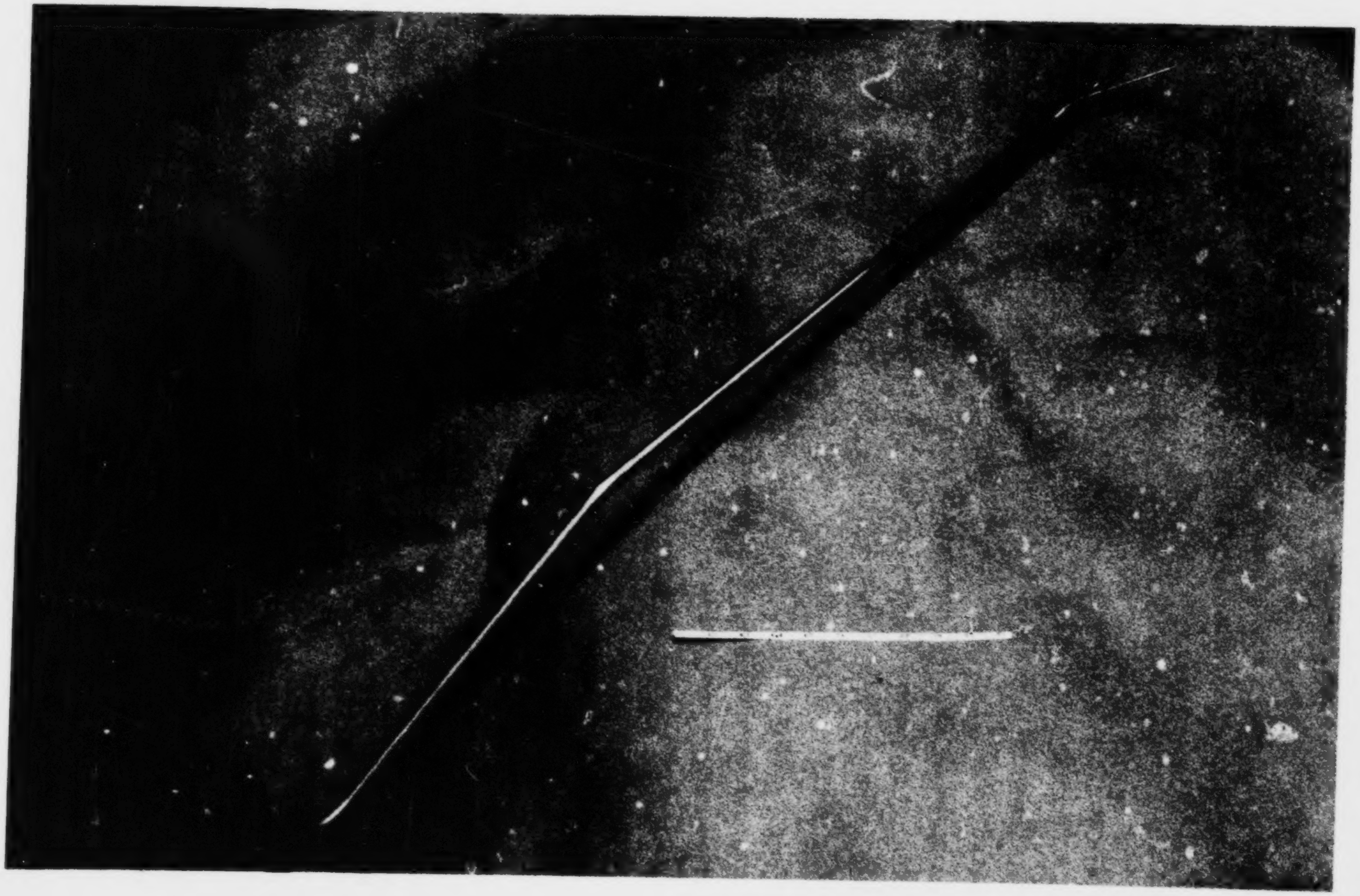

50A66/6/7/73-S1B

Figure 7. Five-hole pitot-type velocity probe

externally-splined tube. A cover is electroformed over the channels, and a second, larger, coaxial tube is used to provide an annular return passage for cooling water.

The channel construction of the species sampling probe design allows several different fluids (e.g., sample gas, quench gas, and probe coolant) to be transported to and from the probe tip without introducing the complicated fabrication requirements associated with multiple coaxial tubes. Also, by using thin walls between the channels, a relatively large proportion of the probe cross-sectional area is available for flow. The sample probe includes a venturi head (see Fig. 8), which has the potential capability of self-induced aspiration of cooled sample gas for quenching of the hot gas being withdrawn from the combustion environment. The venturi shape induces the aspiration by reducing the local static pressure at the probe tip.

The temperature at which the NO reaction is effectively nullified (quenched) was discussed with EPA and Dr. Heap. The quick quench of combustion gas from 3600 F to between 1110 to 1830 F (600 to 1000 C)* was believed to be sufficient to preclude further NO reaction. A quartz liner could be used to decrease surface reactions, but it was felt that these could also be minimized by rapid cooling with a metal wall, whereas the quartz would inhibit the cooling. The concensus was that sufficient cold recycle gas should be introduced at the upstream venturi throat so as to cool the sample gas to a temperature of at least 1830 F (1000 C).

Assuming a recycle gas temperature of 250 F, the species probe was calculated to require a cooled combustion gas recycle flowrate equal to 56-percent of the total mass flowrate of combustion gas (sample plus cooled

---

*The value of 1000 C (1832 F) assumes no carbon deposition on the inside probe walls. If carbon deposition is a problem, the quench temperature of 600 C (1112 F) is recommended.

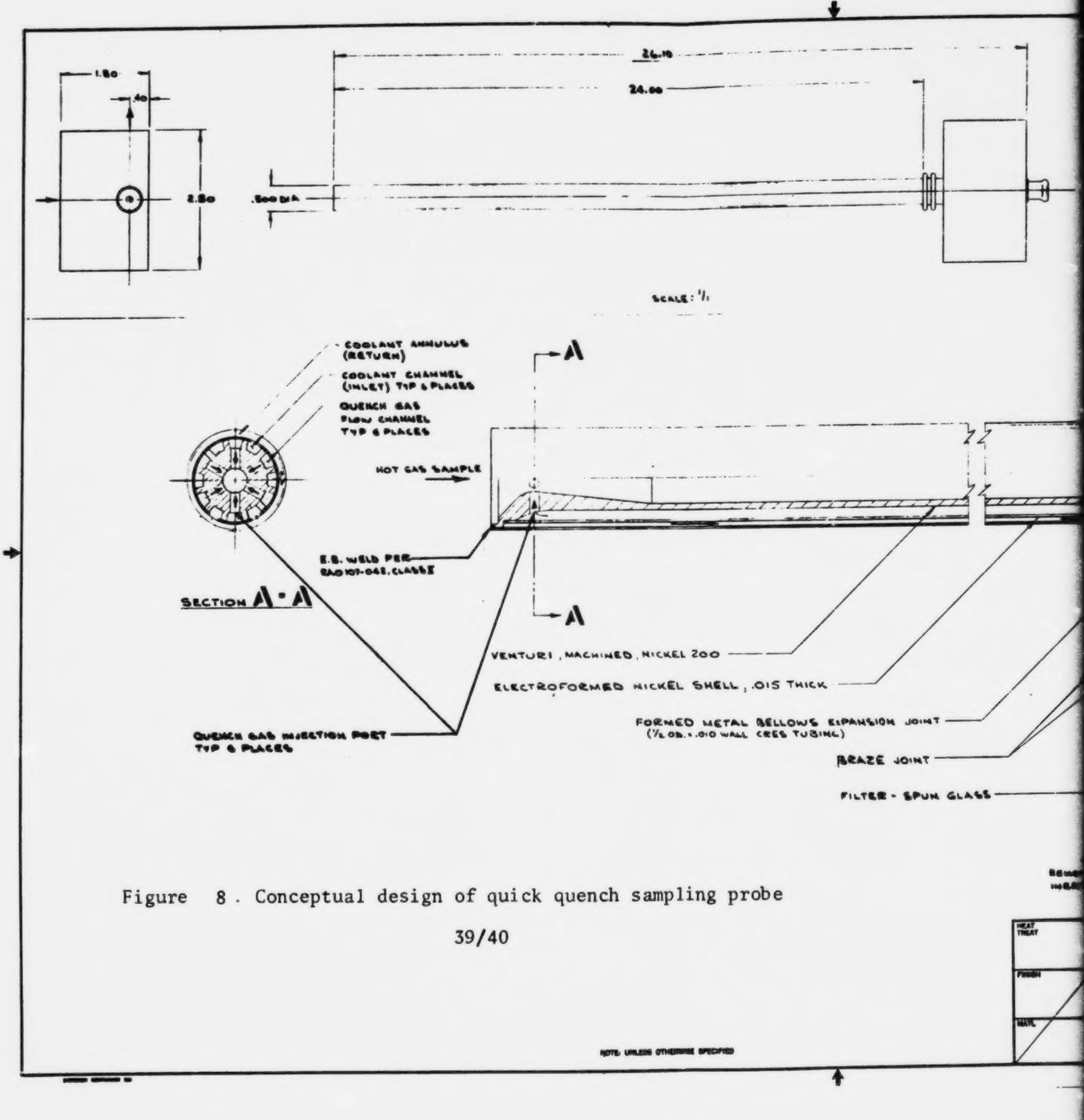
1.80
.40
2.80
.500 DIA
26.10
24.00
SCALE: 1/1
COOLANT ANNULUS (RETURN)
COOLANT CHANNEL (INLET) TYP 6 PLACES
QUENCH GAS FLOW CHANNEL TYP 6 PLACES
HOT GAS SAMPLE
A
A
E.B. WELD PER RAO107-042, CLASS I
SECTION A-A
VENTURI, MACHINED, NICKEL 200
ELECTROFORMED NICKEL SHELL, .015 THICK
FORMED METAL BELLOWS EXPANSION JOINT (1/2 OD. × .010 WALL CRES TUBING)
BRAZE JOINT
FILTER - SPUN GLASS
QUENCH GAS INJECTION PORT TYP 6 PLACES
HEAT TREAT
FINISH
MATL
NOTE: UNLESS OTHERWISE SPECIFIED

Figure 8. Conceptual design of quick quench sampling probe

A

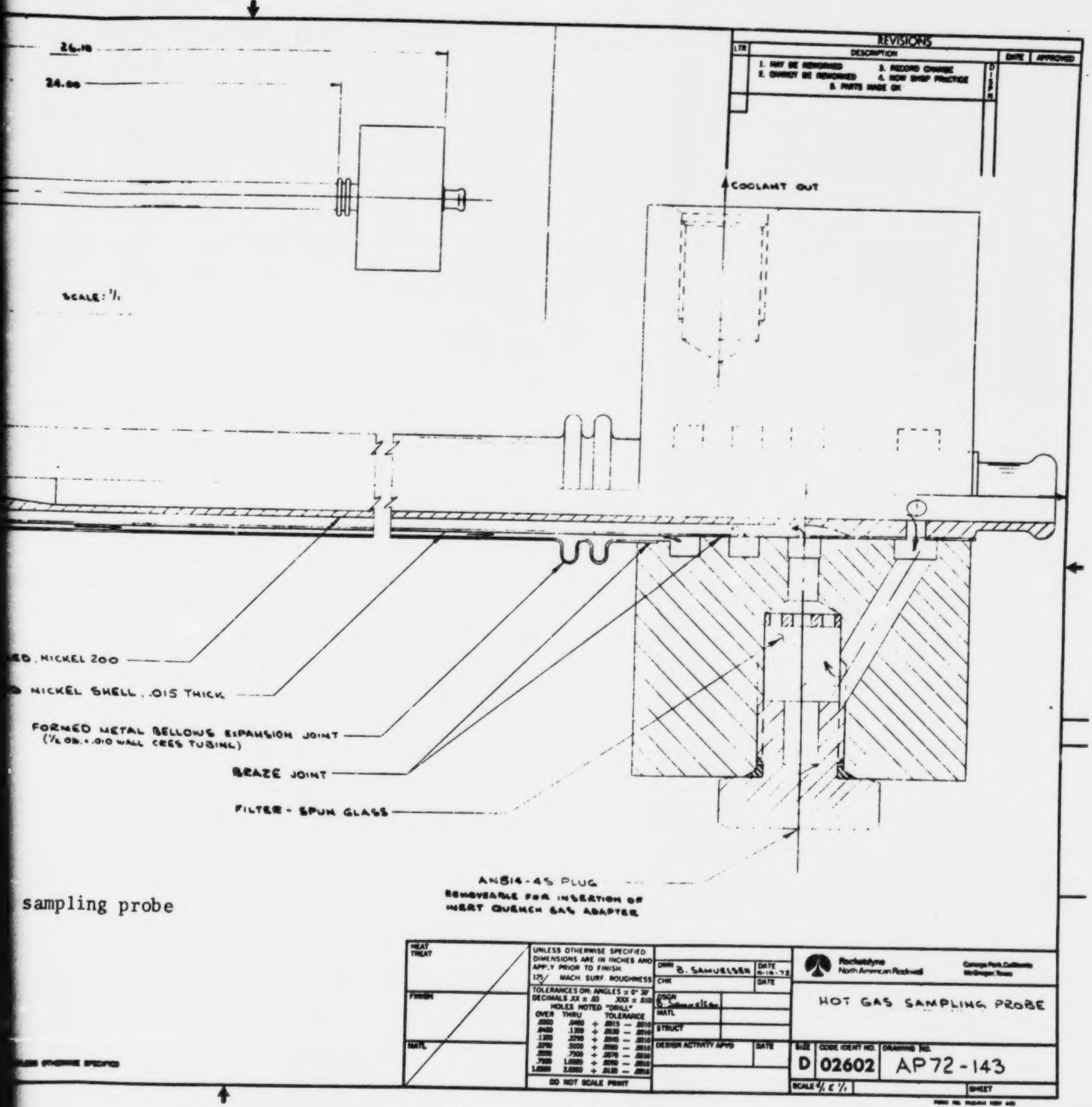
26.10
24.00
SCALE: 1/1
COOLANT OUT
ED, NICKEL 200
D NICKEL SHELL, .015 THICK
FORMED METAL BELLOWS EXPANSION JOINT
(1/2 OD. × .010 WALL CRES TUBING)
BRAZE JOINT
FILTER - SPUN GLASS
AN814-4S PLUG
REMOVEABLE FOR INSERTION OF
INERT QUENCH GAS ADAPTER
REVISIONS
LTR
DESCRIPTION
DATE
APPROVED
1. MAY BE REWORKED
2. CANNOT BE REWORKED
3. RECORD CHANGE
4. NOW SHOP PRACTICE
5. PARTS MADE OK
HEAT TREAT
FINISH
MATL
UNLESS OTHERWISE SPECIFIED
UNLESS OTHERWISE SPECIFIED DIMENSIONS ARE IN INCHES AND APPLY PRIOR TO FINISH.
125/ MACH. SURF. ROUGHNESS
TOLERANCES ON: ANGLES ± 0° 30'
DECIMALS XX ± .03 XXX ± .010
HOLES NOTED "DRILL"
OVER THRU TOLERANCE
DO NOT SCALE PRINT
DRWN B. SAMUELSEN
DATE 6-14-72
CHK
DATE
DSGN B. Samuelsen
MATL
STRUCT
DESIGN ACTIVITY APVD
DATE
Rocketdyne
North American Rockwell
Canoga Park, California
McGregor, Texas
HOT GAS SAMPLING PROBE
SIZE D
CODE IDENT NO. 02602
DRAWING NO. AP72-143
SCALE 1/1 & 1/1
SHEET

sampling probe

B

recycle for quench) to quick quench 3600 F sample (combustion) gas to a temperature of 1830 F. The use of such a recycle rate of cooled combustion gas will increase the response time of the probe by approximately 0.2 second. In spite of the relatively large amount of required recycle, and its adverse effect on response time, cooled combustion gas was chosen for quenching rather than an inert gas such as helium. The use of ambient temperature helium for quench purposes would require (for quenching to 1830 F) an amount equal to 66 percent of the resultant sample gas. This amount should serve to dilute the sample gas to such a degree that identification of trace amounts of certain species would be severely hampered. The use of cooled combustion gas having the same species concentration as the hot combustion gas does not result in such a dilution problem.

An evaluation of the species probe heat transfer indicated that the sample gas/quench gas (recycle) mixture can easily be cooled from 1830 F at the venturi throat to ~250 F at a position 3-feet downstream, thus ensuring adequate quenching of the sample gas with a minimum amount of cool gas recycle. An examination of the potential for heat transfer to the various streams (shown schematically below) indicated that heat

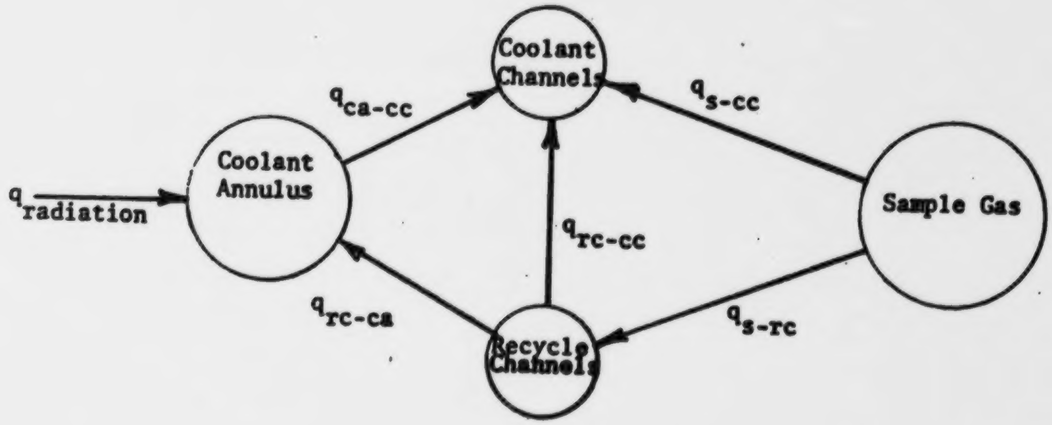

transfer between the sample combustion gas and the recycle gas streams (q_{s-rc}), as well as heat transfer between the coolant channels and the recycle channels (q_{rc-cc}), is small compared to heat transfer between other streams, and therefore, may be ignored. On the other hand, it was revealed that, because of heat transfer between the coolant in the annulus and the recycle gas stream, further substantial cooling of the recycle gas should be expected. The temperature of the recycle gas stream, before its injection at the venturi throat, was calculated to approach closely that of the coolant in the annulus. Therefore, water vapor should be removed from the recycled gas before it is reintroduced into the probe in order to avoid:

1. Condensation of water in the pump and possible damage to the pump
2. Excessive pressure drop in the recycle gas channel.

The ability of the quick-quench probe to self-aspirate the necessary amount of cooled combustion gas was not pursued. The presence of the venturi was believed to be of possible value in enhancing the mixing of the recycle gas with the hot sample gas and, therefore, the venturi throat was retained.

The preliminary probe design shown in Fig. 8 was reviewed with the EPA technical monitor and his consultant, Dr. M. Heap. Based on this review, the probe was redesigned. The overall probe OD of 0.56 inch was left unchanged but the convergent entrance of the probe was truncated from 0.5 inch (see Fig. 8) to 0.25 inch (followed by convergence to an 0.125-inch throat), a value commensurate with the probe inside diameter of 0.25 inch. The design of the gas and coolant channels was revised (from that indicated in Fig. 8) to achieve a minimum cooling water pressure drop. The resultant detail design drawing of the species probe is shown in Fig. 9 . A total cooling water pressure drop of about 25 psi and a recycle gas pressure drop of about 1 psi were estimated for this design.

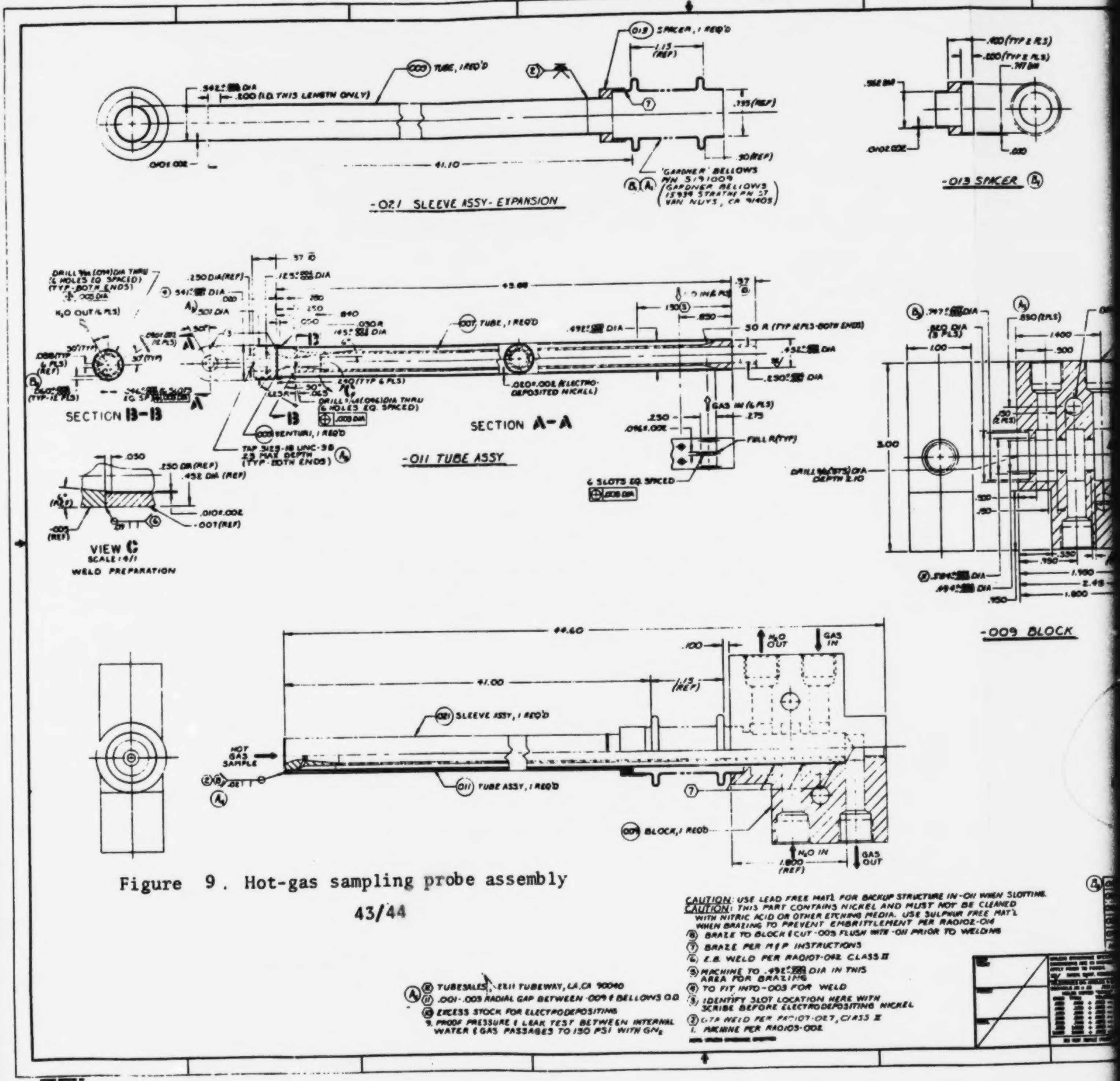
-021 SLEEVE ASSY- EXPANSION
-003 TUBE, 1 REQ'D
-013 SPACER, 1 REQ'D
1.15 (REF)
.200 (I.D. THIS LENGTH ONLY)
.795 (REF)
.50 (REF)
41.10
'GARDNER' BELLOWS P/N 5191009 (GARDNER BELLOWS 15939 STRATHERN ST. VAN NUYS, CA 91405)
-013 SPACER
-011 TUBE ASSY
SECTION A-A
SECTION B-B
-007 TUBE, 1 REQ'D
-003 VENTURI, 1 REQ'D
H₂O OUT (6 PLS)
GAS IN (6 PLS)
.020±.002 (ELECTRO-DEPOSITED NICKEL)
DRILL (6 HOLES EQ. SPACED)
TAP .5125-18 UNC-3B 2.2 MAX DEPTH (TYP - BOTH ENDS)
6 SLOTS EQ. SPACED
FULL R (TYP)
.50 R (TYP 12 PLS - BOTH ENDS)
43.68
VIEW C
SCALE 10/1
WELD PREPARATION
.250 DIA (REF)
.452 DIA (REF)
-007 (REF)
-009 BLOCK
3.00
44.60
41.00
1.15 (REF)
.100
H₂O OUT
GAS IN
HOT GAS SAMPLE
-021 SLEEVE ASSY, 1 REQ'D
-011 TUBE ASSY, 1 REQ'D
-009 BLOCK, 1 REQ'D
H₂O IN
GAS OUT
1.800 (REF)
CAUTION: USE LEAD FREE MAT'L FOR BACKUP STRUCTURE IN -011 WHEN SLOTTING.
CAUTION: THIS PART CONTAINS NICKEL AND MUST NOT BE CLEANED WITH NITRIC ACID OR OTHER ETCHING MEDIA. USE SULPHUR FREE MAT'L WHEN BRAZING TO PREVENT EMBRITTLEMENT PER RA0102-014
⑧ BRAZE TO BLOCK & CUT -003 FLUSH WITH -011 PRIOR TO WELDING
⑦ BRAZE PER M&P INSTRUCTIONS
⑥ E.B. WELD PER RA0107-002 CLASS II
⑤ MACHINE TO .492 DIA IN THIS AREA FOR BRAZING
④ TO FIT INTO -003 FOR WELD
③ IDENTIFY SLOT LOCATION HERE WITH SCRIBE BEFORE ELECTRODEPOSITING NICKEL
② G.T.A WELD PER RA0107-027, CLASS II
1. MACHINE PER RA0103-002
⑫ TUBESALES, 2211 TUBEWAY, LA, CA 90040
⑪ .001-.003 RADIAL GAP BETWEEN -009 & BELLOWS O.D.
⑩ EXCESS STOCK FOR ELECTRODEPOSITING
9. PROOF PRESSURE & LEAK TEST BETWEEN INTERNAL WATER & GAS PASSAGES TO 150 PSI WITH GN₂

Figure 9. Hot-gas sampling probe assembly

A

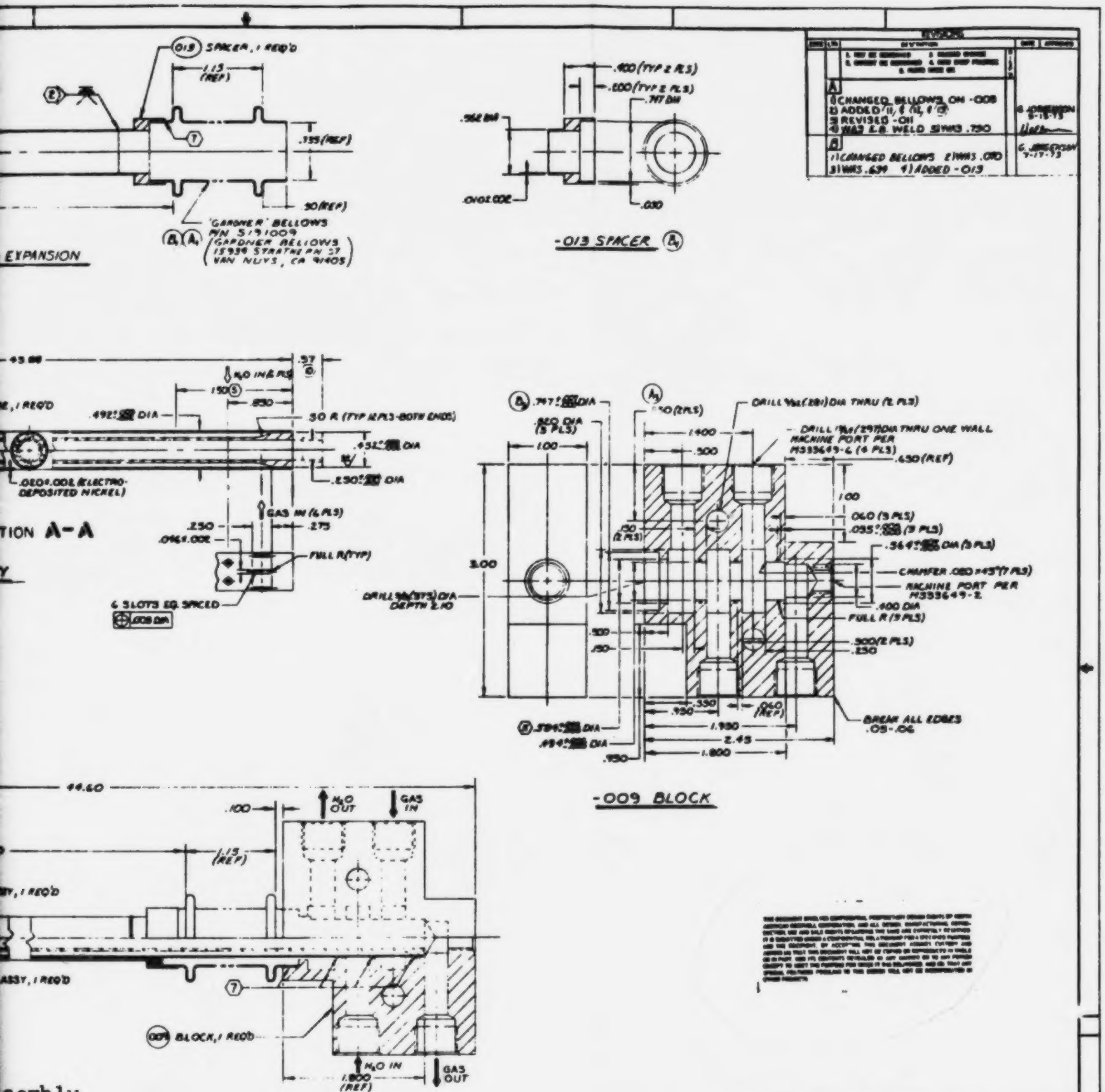
013 SPACER, 1 REQ'D
1.15 (REF)
2
7
.135 (REF)
.50 (REF)
'GARDNER' BELLOWS
P/N 5191009
(GARDNER BELLOWS 15939 STRATHE RN 37 VAN NUYS, CA 91405)
B1 A1
EXPANSION
.400 (TYP 2 PLS)
.200 (TYP 2 PLS)
.747 DIA
.562 DIA
.010±.002
.030
-013 SPACER B4
43.88
.37
H2O IN (6 PLS)
150 5
.850
.492 DIA
.50 R (TYP 12 PLS-BOTH ENDS)
.432 DIA
.230 DIA
.020±.002 (ELECTRO-DEPOSITED NICKEL)
TION A-A
GAS IN (6 PLS)
.250
.275
.096±.002
FULL R (TYP)
6 SLOTS EQ. SPACED
.005 DIA
B4 .747 DIA
A1
.820 DIA (3 PLS)
1.00
.150 (2 PLS)
1.400
.300
DRILL 9/32 (.281) DIA THRU (2 PLS)
DRILL 19/64 (.297) DIA THRU ONE WALL
MACHINE PORT PER MS33649-6 (4 PLS)
.630 (REF)
1.00
.060 (3 PLS)
.035 (3 PLS)
.564 DIA (3 PLS)
3.00
CHAMFER .020×45° (7 PLS)
MACHINE PORT PER MS33649-2
.400 DIA
FULL R (3 PLS)
DRILL 3/8 (.375) DIA DEPTH 2.10
.500
.150
.300 (2 PLS)
.250
.350
.950
.060 (REF)
1.930
2.45
1.800
BREAK ALL EDGES .05-.06
8 .594 DIA
.494 DIA
.950
-009 BLOCK
44.60
.100
H2O OUT
GAS IN
1.15 (REF)
Y, 1 REQ'D
ASSY, 1 REQ'D
7
009 BLOCK, 1 REQ'D
H2O IN
1.800 (REF)
GAS OUT

sembly

CAUTION: USE LEAD FREE MAT'L FOR BACKUP STRUCTURE IN -011 WHEN SLOTTING.
CAUTION: THIS PART CONTAINS NICKEL AND MUST NOT BE CLEANED WITH NITRIC ACID OR OTHER ETCHING MEDIA. USE SULPHUR FREE MAT'L WHEN BRAZING TO PREVENT EMBRITTLEMENT PER RA0102-014

⑧ BRAZE TO BLOCK & CUT -005 FLUSH WITH -011 PRIOR TO WELDING
⑦ BRAZE PER M&P INSTRUCTIONS
⑥ E.B. WELD PER RA0107-042 CLASS II
⑤ MACHINE TO .492 DIA IN THIS AREA FOR BRAZING
④ TO FIT INTO -003 FOR WELD
⑤ IDENTIFY SLOT LOCATION HERE WITH SCRIBE BEFORE ELECTRODEPOSITING NICKEL
② GTA WELD PER RA0107-027, CLASS II
1. MACHINE PER RA0103-002

…1 TUBEWAY, LA, CA 90040
…L GAP BETWEEN -009 & BELLOWS O.D
…OR ELECTRODEPOSITING
…& LEAK TEST BETWEEN INTERNAL
…SSAGES TO 150 PSI WITH GN2

A 1) CHANGED BELLOWS ON -008 2) ADDED ⑪, & ⑫, & ⑬ 3) REVISED -011 4) WAS E.B. WELD SYMS .750	G. JORGENSON 5-15-73
B 1) CHANGED BELLOWS 2) WAS .030 3) WAS .639 4) ADDED -013	G. JORGENSON 7-17-73

NO	MAT'L	SIZE	SPEC
013 (B4)	NICKEL 200	.88 DIA × 1.25	
009	347 CRES	1.10 × 3.10 × 2.55	
007	NICKEL 200	1.00 DIA × 44.00	
005	NICKEL 200	1.00 DIA × 1.50	
003	321 CRES	1/4 O.D. TUBE × .010 WALL × 48.00	12

G. JORGENSON

HOT-GAS SAMPLING
PROBE ASSEMBLY

E 02602 AP73-067

2/1

B

Fabrication

Initially, an attempt was made to fabricate the tubular nickel body of the species probe by gun-drilling a nickel bar. However, an x-ray examination of the bar revealed an irreparable nonconcentricity of the center (gun-drilled) hole. Consequently, another fabrication technique was adopted. This time the nickel probe body was built up by electroforming over a tubular aluminum base. Upon completion of the electroforming process, examination of the completed probe body indicated uniform nickel deposition. However, some slight curvature of the tube was caused by the build-up weight of the long tube, which was supported only at the ends while in the electroforming solution. The tube was straightened successfully and the aluminum mandrel was etched out to obtain a thick-walled nickel tube. The external, axial channels were machined into the tubular nickel probe body and, with these channels temporarily filled with wax, the outer expansion sleeve was electroformed onto its outer diameter. After brazing of the manifold block to the probe body, a leak check of the assembly revealed leaks between the coolant and gas recycle inlet and exit passages. A second (repair) braze cycle was then attempted but subsequently halted when indications were found that some coolant passages were plugged. The block was then machined from the probe and replaced by a modified configuration (see Fig. 10), which allowed sequential assembly with hand brazing in order to achieve a leak-free assembly. This approach was successful. A photograph of the completed species probe is shown in Fig. 11.

TEMPERATURE PROBE

The conceptual design for a pneumatic venturi pyrometer was based on results from both the literature evaluation and a heat transfer analysis. This design is shown in Fig. 12 . To eliminate or minimize the reported effect of the external flowfield on the temperature measurement (Ref. 11), the upstream "hot" venturi pressure taps were positioned in the convergent section of this venturi as was done by the BCURA investigators (Ref. 8 and 9). Additionally, a piezometer ring with six taps was also employed

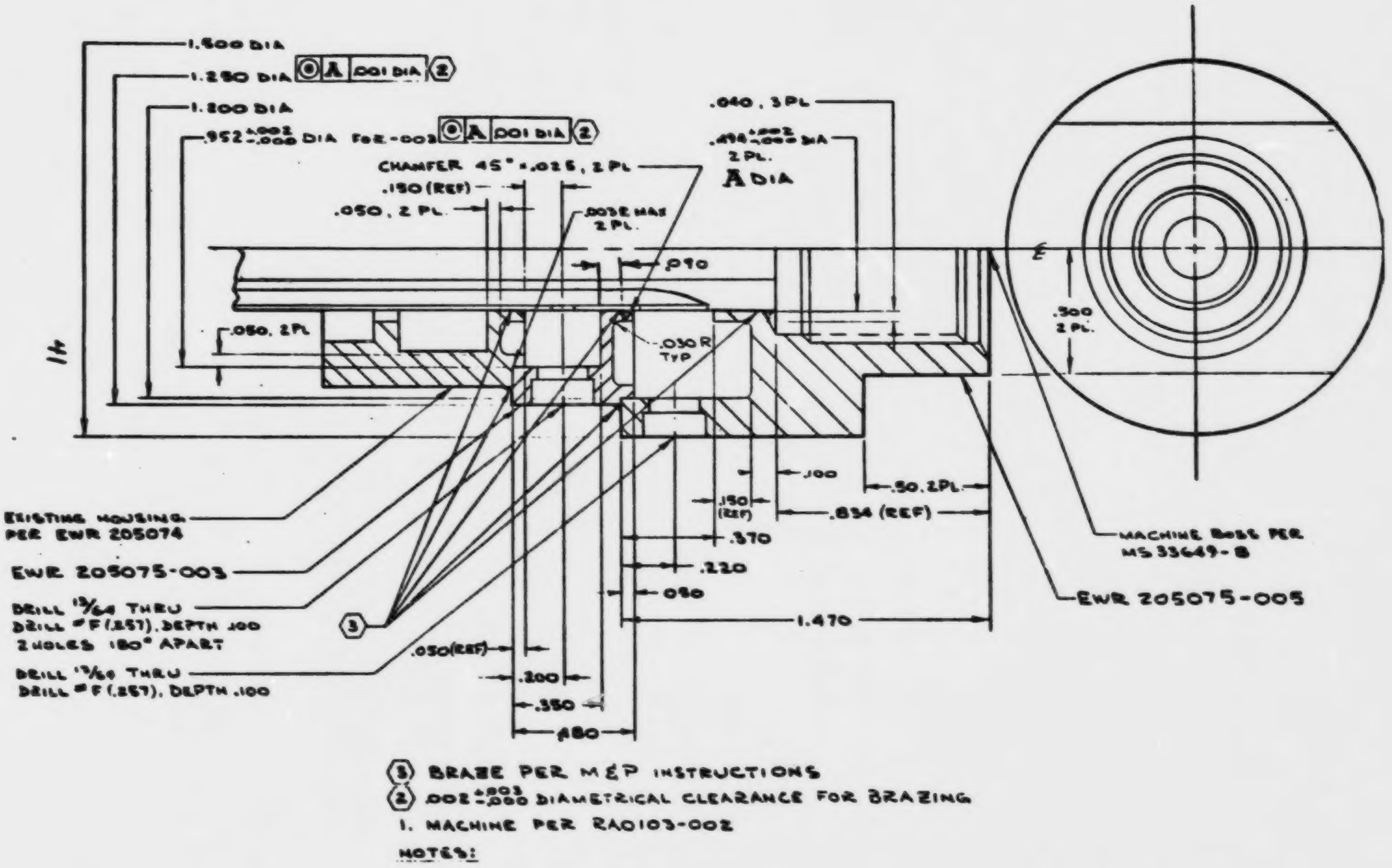
1.500 DIA
1.250 DIA ◎ A .001 DIA ②
1.200 DIA
.952 +.002 -.000 DIA FOR -003 ◎ A .001 DIA ②
CHAMFER 45° × .025, 2 PL
.150 (REF)
.050, 2 PL.
.003E MAX 2 PL.
.040, 3 PL
.494 +.002 -.000 DIA 2 PL.
A DIA
.090
.030 R TYP
.050, 2 PL
.300 2 PL.
℄
.100
.50, 2PL.
.150 (REF)
.834 (REF)
.370
.220
.090
1.470
.050 (REF)
.200
.350
.480
EXISTING HOUSING PER EWR 205074
EWR 205075-003
DRILL 13/64 THRU
DRILL #F (.257), DEPTH .100
2 HOLES 180° APART
DRILL 13/64 THRU
DRILL #F (.257), DEPTH .100
③
MACHINE BOSS PER MS 33649-8
EWR 205075-005
③ BRAZE PER M&P INSTRUCTIONS
② .002 +.003 -.000 DIAMETRICAL CLEARANCE FOR BRAZING
1. MACHINE PER RA0103-002
NOTES:

Figure 10. Rework of hot-gas sampling probe

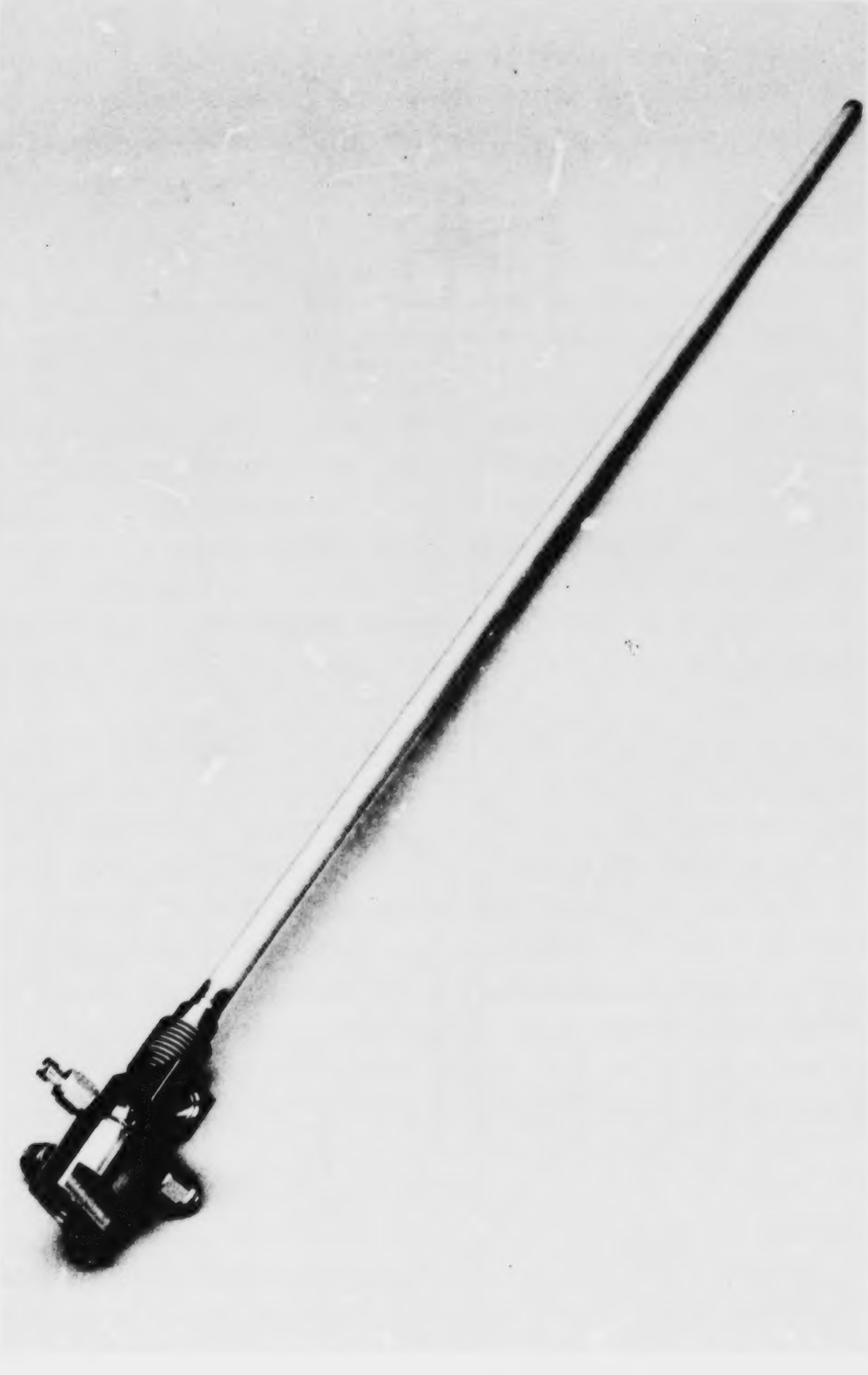

5AD43-8/14/73-C1*

Figure 11. Quick quench species probe

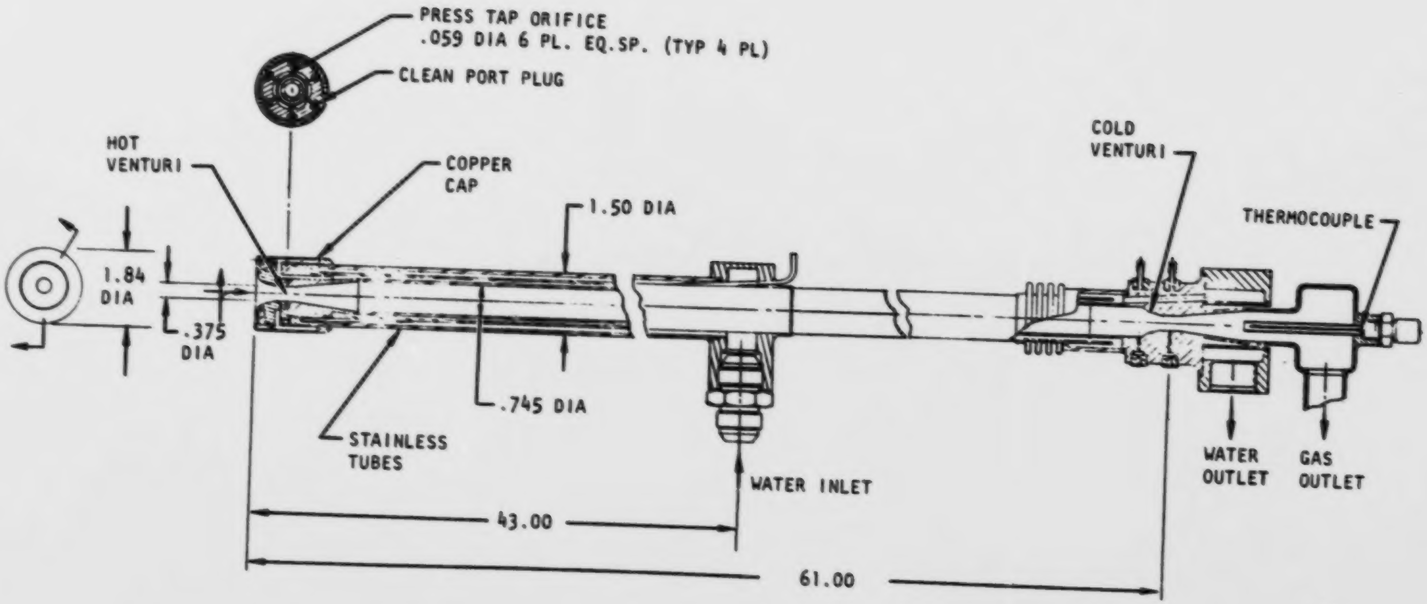
PRESS TAP ORIFICE
.059 DIA 6 PL. EQ.SP. (TYP 4 PL)
CLEAN PORT PLUG
HOT VENTURI
COPPER CAP
1.50 DIA
COLD VENTURI
THERMOCOUPLE
1.84 DIA
.375 DIA
.745 DIA
STAINLESS TUBES
WATER INLET
WATER OUTLET
GAS OUTLET
43.00
61.00

Figure 12 . Pneumatic venturi pyrometer - initial conceptual layout drawing to eliminate sensitivity to external-flow direction (Ref. 8 and 9). Provisions were made to allow ready access to the individual taps for physically cleaning or unplugging the pressure taps, through use of a copper cap (see Fig. 12).

A venturi diameter of 3/8-inch was selected. This size is intermediate between the 1/2-inch size "successfully" used in BCURA work (Ref. 8 and 9) and the approximately 1/4-inch size used without much success at IFRF, IJmuiden (Ref. 11). The probe shown in Fig. 12 was designed for insertion perpendicular to the main flow and in this respect is similar to the BCURA probe and unlike the 1/4-inch diameter venturi probe used by Pengally at IFRF, IJmuiden. A cooling length requirement of 60 inches between the hot and cold venturi tubes was calculated for cooling the combustion gases from 3600 to 500 F in the 3/4-inch inside diameter section over a reasonable range of suction velocities. A maximum insertion length of 36 inches in the 3600 F flame was assumed for design purposes.

The design of this venturi pyrometer in Fig. 12 was reviewed with the EPA technical monitor and his consultant, Dr. M. Heap. The design was generally satisfactory, but the 1.84-inch OD was considered too large to permit accurate resolution of local temperature differences within a flame combustion flowfield. Therefore, this design was revised to reduce the OD of the probe to a maximum value of 1.0-inch while maintaining a minimum venturi diameter of 0.20 inch and retaining the design features shown in Fig. 12 . Both a splined-channel design (instead of concentric tubes) and a higher temperature cold venturi were considered as methods of reducing the OD while maintaining a reasonable cooling water pressure drop.

An extensive analysis of the heat transfer and cooling water pressure drop in the venturi pyrometer as functions of OD, ID, gas flowrate, water flowrate, probe length, and water flow area indicated that construction of a venturi pyrometer with a venturi throat diameter of 0.25-inch and an OD of 1 inch or less was feasible. However, the use of a splined-channel fabrication design was expected to allow only about a 10-percent reduction in probe OD for equal water ΔP, so the concentric tube design concept was retained.

A detail design drawing of the selected configuration for the venturi pyrometer is shown in Fig. 13 . This design features a 1.0-inch OD by 0.50-inch ID probe with 0.25-inch diameter venturi throat. Assuming suction velocities of sample gas through the probe of 50 and 150 fps, and a cold (downstream) venturi temperature of 500 F, the following coolant water flowrate, length between upstream and downstream venturi tubes, and total coolant pressure drop were calculated:

Suction velocity (fps)	50	150
Coolant water flowrate (gph)	167	171
Length between venturi tubes (inch) for 500 F cold venturi temperature	37	46
Total coolant ΔP (psi)	2	2

These results indicate the design length of 42 inches is adequate for cooling the gas sample to a temperature of approximately 500 F before it enters the downstream venturi. Although the predicted coolant pressure drop is low enough to permit further size reductions, the outside probe diameter could not be further reduced because of the spatial requirements of the pressure tap passages. Six pressure taps were used in the convergent section upstream of the hot venturi. Three pressure taps were used in the hot venturi throat and two taps each at the upstream and throat locations of the cold venturi. The hot venturi head of the probe was made of nickel to aid cooling while the remainder of the probe was made of stainless steel.

In order to reduce the probe OD from the 1.84 inches shown in Fig. 12 to the 1.0 inch shown in Fig. 13, the ability to easily clean the hot

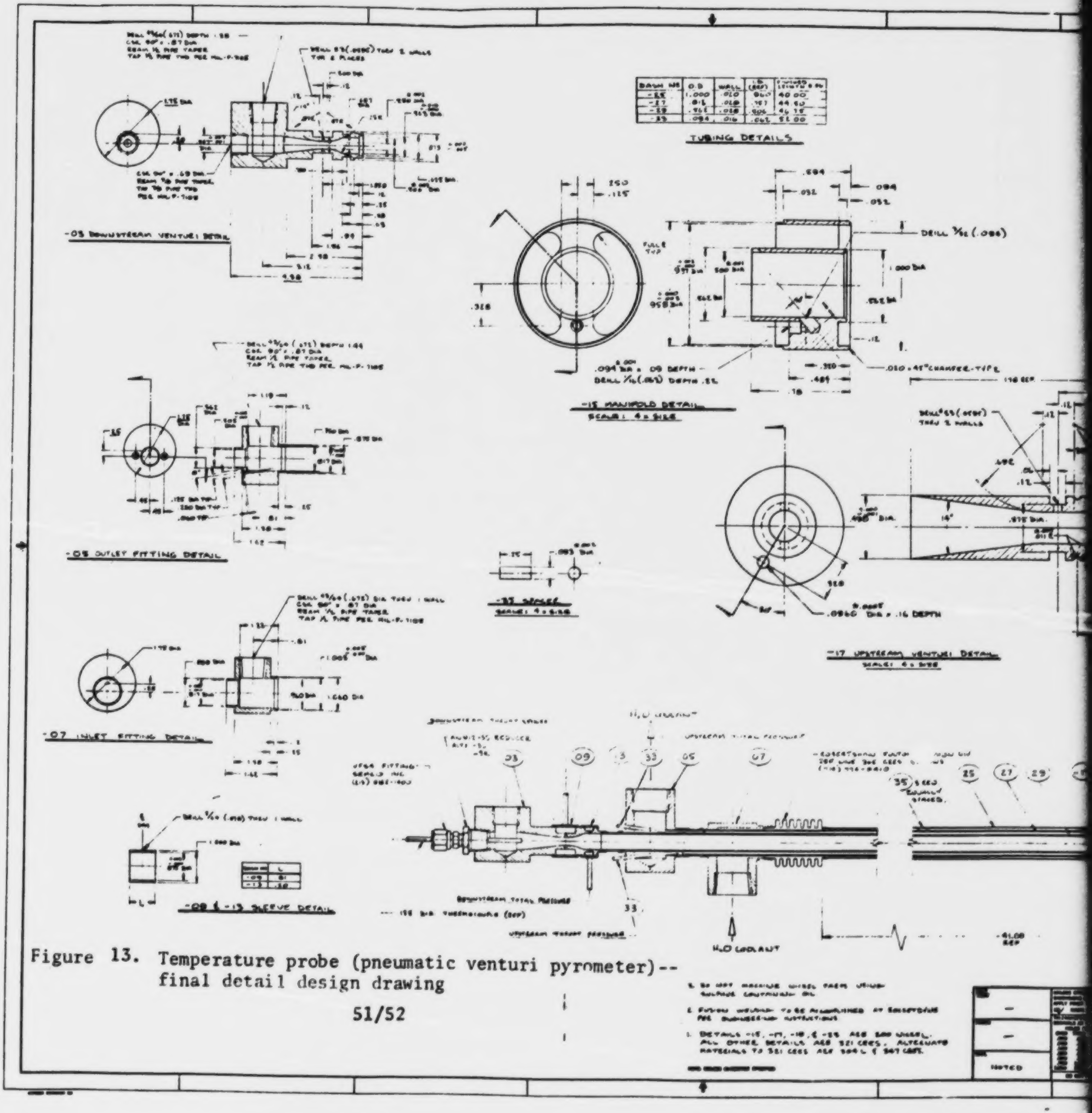
-03 DOWNSTREAM VENTURI DETAIL
TUBING DETAILS
DASH NO. | O.D. | WALL | I.D. (REF) | FINISHED LENGTH
-25 | 1.000 | .020 | .960 | 40.00
-27 | .81 | .020 | .787 | 44.50
-29 | .561 | .018 | .606 | 46.15
-33 | .094 | .016 | .062 | 52.00
DRILL 3/32 (.094)
1.000 DIA
.030 x 45° CHAMFER-TYP 2
-15 MANIFOLD DETAIL
SCALE: 4 x SIZE
-05 OUTLET FITTING DETAIL
-33 SPACER
SCALE: 4 x SIZE
.0960 DIA x .16 DEPTH
-17 UPSTREAM VENTURI DETAIL
SCALE: 4 x SIZE
-07 INLET FITTING DETAIL
DOWNSTREAM THROAT PRESSURE
H2O COOLANT
UPSTREAM TOTAL PRESSURE
03
09
13
33
05
07
35
25
27
29
DOWNSTREAM TOTAL PRESSURE
UPSTREAM THROAT PRESSURE
H2O COOLANT
-09 & -13 SLEEVE DETAIL
NOTED

Figure 13. Temperature probe (pneumatic venturi pyrometer)--final detail design drawing

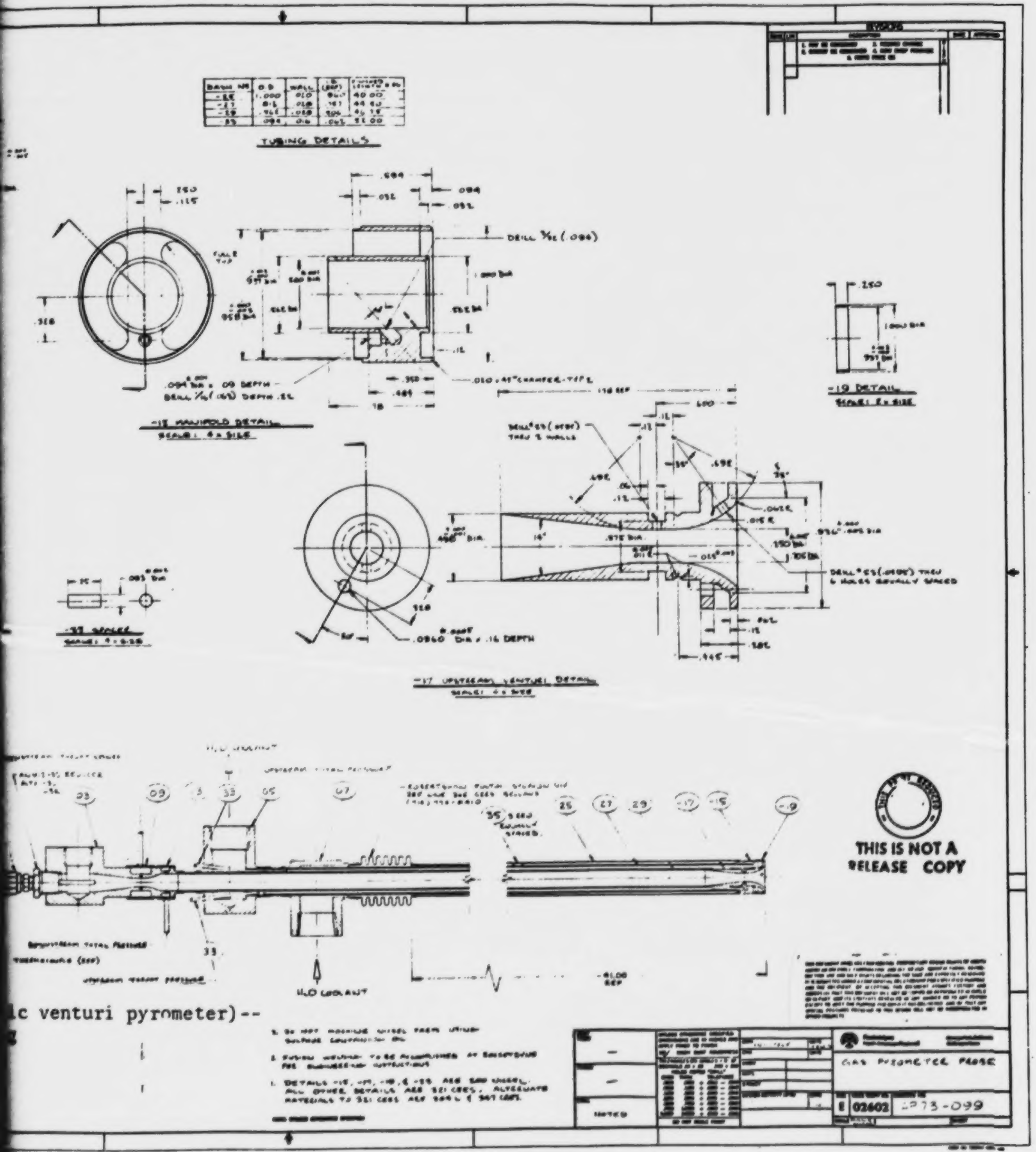
TUBING DETAILS
-13 MANIFOLD DETAIL
SCALE: 4 x SIZE
DRILL 3/32 (.094)
.010 x 45° CHAMFER-TYP 2
-19 DETAIL
SCALE: 2 x SIZE
-37 SPACER
-17 UPSTREAM VENTURI DETAIL
SCALE: 4 x SIZE
.0960 DIA x .16 DEPTH
H2O COOLANT
UPSTREAM TOTAL PRESSURE
DOWNSTREAM TOTAL PRESSURE
THERMOCOUPLE (REF)
23
09
33
05
07
35
25
27
29
-17
-15
-19
41.00 REF
THIS IS NOT A RELEASE COPY
GAS PYROMETER PROBE
E 02602 2P73-099
NOTED

lc venturi pyrometer)--
g

3

venturi pressure taps was sacrificed to some degree. The original conceptual design (Fig. 12) included a copper cap for the probe head that could be removed to permit insertion of a drill in the hot venturi pressure taps from the outside. The final design, Fig. 13 , included only the option of incorporating small setscrews on the outside probe diameter. These setscrews could be removed to allow insertion of a drill in the venturi taps. However, a special tool would be needed to clean the venturi taps from the inside of the probe. Photographs of the completed temperature probe are shown in Fig. 14 and 15.

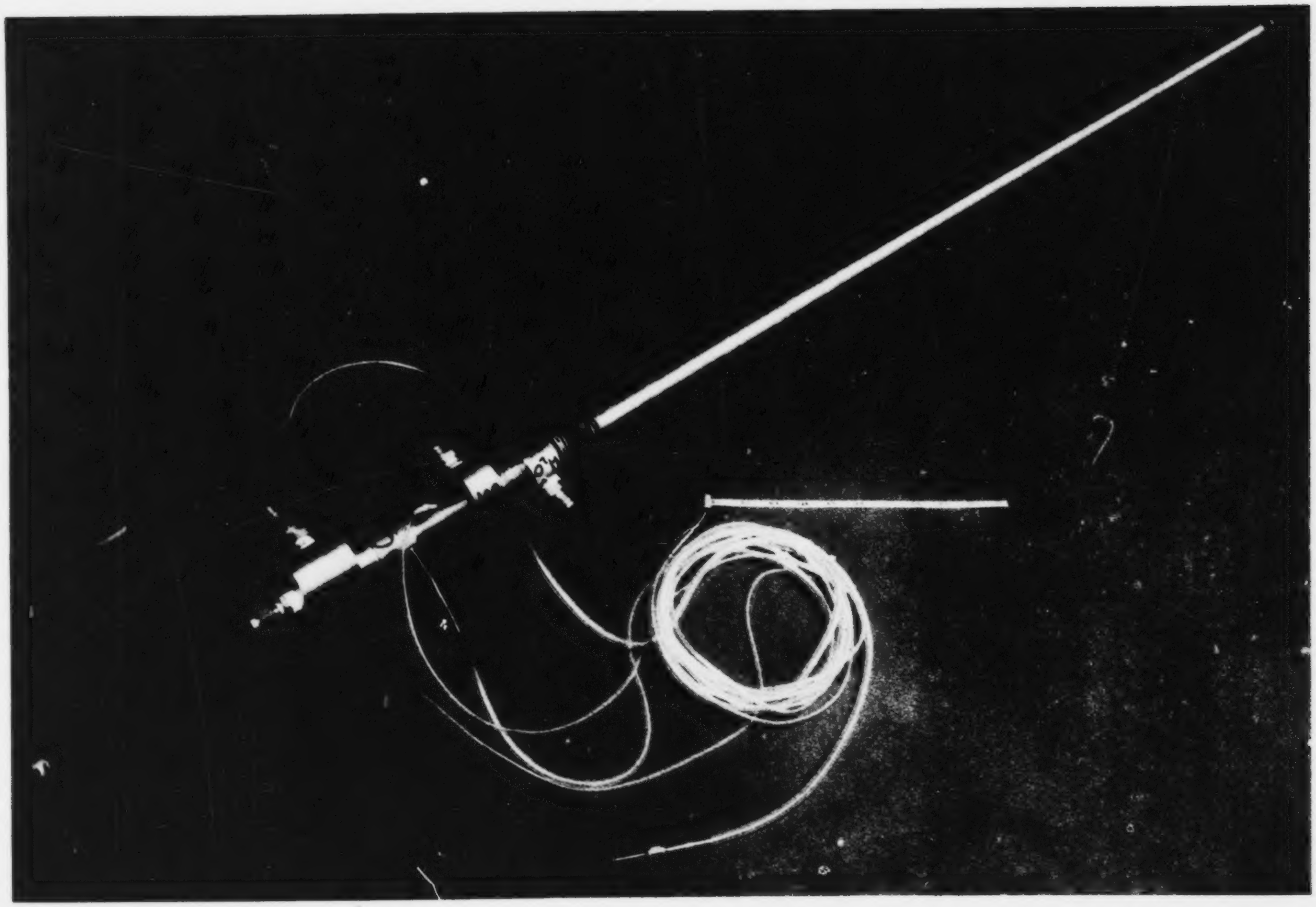

50A66-6/13/73-S1A

Figure 14 . Pneumatic venturi temperature probe

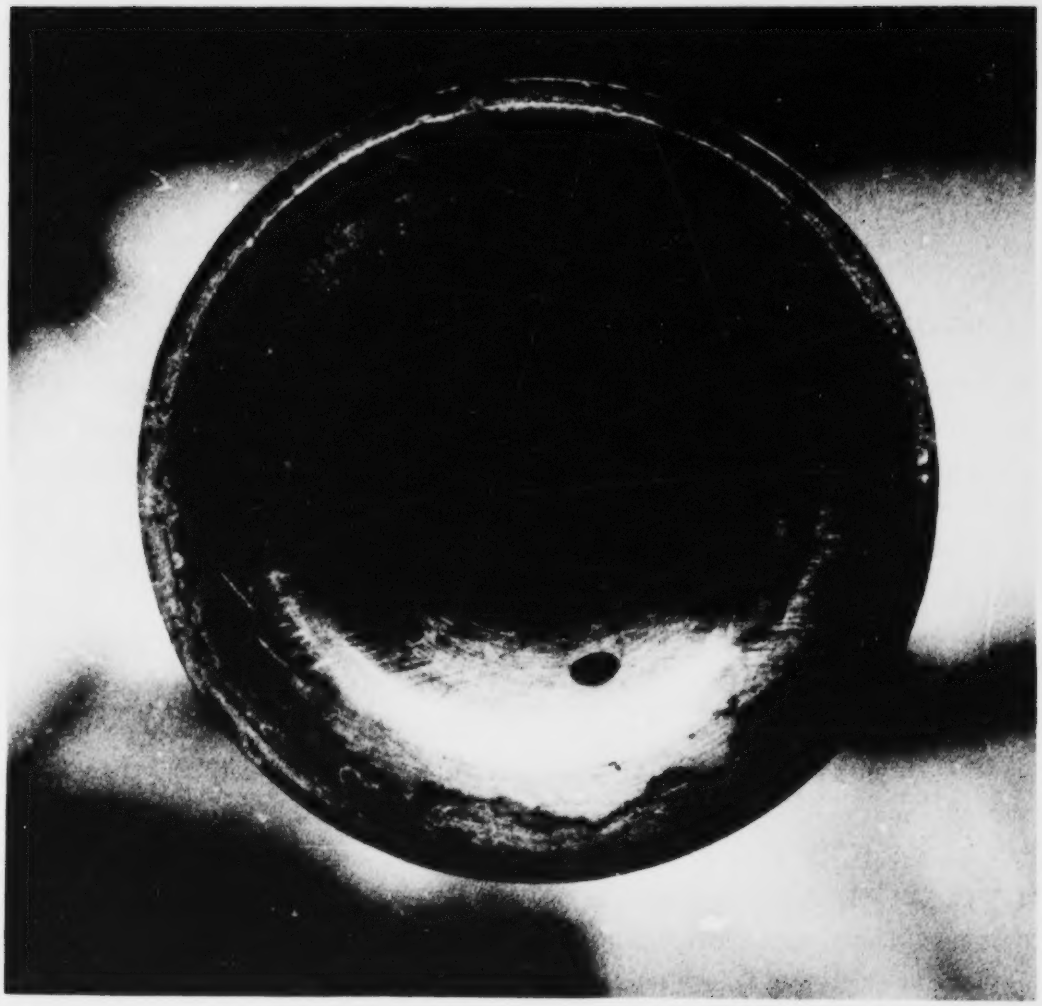

50A66-6/13/73-S1B

Figure 15. Temperature probe - end view of upstream venturi

VELOCITY PROBE CALIBRATION

CALIBRATION MEASUREMENTS

A 5-hole pitot probe can be used to determine both the magnitude and direction of the velocity from measurement of three differential pressures, once the probe is properly calibrated. Typical calibration curves are in Ref. 4 and Fig. 16 .

The newly-fabricated velocity probe shown in Fig. 6 was calibrated using a system consisting of a rotatable lathe table, on which the probe could be mounted, and a 2-in. diameter steel tube through which a regulated supply of gaseous nitrogen was flowed (Fig. 16). The probe was mounted on the lathe table so that both pitch (β) and yaw (α) angles could be varied separately (Fig. 17). Calibrations were done at a GN_2 flow velocity of about 100 ft/sec. The location of the probe tip was varied between 0.5 and 3.0 inch above the exit of the 2-in. diameter tube. Horizontal traverses were made with the probe to ascertain that the measurements were made in a region with a flat velocity profile.

Employing the notation shown in Fig. 18 , variations in the pressure differences P_4-P_2, P_o-P_2, P_3-P_1, P_o-P_1, and P_o-P_3 were measured (in addition to P_o-$P_{ambient}$) with probe rotation in either the pitch or yaw directions. These data were plotted as delta pressure ratios, as shown in Fig. 19, for comparison with typical calibration data obtained at the IFRF (Ref. 4).

The calibration data exhibited very good agreement between corresponding delta pressure ratios, $(P_4-P_2)/(P_o-P_1)$ and $(P_1-P_3)/(P_o-P_2)$, when the respective pitch or yaw angle was varied an equal amount, confirming symmetry of the probe tip.

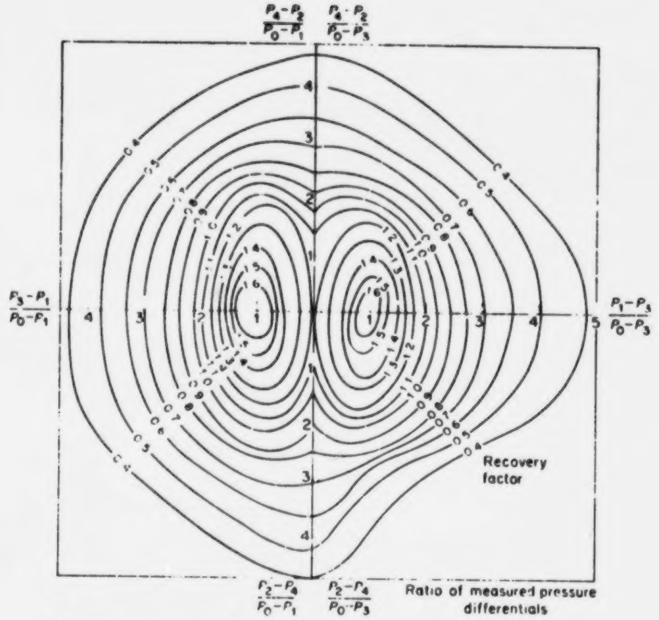

Five-hole probe; measurement of angles

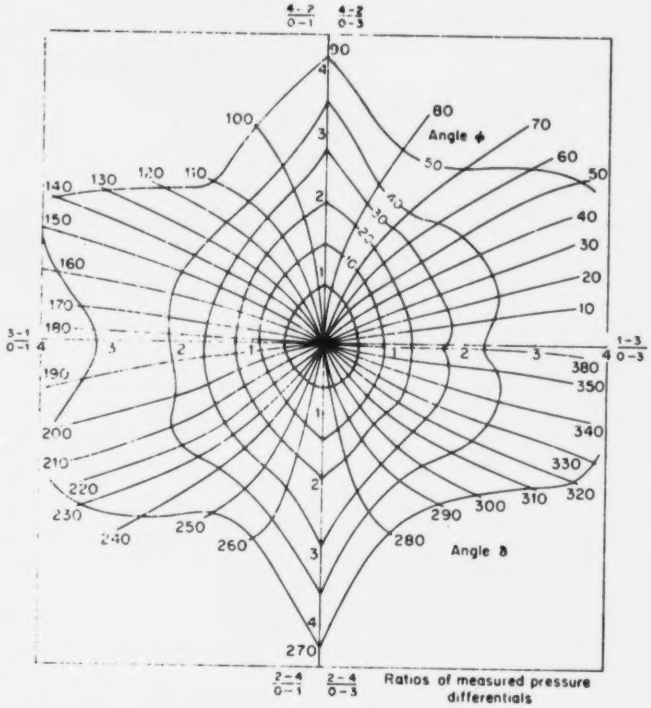

Five-hole probe; measurement of velocity magnitude

Figure 16. Typical velocity calibration curves (Ref. 4)

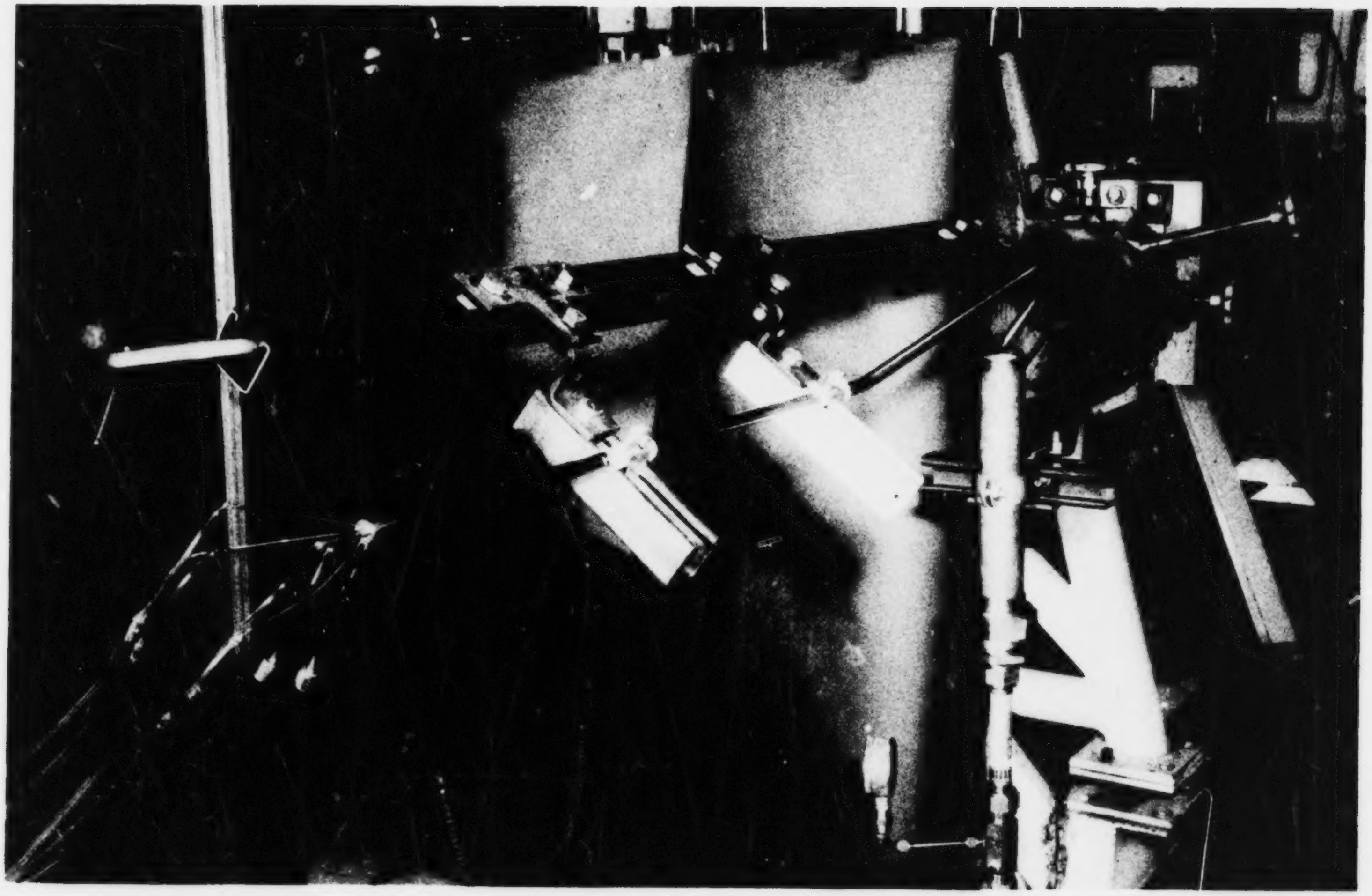

5AH21-7/6/73-S1

Figure 17. Velocity probe calibration rig

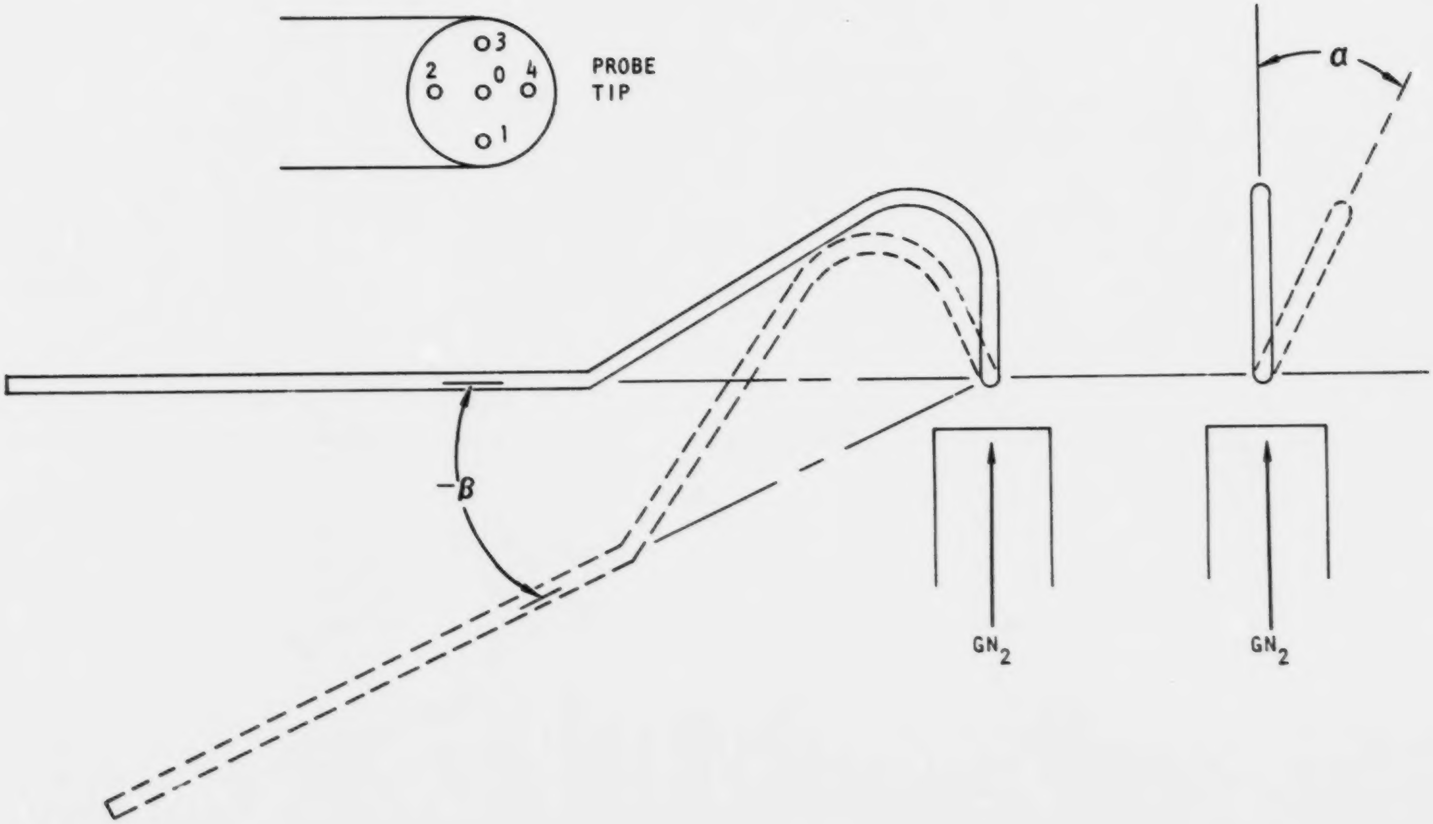
3
2
0
4
1
PROBE TIP
α
$-\beta$
GN_2
GN_2

Figure 18. Velocity probe calibration orientation

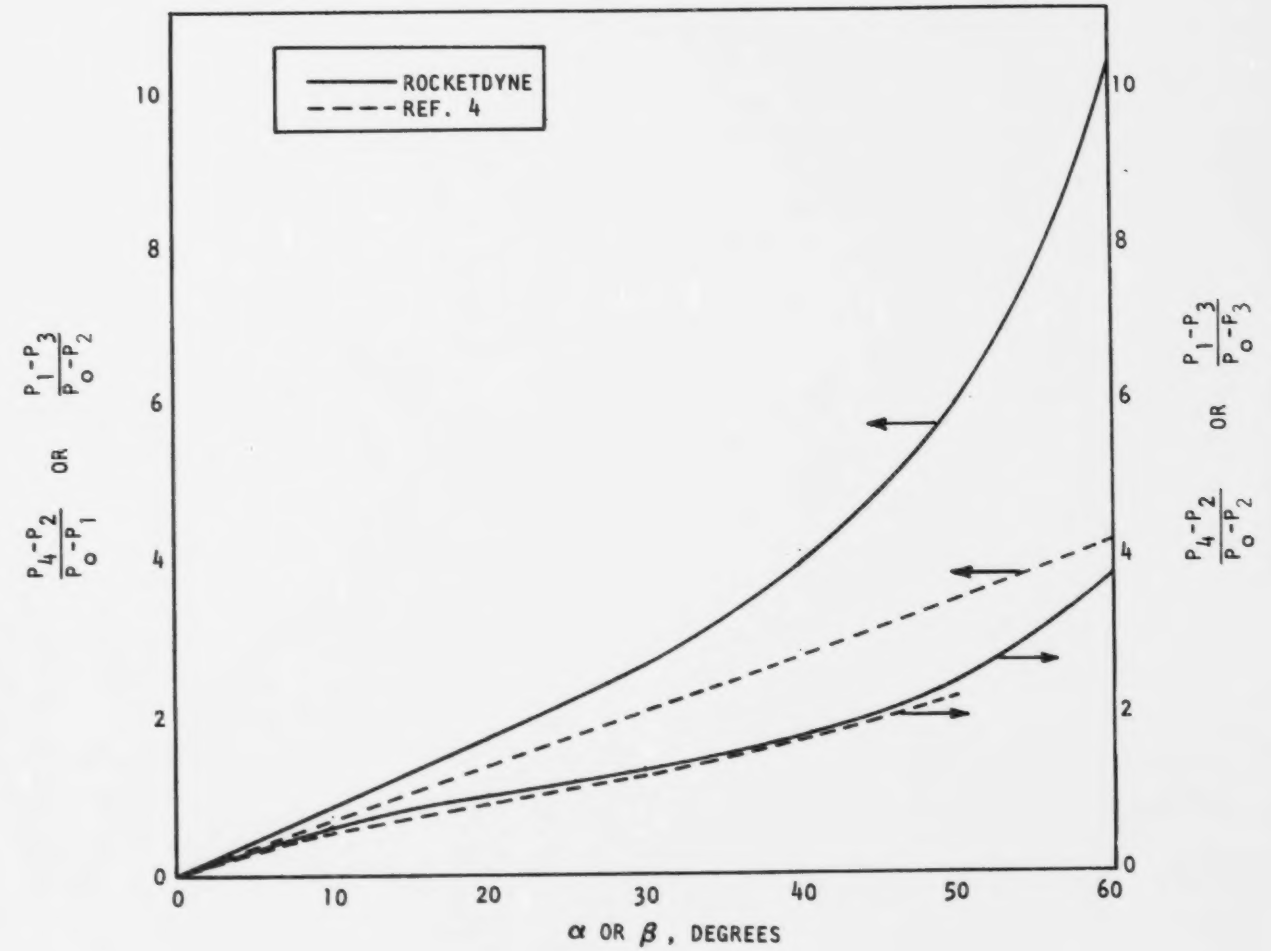

Figure 19. Velocity probe calibration chart for yaw (α) and pitch (β)

Comparison of the Rocketdyne calibration data with predictions based on potential flow theory showed acceptable agreement with deviations expected for "real" flow situations. Nevertheless, the difference in the shape of the Rocketdyne curve $(P_4-P_2)/(P_o-P_1)$ vs β (Fig. 19) and the similar curve for the data in Ref. 4 , prompted more detailed calibration testing. This testing involved the experimental measurement of the locations on the probe tip at which (P_i-P_{amb}) equals zero. According to potential flow theory, the stagnation point would have to be rotated an angle of 41.8 degree to record $(P_i-P_{amb}) = 0$.* Calibration testing of the probe indicated an actual angle of 44.85 degree for attainment of zero and the geometrical layout of the probe tip as shown schematically below.

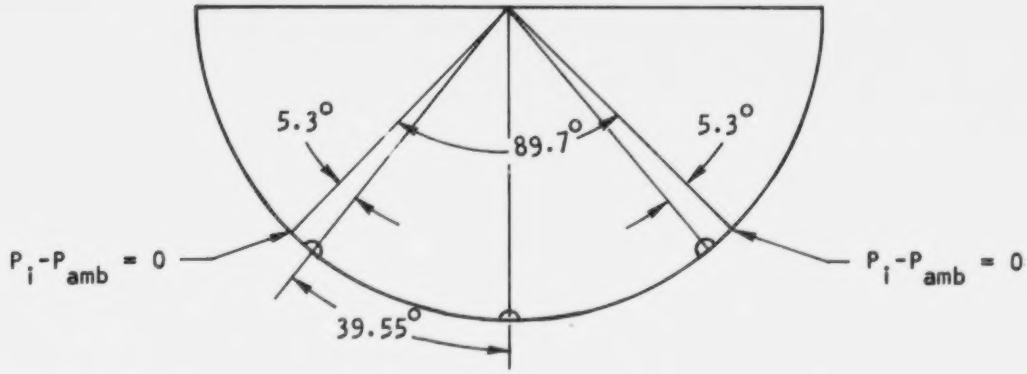

(TYPICAL FOR TWO CROSS-SECTIONS)

In addition the surrounding holes were found to be located at an angle of 39.55 degree relative to the central hole (instead of the design value, 45 degree) and, also, the tip of the 0.50 inch OD probe was not a perfect hemisphere (it had a height of ~0.17 inch, instead of 0.250 inch, corresponding to a radius of curvature of 0.268 inch). These fabrication deviations from the detail design drawing (Fig. 6) are the probable explanation for the differences between the Rocketdyne calibration data and that of Ref. 4 . These deviations, however, do not preclude in any way the use of the velocity probe in its intended capacity because the probe has been calibrated.

---

*$P_i-P_{amb}/1/2\rho V^2 = 1 - 9/4 \sin^2 \theta = 0$ yields $\sin \theta = 2/3$, or $\theta = 41.8$ degrees.

In addition to using the calibration data to calculate differential pressure ratio versus yaw and pitch angle (Fig. 19), the data were also used to calculate velocity recovery factors* versus yaw or pitch angle as shown in Fig. 20 + along with IFRF results. The velocity recovery factor, K_o-K_i, is defined by the relation

$$(K_o-K_i) = (P_o-P_i)/1/2\rho V^2 \tag{1}$$

where position o is the central probe hole as shown in Fig. 18 and position i is that of any surrounding hole.

In addition, the velocity magnitude may also be expressed as

$$V = \sqrt{\frac{2g_c\ (P_{stag}-P_{amb})}{\rho}} \tag{2}$$

where $P_{stag} = P_o$ when yaw and pitch angles are zero

P_{amb} = ambient pressure

---

*The measurement of differential pressure ratios permits determination of flow direction while the additional measurement of the velocity recovery factor permits determination of velocity magnitude as well.

+The data shown in Fig. 19 represent only a change in pitch (β) angle. Owing to probe symmetry, Fig. 19 would also represent a change in yaw (α) angle, if the x-axis was labeled "α, degrees", the left-hand y-axis labeled, "K_o-K_2", and the right-hand y-axis, "K_o-K_3".

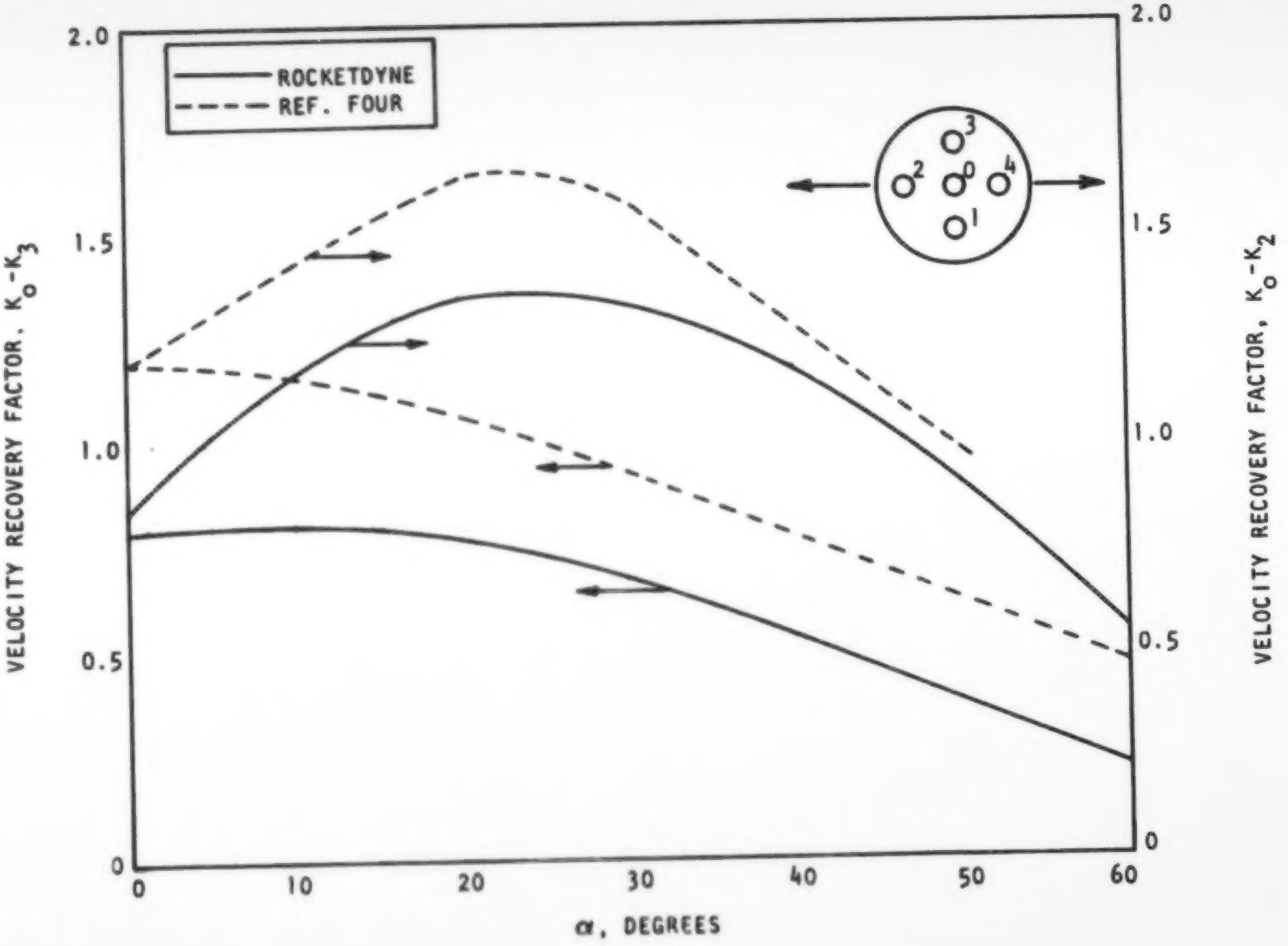

Figure 20. Velocity probe calibration chart for velocity magnitude

CONSTRUCTION OF CALIBRATION CHARTS

By equating Eq. 1 and 2, the velocity recovery factor $K_o - K_i$ was calculated from the calibration data as a function of yaw or pitch angle (Fig. 20).

The results shown in Fig. 19 and 20 are referred to the yaw (α) and pitch (β) angles. However, in Ref. 4 the angles ϕ and δ as shown in Fig. 21 were also used. The angle ϕ is the angle between the velocity vector and the x axis. The angle δ is the angle between the projection of the velocity vector on the zy plane and the y axis. The angle α (yaw angle) is the angle between the projection of the velocity vector on the xz plane and the x axis. The angle β is the angle between the projection of the velocity vector on the xy plane and the x axis. The angles are interrelated through the equations.

$$\tan\delta = \frac{\tan\alpha}{\tan\beta} \quad \text{and} \quad \tan\phi = \frac{\tan\alpha}{\sin\delta}$$

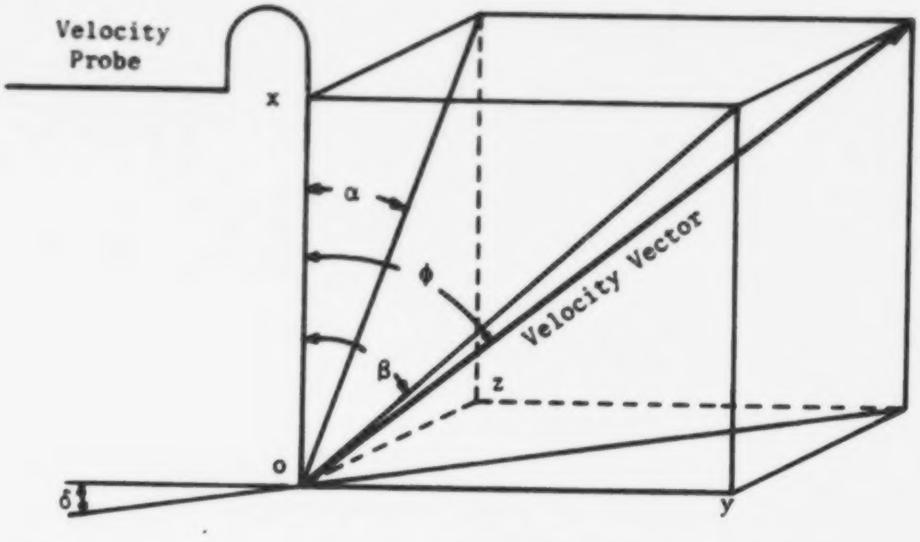

Figure 21. Relation between angles for velocity determination in five-hole pitot probe

A calibration chart for use with the Rocketdyne Velocity probe was constructed in terms of the angles ϕ and δ for definition of the flow angle (as was done in Ref. 4). This chart is shown in Fig. 22 , which was calculated from the experimental calibration data obtained at yaw and pitch angles of zero and 90 degrees. Two procedures for calculating this set of calibration curves were explored; both involved use of the data at the two pitch and yaw angles to estimate the pressures for any angles. Initially, an attempt was made to use the potential flow expression for the pressure distribution over a sphere with the introduction of two empirical coefficients, D_i and Q,

$$\frac{P_i - P_{amb}}{1/2\rho V^2} = D_i \left[1 - \frac{9}{4} \sin^2 (Q\theta) \right]$$

Secondly, the data were used explicitly with interpolation equations, and assuming the flow was symmetrical around the axis of the probe, to calculate the pressures. The second approach was the most successful in describing the available data. Therefore, it was used to calculate the curves shown in Fig. 22 .

A similar calibration chart for determination of velocity magnitude with the Rocketdyne velocity probe was also constructed. This was accomplished through use of the relation $(K_o - K_i) = (P_o - P_i)/1/2\rho V^2$, where the value of P_o and P_i were determined as described above for any flow direction. The resulting velocity magnitude calibration chart is shown in Fig. 23.

The calibration charts developed for the velocity probe fabricated during this program, Fig. 21 and 22, are incomplete in as much as only a single quadrant of the total calibration chart is actually shown. As seen in Fig. 16, the total calibration chart consists of four quadrants, which in the case of Fig. 22 and 23 will be mirror images of each other at the x and y axes.

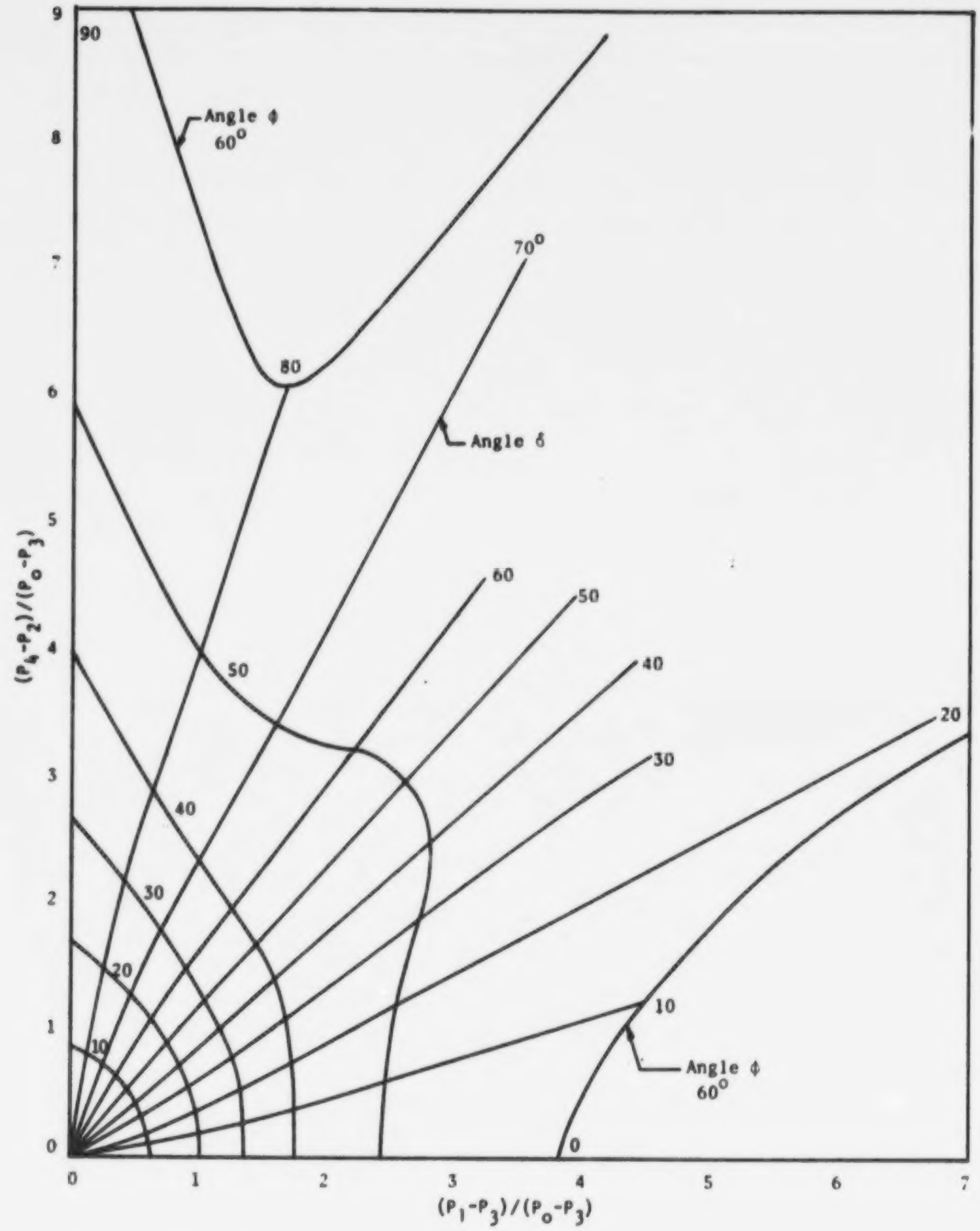

Figure 22. Velocity probe calibration chart for determination of angle of flow

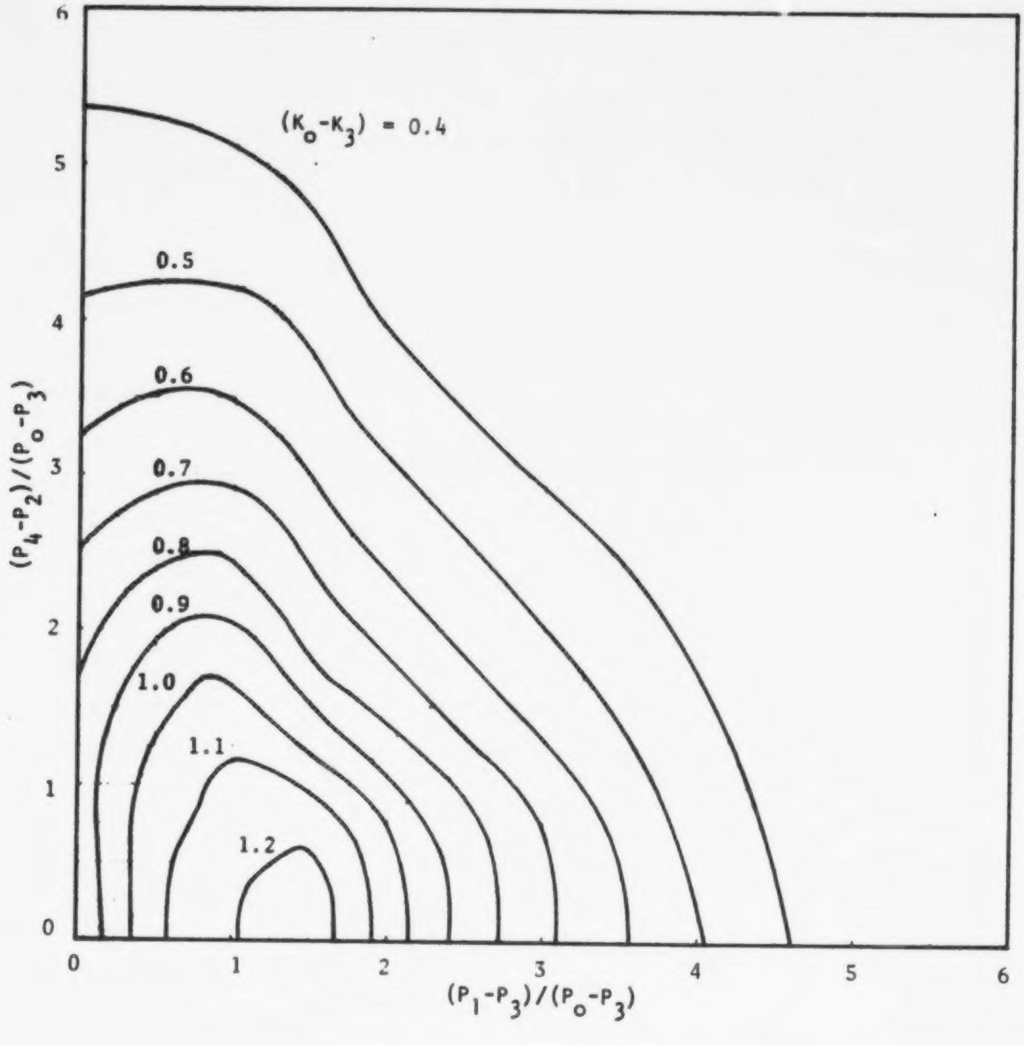

Figure 23. Velocity probe calibration chart for determination of velocity magnitude

The total calibration chart can thus be obtained by reference to Fig. 22 and 23, which represent the upper right-hand quadrant. For example, referring to Fig. 16, the upper left-hand quadrant is a mirror image of the upper right-hand quadrant about the y axis. The lower left-hand quadrant is a mirror image of the upper left-hand quadrant about the x axis and the lower right-hand quadrant is a mirror image of the upper right-hand quadrant about its x axis.

The pressure ratios representing the x and y axes in the various quadrant are not constant and vary as shown in Fig. 16. Similarly, the angle δ has a different range in each of the four quadrant as shown in Fig. 16. Lastly, the velocity recovery factor also varies from quadrant to quadrant. A velocity recovery factor of (K_o-K_3) applies in the upper and lower right-hand quadrants while a recovery factor of (K_o-K_1) applies in the upper and lower left-hand quadrants.

USE OF CALIBRATION CHARTS

The use of the velocity probe calibration charts is most simple. Measurement of three differential pressures (P_4-P_2, P_o-P_3, and P_1-P_3) are sufficient to determine the flow direction as defined by the angles ϕ and δ using Fig. 22. The same three differential pressures also allow determination of the velocity recovery factor using Fig. 23. Velocity magnitude can be calculated from the definition of the recovery factor, i.e.,

$$V = \sqrt{\frac{2g_c\ (P_o-P_3)}{\rho\ (K_o-K_3)}}$$

It is again mentioned that the calibration charts presented in Fig. 22 and 23 are applicable only to the particular velocity probe fabricated under this contract. A different instrument would require its own separate calibration.

PROBE CHECKOUT AND EVALUATION AT ROCKETDYNE

A special gas burner (Fig. 24) was designed and built at UCLA for use in the molecular beam mass spectroscopy portion of this program conducted at UCLA. A second gas burner identical in most respects to the UCLA burner was also fabricated at Rocketdyne for use in the preliminary evaluation of the newly fabricated probes. A 2.66-inch diameter porous ceramic disk was used in the burner head to create and hold a flat premixed methane/air flame within a 3-inch diameter, 4-foot-long quartz tube. To promote mixing of the air and fuel, five layers of brass screens were placed below the flame holder, as shown in Fig. 24 .

TEMPERATURE PROBE

Initial tests of the temperature probe were made in a premixed gas flame with the setup shown schematically in Fig. 25 . The hot-gas temperature is calculated from the venturi pyrometer measurements by

$$T_H = F \frac{\Delta P_H}{\Delta P_c} T_c$$

where T_H = gas temperature at upstream (hot) venturi, R
T_c = gas temperature at downstream (cold) venturi, R
ΔP_H = pressure drop across hot venturi
ΔP_c = pressure drop across cold venturi
F = instrument constant

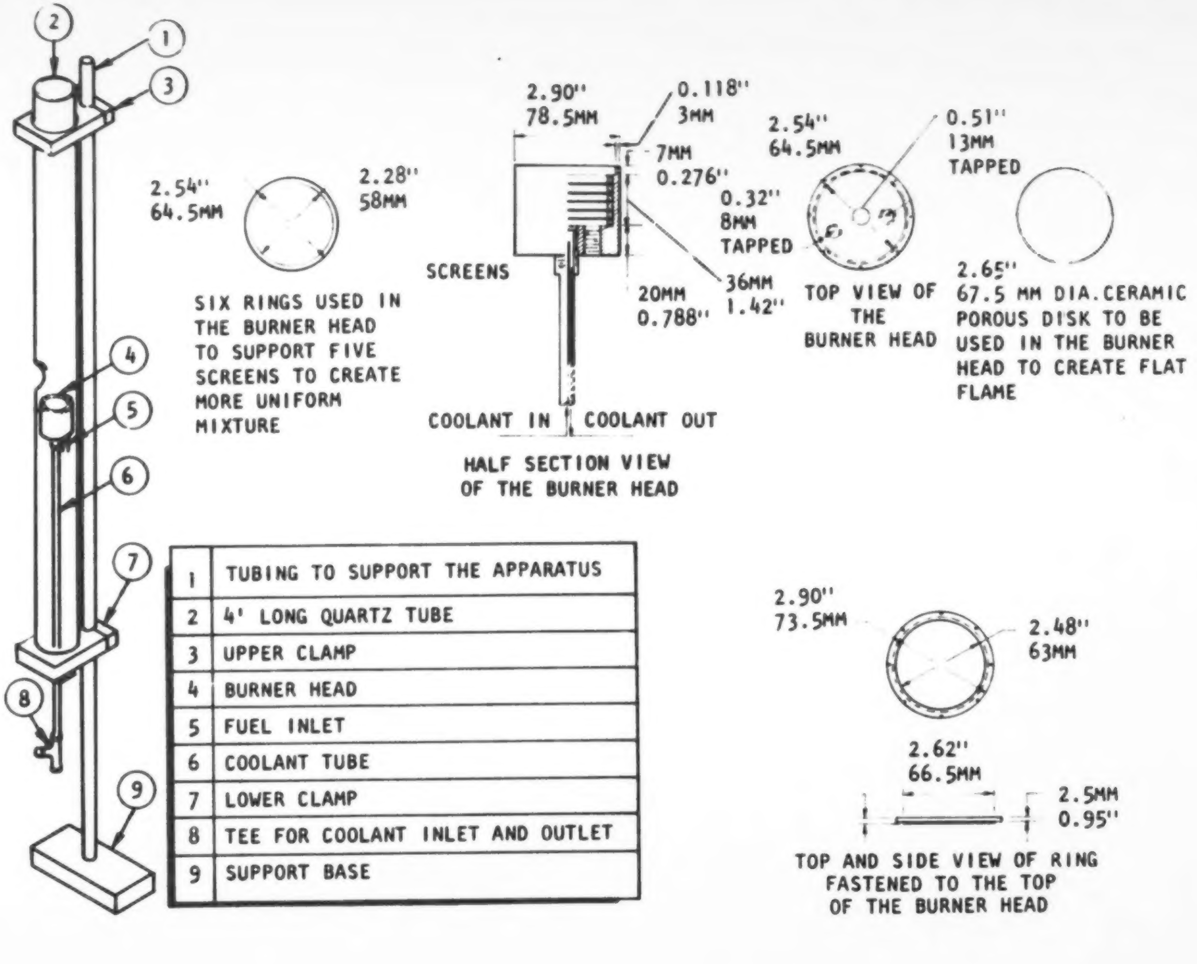
2
1
3
2.54''
64.5MM
2.28''
58MM
SIX RINGS USED IN THE BURNER HEAD TO SUPPORT FIVE SCREENS TO CREATE MORE UNIFORM MIXTURE
4
5
6
7
8
9
2.90''
78.5MM
0.118''
3MM
7MM
0.276''
0.32''
8MM
TAPPED
SCREENS
20MM
0.788''
36MM
1.42''
COOLANT IN
COOLANT OUT
HALF SECTION VIEW OF THE BURNER HEAD
2.54''
64.5MM
0.51''
13MM
TAPPED
TOP VIEW OF THE BURNER HEAD
2.65''
67.5 MM DIA.CERAMIC POROUS DISK TO BE USED IN THE BURNER HEAD TO CREATE FLAT FLAME
2.90''
73.5MM
2.48''
63MM
2.62''
66.5MM
2.5MM
0.95''
TOP AND SIDE VIEW OF RING FASTENED TO THE TOP OF THE BURNER HEAD

1	TUBING TO SUPPORT THE APPARATUS
2	4' LONG QUARTZ TUBE
3	UPPER CLAMP
4	BURNER HEAD
5	FUEL INLET
6	COOLANT TUBE
7	LOWER CLAMP
8	TEE FOR COOLANT INLET AND OUTLET
9	SUPPORT BASE

Figure 24. Gas burner design

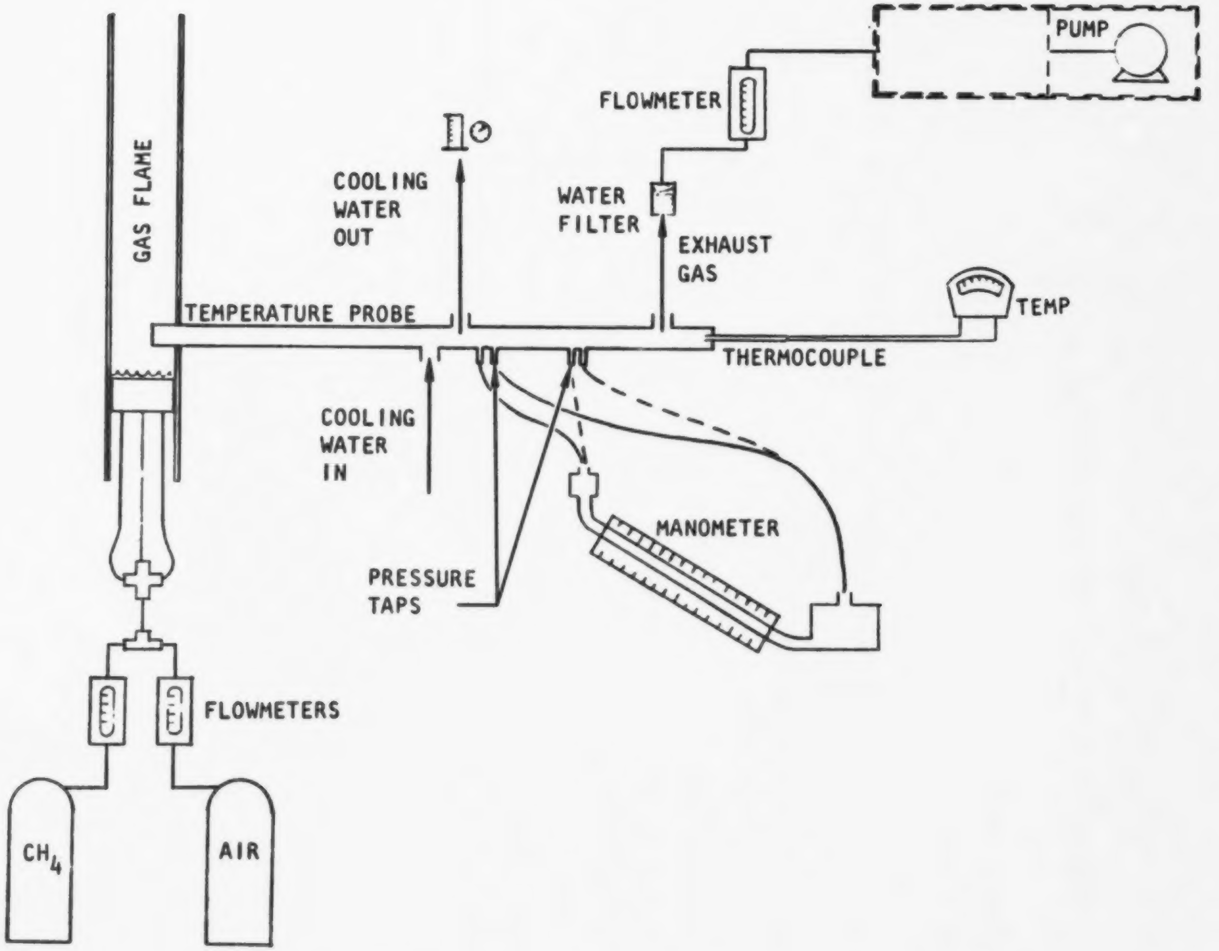
PUMP
FLOWMETER
WATER
FILTER
EXHAUST
GAS
COOLING
WATER
OUT
GAS FLAME
TEMPERATURE PROBE
TEMP
THERMOCOUPLE
COOLING
WATER
IN
MANOMETER
PRESSURE
TAPS
FLOWMETERS
CH_4
AIR

Figure 25. Temperature probe/gas burner schematic

The instrument constant, F, was obtained in preliminary cold-flow tests. The maximum suction flowrate of room temperature air was drawn through the probe by means of a series of three vacuum pumps installed in conjunction with the analysis equipment. Using the measured values of ΔP_H and ΔP_c (obtained with an inclined manometer), and noting that $T_c = T_H =$ ambient, a value of F = 1.225 was calculated.

The pneumatic venturi pyrometer was then used (Fig. 26) to obtain the gas temperature in a fuel-lean methane-air flame with an equivalence ratio* of 0.75. The measurement was made in the center of the 3-inch tube diameter at a distance of 2-inches downstream of the burner head. A gas flame temperature of 2930 R (1626 K) was calculated from the measured ΔP's and the instrument constant⁺.

The theoretical maximum flame temperature of a methane-air flame was calculated as a function of equivalence ratio using the Rocketdyne n-element propellant performance program. This computer program accounts for the establishment of definite equilibrium conditions between products and reactants. Results are summarized in Appendix D. The theoretical temperature of a methane-air flame having an ER = 0.75 is 1922 K. The relatively large 296 K difference between the 1922 K theoretical flame temperature and the measured value of 1626 K is believed due to:

1. Loss of heat from the flame
2. Inherent inaccuracy involved in the method of pneumatic pyrometry.

The accuracy of the pneumatic pyrometry technique was investigated further by comparison with the molecular-beam mass spectrometer technique. These results are reported in a later section of this report.

---

*ER = $(CH_4/\text{air})/(CH_4/\text{air})_{\text{stoichiometric}}$

⁺$T_H = F\ \Delta P_H/\Delta P_c\ T_c = 1.225(0.925 \text{ inch } H_2O/0.320 \text{ inch } H_2O)(366 + 460) =$ 2930 R

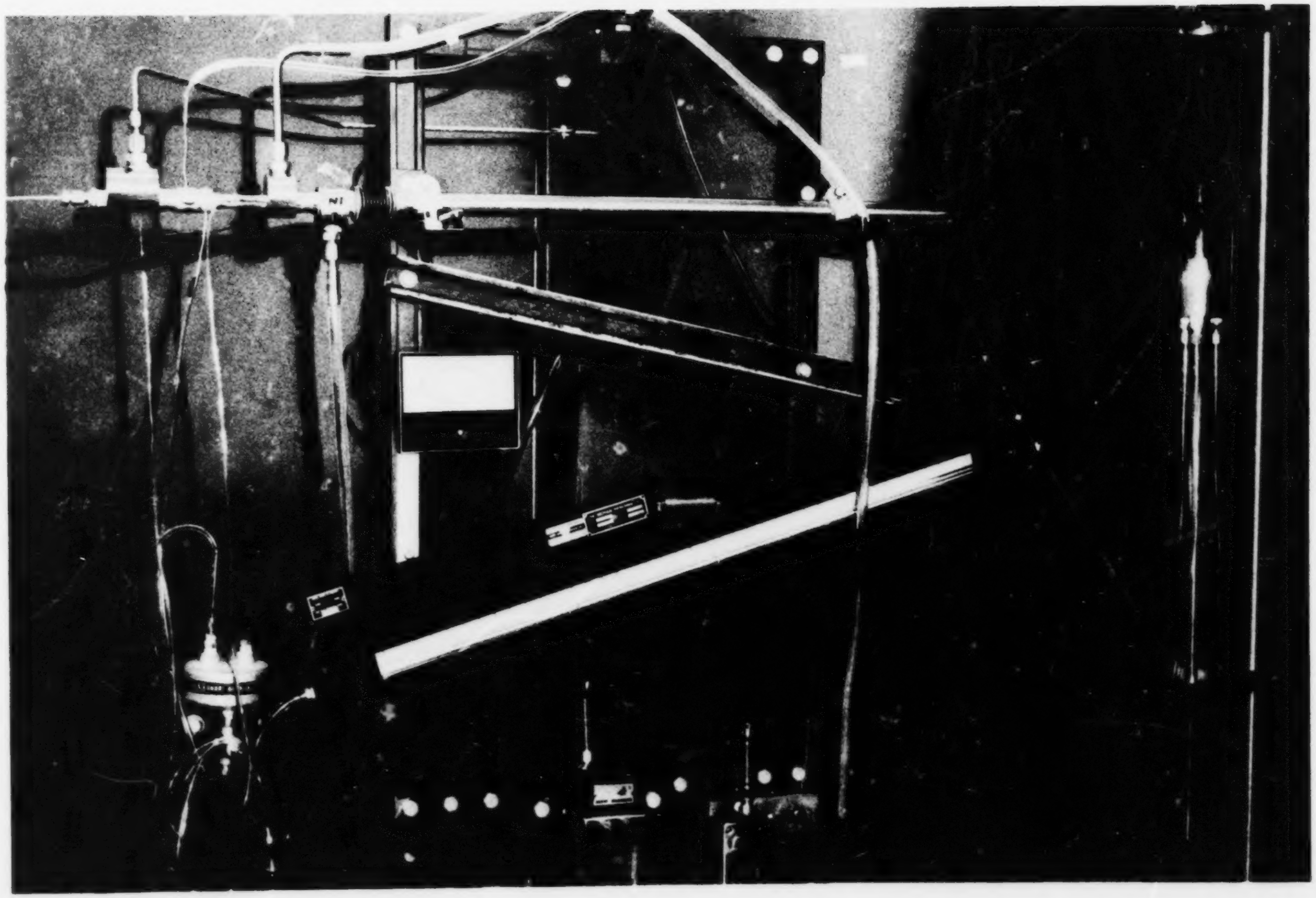

50A66-6/7/73-S1A

Figure 26. Evaluation of temperature probe in premixed gas flame

It is interesting to note, however, that Perry (Ref. 17) reports that, for a stoichiometric methane-air mixture, a theoretical maximum flame temperature of 2340 K is calculated although the experimentally determined flame temperature (sodium line reversal) is only 2148 K, a difference of 192 K.

The response time of the temperature probe was calculated to be on the order of tens of seconds (Ref. 4 , p. 42). The use of a low-response device such as the manometer for pressure recording, of course, adds to this value. A posttest calibration with room temperature air yielded an instrument constant within 1-percent of the pretest value.

During operation of the temperature probe in the gas flame, it was observed that care was required to avoid overcooling the probe. Overcooling results in condensation of water vapor (present in the methane/air combustion products) within the probe that ultimately leads to the presence of water in the annular piezometric rings used to measure pressure drop across the venturi tubes and adversely affects the pressure drop measurement.

VELOCITY PROBE

The velocity probe was also initially tested in a premixed methane/air gas flame (Fig. 27). The primary purpose of this test was to verify the adequacy of the probe cooling capability. Meaningful velocity measurement was not expected because the estimated gas velocity in the 3-inch OD quartz tube was on the order of only 6 fps. This value is equivalent to a manometer reading of only 0.008 inch of water--less than the smallest scale division on the manometer (0.01 inch of water). No significant velocity was indicated by the manometer.

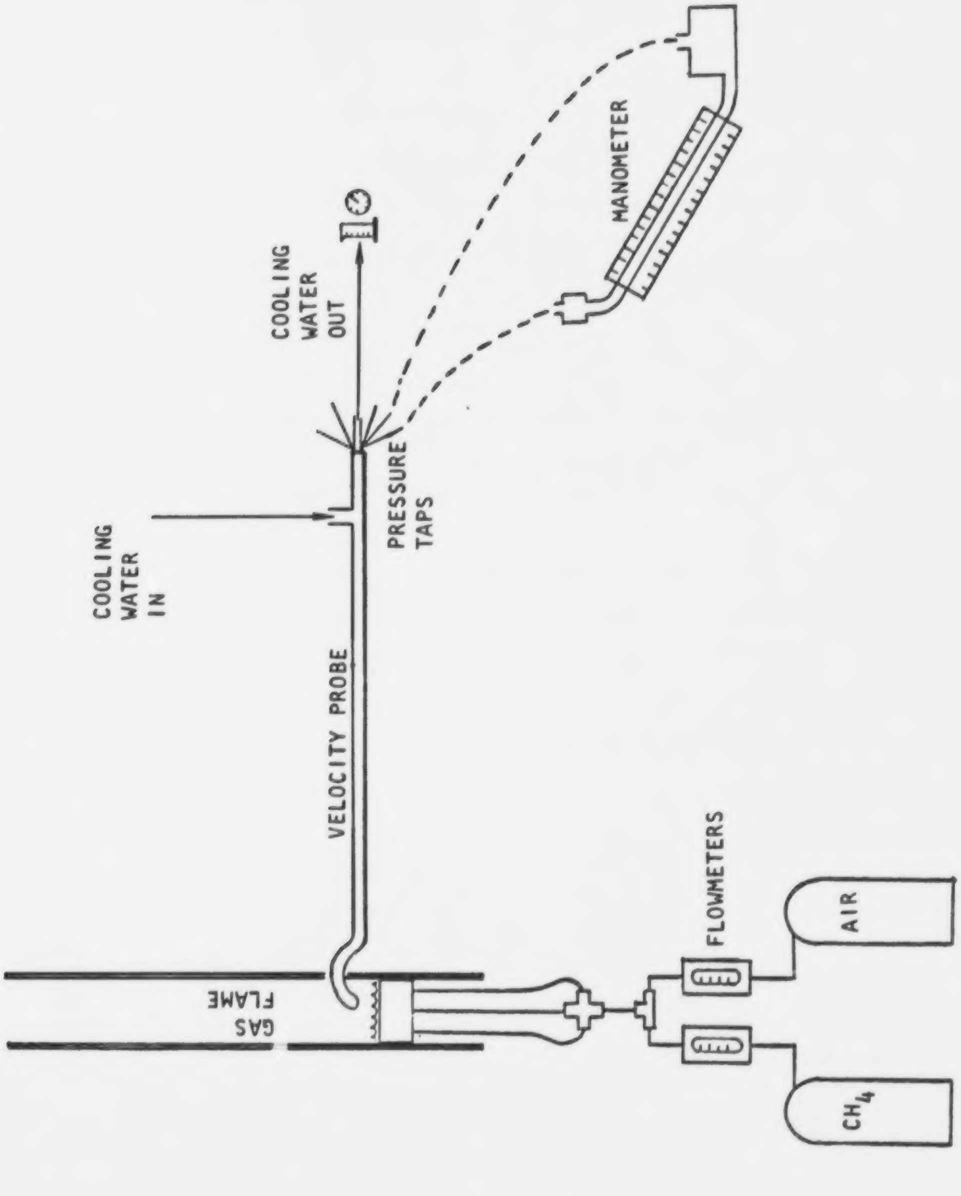
COOLING WATER OUT
COOLING WATER IN
PRESSURE TAPS
MANOMETER
VELOCITY PROBE
GAS FLAME
FLOWMETERS
AIR
CH_4

Figure 27. Velocity probe/gas burner schematic

SPECIES PROBE

The species probe was also inserted into a premixed methane/air gas flame (2 inches downstream of the burner head) for initial checkout (Fig. 28). With a fixed water coolant flowrate, concentrations of CO, CO_2, and NO_x in the combustion gas were measured as functions of the fraction of the combustion gas flow being drawn into the probe that was recycled after cooling. Data analysis showed the following variations with percentage of recycle gas.

ER	Percent Recycle	CO, ppm	CO_2, percent	O_2, percent	NO_x, ppm
0.75	48	1391	8.59	5.90	10
0.75	43	1452	8.59	5.90	8
0.70	18	1300	8.13	7.00	10

The effect of percent recycle on composition shown by these results is not considered significant. Percentages of CO_2 and O_2 were quite close to theoretical values* obtained using the Rocketdyne n-element propellant performance model (Appendix D). No abnormalities were evident during testing and operation of the species probe in the flame appeared satisfactory.

---

*Theoretical calculations yield (on a water-free basis)

ER	CO_2, percent	O_2, percent
0.75	8.51	5.50
0.70	7.92	6.65

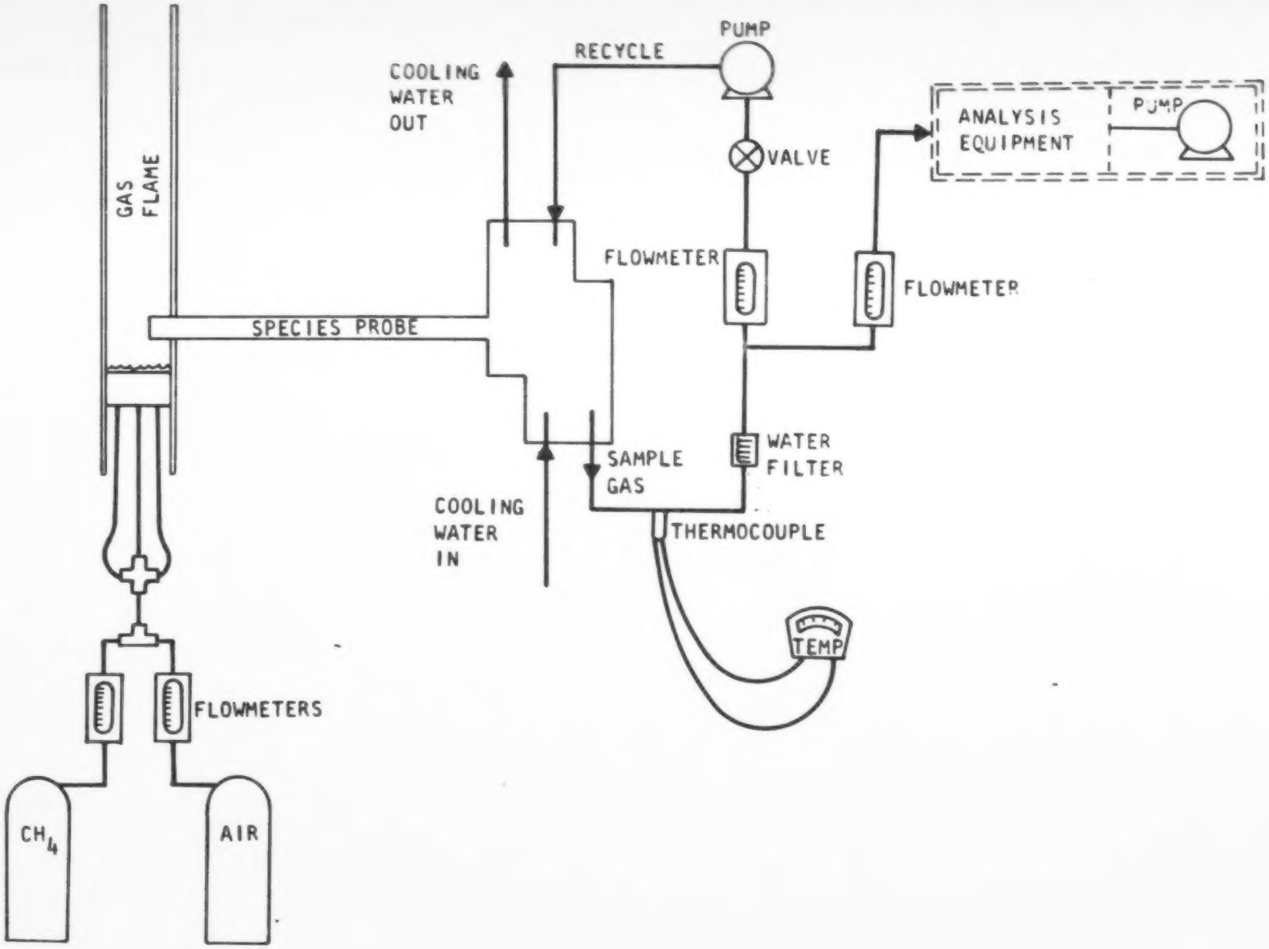
GAS
FLAME
SPECIES PROBE
COOLING
WATER
OUT
RECYCLE
PUMP
VALVE
ANALYSIS
EQUIPMENT
PUMP
FLOWMETER
FLOWMETER
SAMPLE
GAS
WATER
FILTER
COOLING
WATER
IN
THERMOCOUPLE
TEMP
FLOWMETERS
CH4
AIR

Figure 28. Species probe/gas burner schematic

MOLECULAR-BEAM MASS SPECTROSCOPY AT UCLA

A molecular-beam mass-spectrometer system, in existence at UCLA at the beginning of the program, was substantially modified and improved to quantitatively determine the molecules and radicals present in a premixed methane/air flame. Determination of the stable, as well as the unstable species existing in the flame was planned as well as the flame temperature itself.

EXPERIMENTAL APPARATUS

The experimental apparatus employed in the molecular-beam mass-spectrometer system consisted of the following:

A. Gas Burner

A special gas burner designed and built for these studies was described earlier and is shown in Fig. 24. The flame holder consists of a 2.66-inch-diameter porous ceramic disk to produce vertical-flow flat flames. The flame holder was movable in the vertical direction to facilitate sampling from different locations within the flames. It was water-cooled by means of two concentric stainless-steel tubes, which also serve as the burner mount. Air and fuel flowrates were measured with flowmeters, which in turn, were calibrated with a wet testmeter (Precision Scientific No. 63125).

The flame-holder assembly was inserted in a 4-foot long, 3-inch diameter quartz tube. A 2.5-inch diameter hole in the wall of the tube admitted a conical, quartz sampling probe. The probe had an apex angle of 90 degrees and a sampling orifice diameter of 0.059 cm. Three layers of asbestos sheet sealed the probe-tube junction. The integrity of the seal was checked by:

1. Blowing air on it and looking for a change in the flame shape
2. Analyzing for O_2 in fuel-rich flames.

No air leaks were detected in the experiments reported herein.

Since the primary reaction zone was always below (upstream of) the sampling probe, the presence of the probe did not influence the flatness of the flame. The flame flatness was influenced, however, by the fuel-air ratio. A relatively flat flame was realized at and near $\phi = 1$,* whereas, a less stable flame, containing small conical regions, was realized at $\phi = 0.75$ and 1.30.

All measurements were believed to be made outside the boundary layer formed as a result of the flow through the quartz tube. The (displacement) boundary-layer thickness was calculated to be 0.12 inch; the sampling cone penetrated 0.8 inch into the gas stream.

B. Vacuum System

As shown in Fig. 29, the vacuum system consisted of three separate chambers. The sampling gas was accelerated aerodynamically through the sampling orifice and into the source chamber. This chamber was maintained near 10^{-2} torr by a 16-inch Stokes booster diffusion pump in series with a Stokes mechanical pump.

The core of the supersonic jet enters the collimating chamber through a skimmer. The skimmer has an internal half angle of 16 degrees, an

---

*ϕ = equivalence ratio = $(CH_4/air)/(CH_4/air)_{stoichiometric}$

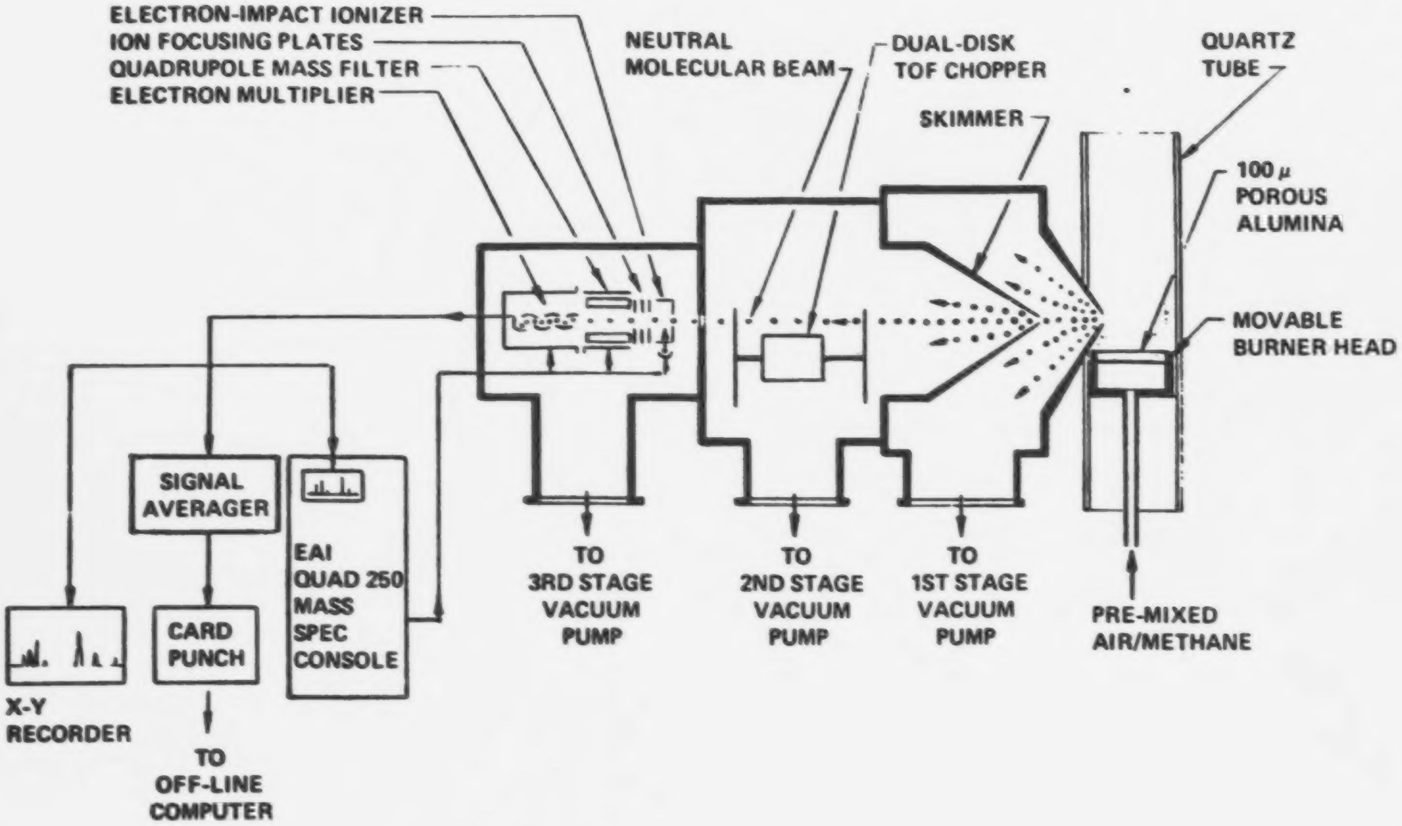
ELECTRON-IMPACT IONIZER
ION FOCUSING PLATES
QUADRUPOLE MASS FILTER
ELECTRON MULTIPLIER
NEUTRAL MOLECULAR BEAM
DUAL-DISK TOF CHOPPER
SKIMMER
QUARTZ TUBE
100 μ POROUS ALUMINA
MOVABLE BURNER HEAD
PRE-MIXED AIR/METHANE
TO 1ST STAGE VACUUM PUMP
TO 2ND STAGE VACUUM PUMP
TO 3RD STAGE VACUUM PUMP
EAI QUAD 250 MASS SPEC CONSOLE
SIGNAL AVERAGER
CARD PUNCH
TO OFF-LINE COMPUTER
X-Y RECORDER

Figure 29. The mass spectrometer is used to analyze the chemical composition. The time-of-flight technique is used to measure the temperature of the flame. The burner head position is varied to study the flame structure.

external half angle of 20 degrees, and an orifice diameter of 0.043 inch (0.11 centimeter). The collimating chamber is evacuated by a 10-inch CVC diffusion pump in series with a Hereaus mechanical pump. The pressure in this chamber is typically about 2 x 10^{-5} torr during the sampling.

The molecular beam passes through a slit in the rear wall of the collimating chamber into the detection chamber. The detection chamber is evacuated by a 6-inch NRC diffusion pump and a liquid-nitrogen-cooled cryosurface. The detection chamber pressure is maintained at about 3 x 10^{-7} torr during sampling from the flame.

C. Sampling System

During this program, the existing molecular-beam mass-spectrometer system was adapted for sampling from the burner (Fig. 30) as follows:

1. A logarithmic amplifier was designed and constructed for measurement of a low concentration species in flames. This amplifier uses a baseline compensator to compensate for background signals produced by metastable molecules.
2. A heated effusive source was built to facilitate the determination of temperature effects on mass-spectrometer fragmentation patterns.
3. A liquid-nitrogen shroud was added to the detection chamber to reduce the background noise.
4. A new time-of-flight chopper (Fig. 31) was constructed and installed for flame-temperature measurements. The time-of-flight chopper has been described in detail by Young (Ref. 13); data-reduction procedures are discussed in a later section of this report (page 87).

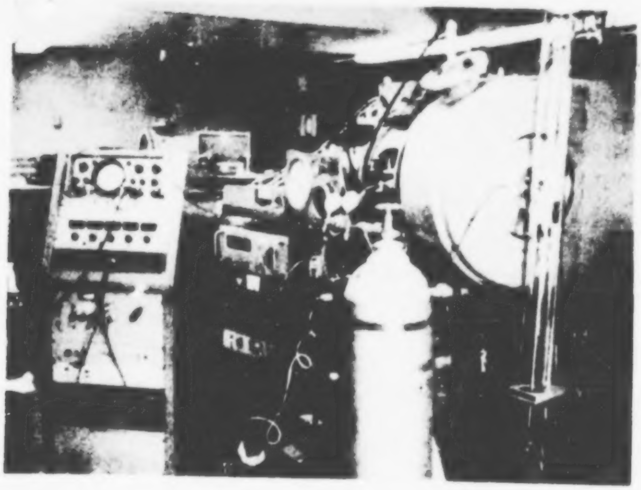

Figure 30. Flame sampling system

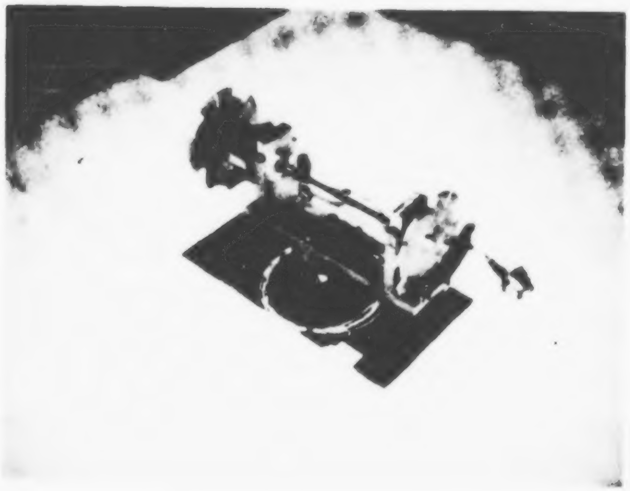

Figure 31. Dual-Disk TOF Chopper

D. Mass Spectrometer

The EAI quadrupole mass spectrometer, shown schematically in Fig. 29, consists of three primary components: the ionizer, the quadrupole mass filter, and the electron multiplier. The gas to be analyzed enters the ionizer, where a small percentage of the gas is ionized by electron bombardment. These ions are then accelerated and focused in the quadrupole section. The quadrupole assembly is composed of four stainless-steel rods, each approximately 5 inches long and 1/4-inch in diameter. A DC potential and a superimposed RF potential are applied to the rods. An electrostatic field is thereby generated in the region between the rods.

Most ions entering this region oscillate, collide with one of the poles, and are removed from the ion beam. Only ions in a very narrow range of charge-to-mass ratio can pass through the quadrupole. Those ions that do pass through the quadrupole strike the EAI beryllium-copper electron multiplier. The multiplier output current can be conveniently displayed on many types of instruments (such as oscilloscopes and X-Y recorders) to show the quantitative abundance as a function of atomic mass.

E. Signal Amplifying and Averaging System

For time-of-flight measurements of flame temperature, the output of the electron multiplier was amplified. The amplified signals were then averaged by a Northern Scientific Model 513 Digital Signal Averager. The averaging time depends upon the signal-to-noise ratio.

EXPERIMENTAL MEASUREMENTS AND DATA REDUCTION

The experimental measurements and data reduction methods employed are summarized as follows:

Composition Measurements

Two different data sets were taken in the composition measurements. First, a primary data set was taken in which the flame compositions were measured at equivalence ratios of 0.75, 0.80, 0.90, 1.00, 1.10, 1.25, and 1.30 and at sampling-orifice to flame-holder distances of 0.75, 1.00, 1.25, 1.50, 1.75, 2.00, 2.25, 2.50, 2.75, and 3.00 inches. The second data set was taken for measurement comparison with the Rocketdyne probe (discussed in a later section) and was taken for equivalence ratios of 0.90, 1.00, and 1.10 at a distance of 2.00 inches. Signals for mass-to-charge (m/e) ratios ranging from 1 to 44 were recorded. In order to minimize fragmentation, the ionizing electron energy was set at 20 ev.

Temperature Measurements

Flame temperatures were measured using the dual-disk time-of-flight (TOF) chopper with the signal from m/e = 28. In molecular beam sampling at high Reynolds numbers, based on the source conditions, the hydrodynamic speed V is the same for all species. Therefore, one may use any species or m/e present in the beam to determine V. The most convenient choice is m/e = 28, which provides the strongest signal. These measurements were made at equivalence ratios of 0.75, 0.80, 0.90, 1.00, 1.10, 1.25, and 1.30 and for sampling to flame-holder distances of 1.00, 2.00, and 3.00 inches. The TOF signals were punched on computer cards and then analyzed with a computer program generated for that purpose.

Flame temperatures were also measured using a platinum/platinum-10-percent rhodium thermocouple for the aforementioned equivalence ratios and for a sampling to flame-holder distance of 2.00 inches.

Mass-Spectrometer Calibration

The mass spectrometer was calibrated for gases at elevated temperatures. to determine:

1. Temperature effects on mass-spectrometer fragmentation patterns
2. Ionization efficiencies for CH_4, NO, H_2, and CO_2.

Using a heated effusive source, these calibrations were carried out for known CH_4-N_2, NO-N_2, H_2-N_2, and CO-N_2 mixtures at room temperature, 250, 500, 750, and 900 C. During the flame composition measurements, the mass-spectrometer was additionally calibrated with a supersonic room-temperature air beam.

Data Reduction for Composition Measurements

To determine the compositions of stable species and radicals in flames, the mass spectrometer signals for mass-to-charge (m/e) ratios of 1, 2, 14, 15, 16, 17, 18, 28, 29, 30, 32, 40, and 44 were analyzed. The supersonic-air-beam calibration data were used to determine the contributions of m/e = 32 to 16, 18 to 17, and 18 to 1 because of fragmentations. No appreciable changes in fragmentation patterns of CH_4, CO_2, H_2, and NO were observed for temperatures from room temperature to 900 C.

For those cases in which the analysis is qualitative (caused by lack of ionization cross-section values), the species signal was multiplied by the mole fraction of N_2 and divided by the N_2 signal.*

For those cases in which the effusive-source calibration data were available, these data were used to determine the relative ionization efficiencies. For example, for an N_2-H_2 mixture, the relative ionization efficiency is determined from

$$\text{R.I.E.} = \frac{\sigma(H_2)}{\sigma(N_2)} = \left(\frac{\Delta H_2}{\Delta N_2}\right)\left(\frac{x_{N_2}}{x_{H_2}}\right)\sqrt{\frac{m_{N_2}}{m_{H_2}}}$$

where $\sigma(H_2)$ = ionization probability for H_2 molecules
$\sigma(N_2)$ = ionization probability for N_2 molecules
ΔH_2 = H_2 signal level in the calibration data
ΔN_2 = N_2 signal level in the calibration data

---

*Qualitative data so derived are employed in some of the data plots presented later with ordinates labeled "Beam Signal, Arbitrary Scale."

x_{H_2} = H_2 mole fraction in the mixture
x_{N_2} = N_2 mole fraction in the mixture
m_{N_2} = molecular weight of N_2
m_{H_2} = molecular weight of H_2

The R.I.E. and the flame sampling signals were used to calculate the mole fraction of H_2 from

$$\frac{[H_2]}{[N_2]} = \left(\frac{S_{H_2}}{S_{N_2}}\right)\left(\frac{1}{\text{R.I.E.}}\right)$$

where $[H_2]$ = H_2 mole fraction in the flame
$[N_2]$ = N_2 mole fraction in the flame
S_{H_2} = H_2 signal level from the flame
S_{N_2} = N_2 signal level from the flame

Since the m/e = 28 signal corresponds to both N_2 and CO molecules, it was not possible to determine the CO concentration directly. However, it is believed that, at $\phi = 0.75$, the contribution of CO is very low and the m/e = 28 signal is only from N_2 molecules, so that one may use data for $\phi = 0.75$ to obtain the ionization cross-section ratio $\sigma(N_2)/\sigma(Ar)$ for use at other values of ϕ. More specifically,

$$\frac{\sigma(N_2)}{\sigma(Ar)} \approx \frac{S_{28}-S_{co}}{S_{40}} = \frac{S_{28}}{S_{40}}\left(1 - \frac{S_{co}}{S_{28}}\right)$$

Data taken with the Rocketdyne probe indicate that S_{co}/S_{28} is less than 0.002 and may be neglected in this determination of cross-section ratio. Therefore, N_2 and Ar signals at $\phi = 0.75$ were used in conjunction with the argon signal at other equivalence ratios to calculate the N_2 contribution to the m/e = 28 signals at these equivalence ratios. The difference between the measured m/e = 28 signal and the calculated N_2 contribution is the CO signal. A literature value for the relative ionization efficiency then determines quantitatively the CO concentration.

Data Reduction for Temperature Measurements

The time-of-flight technique may be used to determine the stagnation temperature of the source by determining the velocities of the molecules in a beam extracted from the source.

Alcalay and Knuth (Ref. 14) developed a moment method to extract the beam density, temperature, and energy from the measured TOF signal. Algebraic relations between the moments of the measured TOF signal, the speed distribution function, the modulator gate function, and the dynamic function of the detector and its electronics were derived. This technique was applied here to N_2 time-of-flight measurements for methane/air flames.

The stagnation temperature of the flame is given by:

$$T_o = T\left(1 + \frac{\gamma-1}{2} M^2\right) = T\left[1 + \frac{\gamma-1}{2}(V/a)^2\right]$$

where T_o = stagnation temperature of the source
T = static temperature in the free jet
γ = specific heat ratio
M = Mach number
V = hydrodynamic velocity
a = speed of sound

Since the static temperature is much less than the stagnation temperature, substitution for the speed of sound, a, yields

$$T_o \cong T\left[\frac{\gamma-1}{2}\ (V/a)^2\right] = T\left[\frac{\gamma-1}{2}\left(\frac{\sqrt{m\ V}}{\sqrt{\gamma\ RT}}\right)^2\right] = \left(\frac{\gamma-1}{2}\right)\left(\frac{mV^2}{\gamma R}\right)$$

where m is the mass (molecular weight) of the beam molecules and R is the universal gas constant. The velocity, V, can be calculated from

$$V = \frac{(L_I - L_{II})^2 \left(1 + \frac{5}{2S^2}\right)}{\left[\eta_I \left\{I_I^+(t)\right\} - \eta_I \left\{I_{II}^+(t)\right\} - \bar{\phi}/\omega\right]^2}$$

where $L_I - L_{II}$ = distance between the two chopper disks

S = hydrodynamic speed ratio

$\eta_I \{\ \}$ = first moment operator

$I^+(t)$ = instantaneous detected signal

t = time

$\bar{\phi}$ = phase angle of the dual-disk chopper

ω = angular speed of the chopper

For a diatomic gas with a molecular weight of 28, the value of $\left((\gamma - 1)/2\right)$ $(m/\gamma R)$ equals 4.81×10^{-4} K sec^2/m^2. The variation of m with ϕ, shown in Fig. 32, was taken into account in the calculations.

As an example, T_o for $\phi = 1.10$ and D = 2.00 inches may be calculated. For these conditions, V was determined experimentally to have a value of 2096 meter/sec. For $\phi = 1.10$, the mean molecular weight of the combustion gases in thermodynamic equilibrium (Ref. 15) is calculated to be 27. Using the relationship $T_o = \left((\gamma-1)/2\gamma R\right)$ (mV^2) T_o = 2036 K is obtained.

EXPERIMENTAL RESULTS

The methane-air flames were sampled directly for the stable products H_2, O_2, H_2O, CO, NO, and CO_2 and for the radicals H, O, and OH. Flame-temperature measurements were made with both the TOF and a thermocouple.

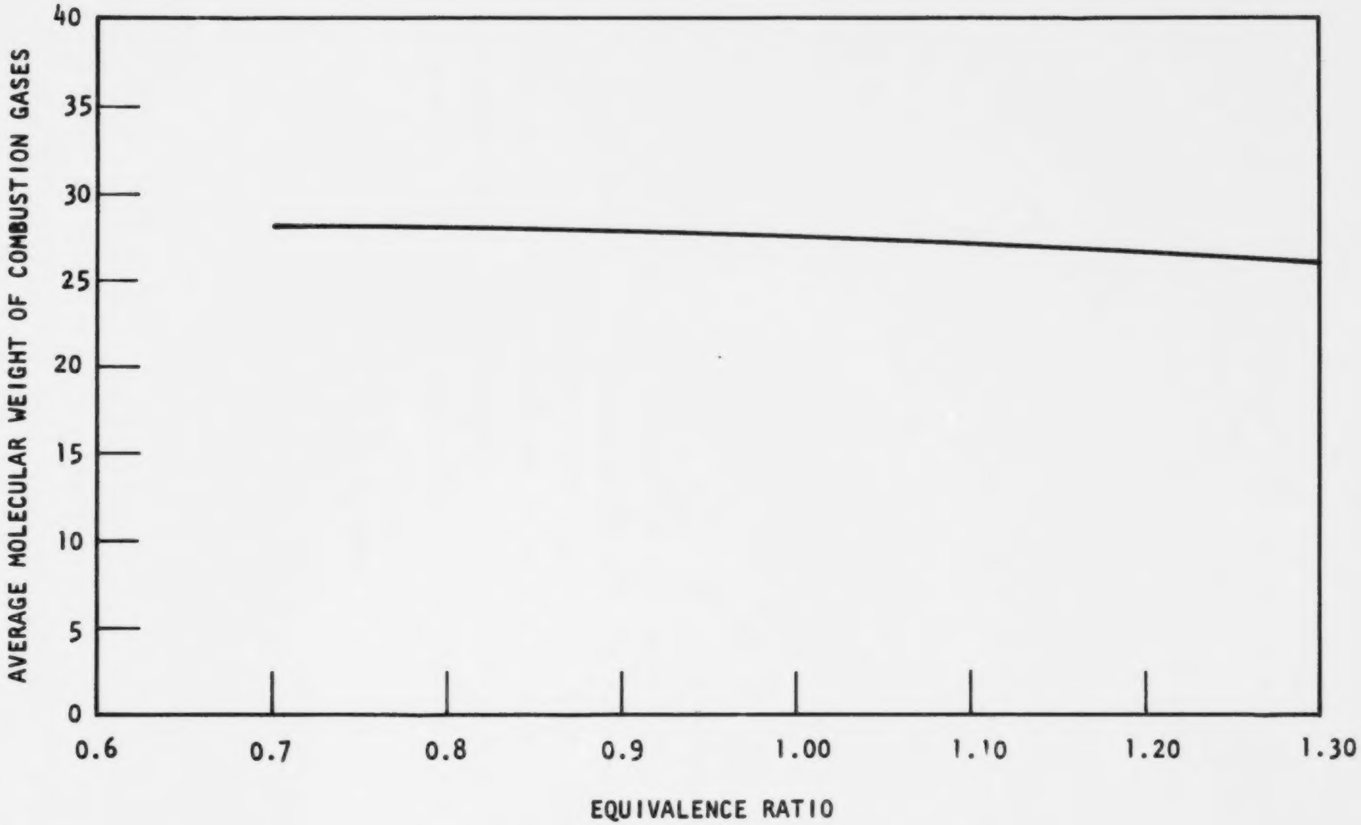

Figure 32. Average molecular weight of combustion gases vs equivalence ratio for methane-air flames

Direct-Sampling Composition Measurements

The results of measurements (qualitative or quantitative, as the case may be) on methane-air flames with D = 2.00 inches are presented versus equivalence ratios in Fig. 33 through 36. The qualitative results have not been converted to mole fractions in those cases where values for the ionization cross section were not available. Tabulations of the data (for several sampling-orifice to flame holder distances and for several equivalence ratios) are provided in Appendix C.

The term "recycled" used in Fig. 34, and subsequently, refers to the gas that was drawn through the Rocketdyne species probe (which employed cooled combustion gas recycle) and then returned to the MBMS sampling system for analysis. These measurements are described in a subsequent section.

The beam signal levels for the radicals H, O, and OH are shown in Fig. 33.* The m/e = 1 signal includes, in general, contributions from H_2O and H_2 fragments as well as from the H radical. In order to isolate the H-radical contribution, the fragmentation of H_2O and H_2 to H was established through a heated-effusive-source calibration. H_2 fragmentation to H at an ionizing electron energy of 20 ev was found to be negligible. H_2O fragmentation to H and OH was small; about 4 percent of the m/e = 1 signal and taken into account. However, the primary source of H atoms in lean methane-air flames is believed to be

$$CH_4 + OH \rightleftarrows CH_3 + H_2O$$

$$CH_3 + O \rightleftarrows CH_2O + H$$

---

*Equivalent readings on the arbitrary "y axis" scale (shown in Fig. 33) for the three radicals H, OH, and O do not correspond to equivalent concentrations. They would so correspond only if the three species had equal ionization cross sections (values are not known for the unstable species).

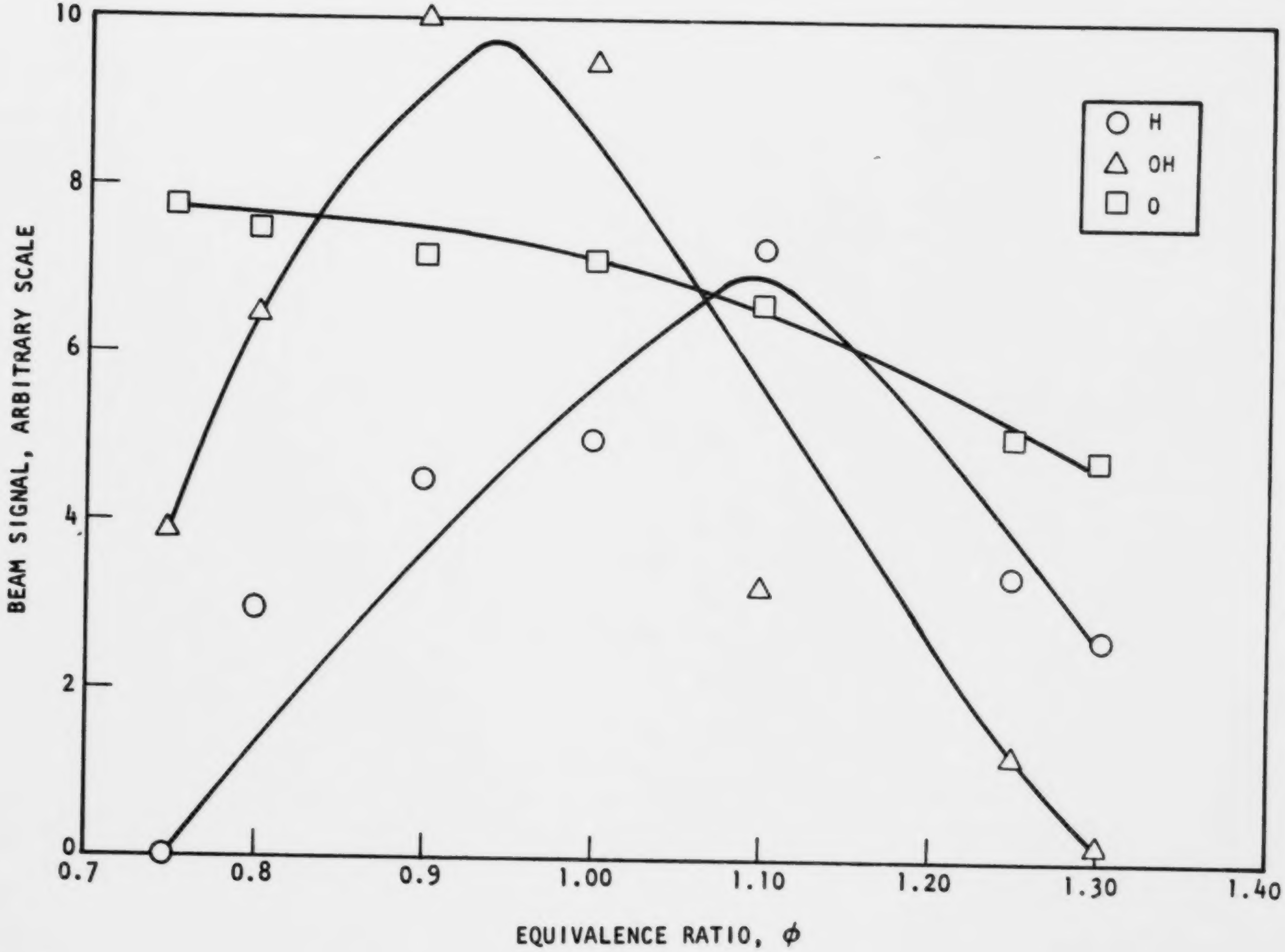

Figure 33. Beam signals for H, OH, and O radicals versus equivalence ratio at D = 2.00 inches

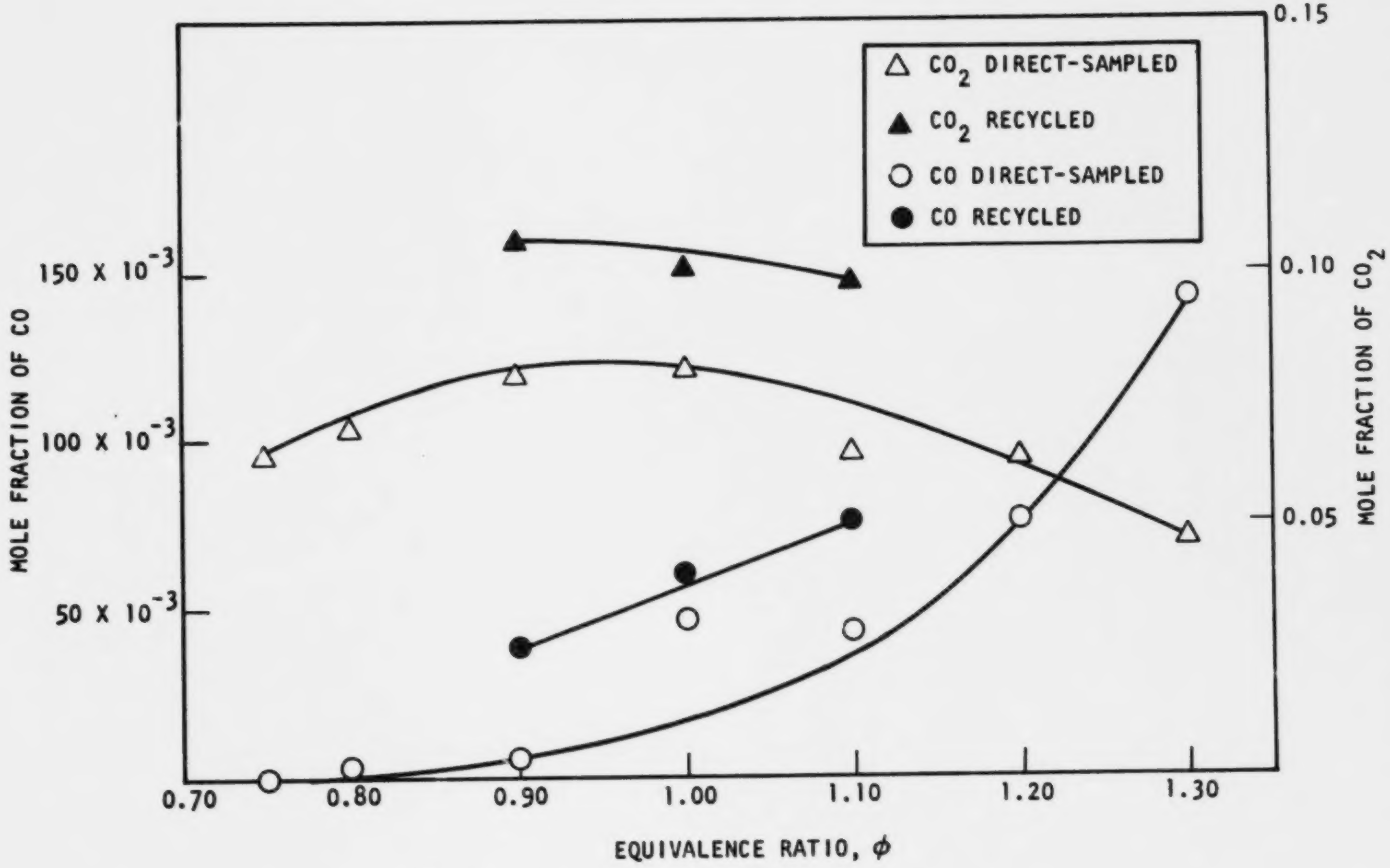

Figure 34. Mole fraction of direct-sampled CO_2 and CO, and recycled CO_2 and CO, versus equivalence ratio at D = 2.00 inches

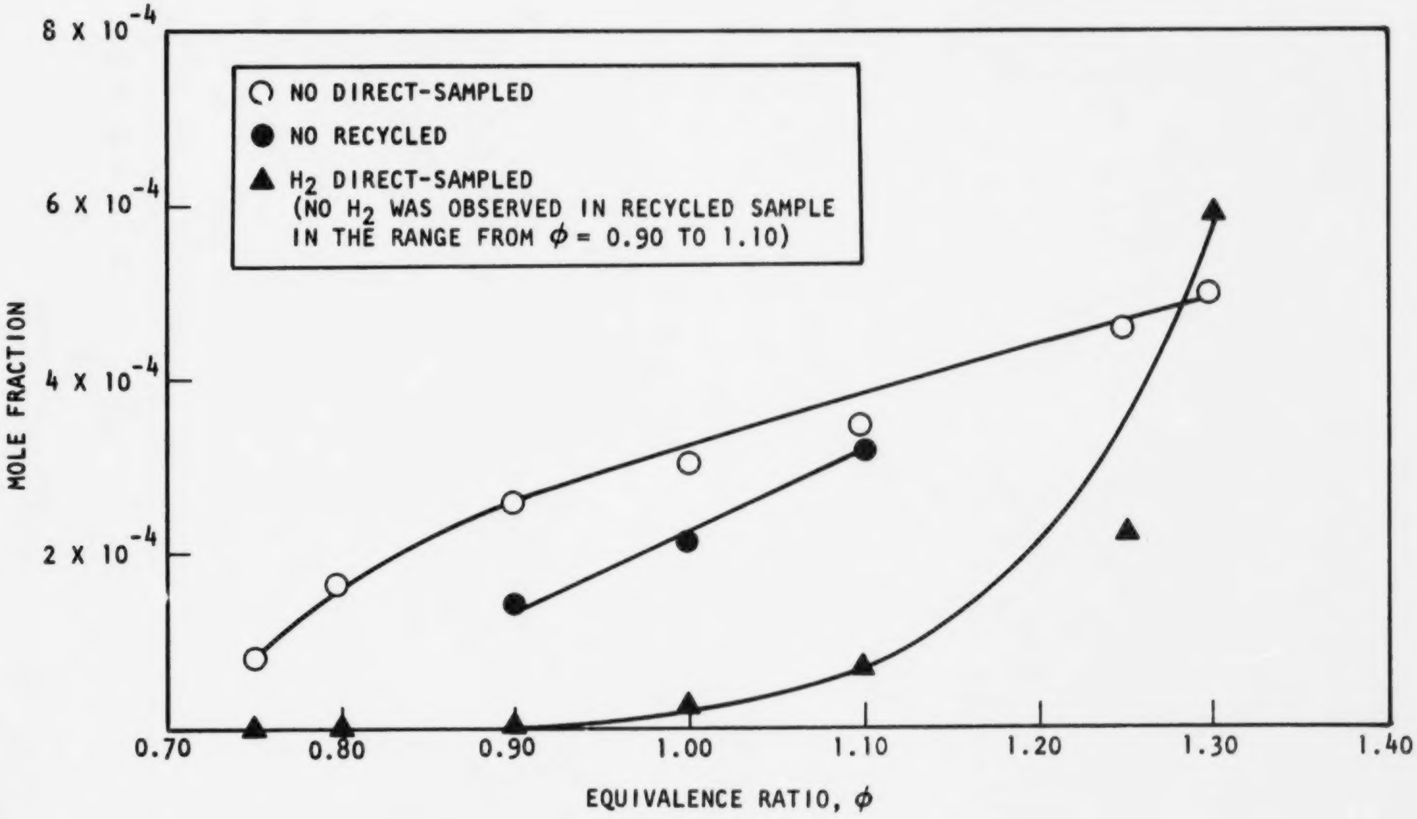

Figure 35. Mole fraction of direct-sampled NO and H_2 and recycled NO versus equivalence ratio for D = 2.00 inches

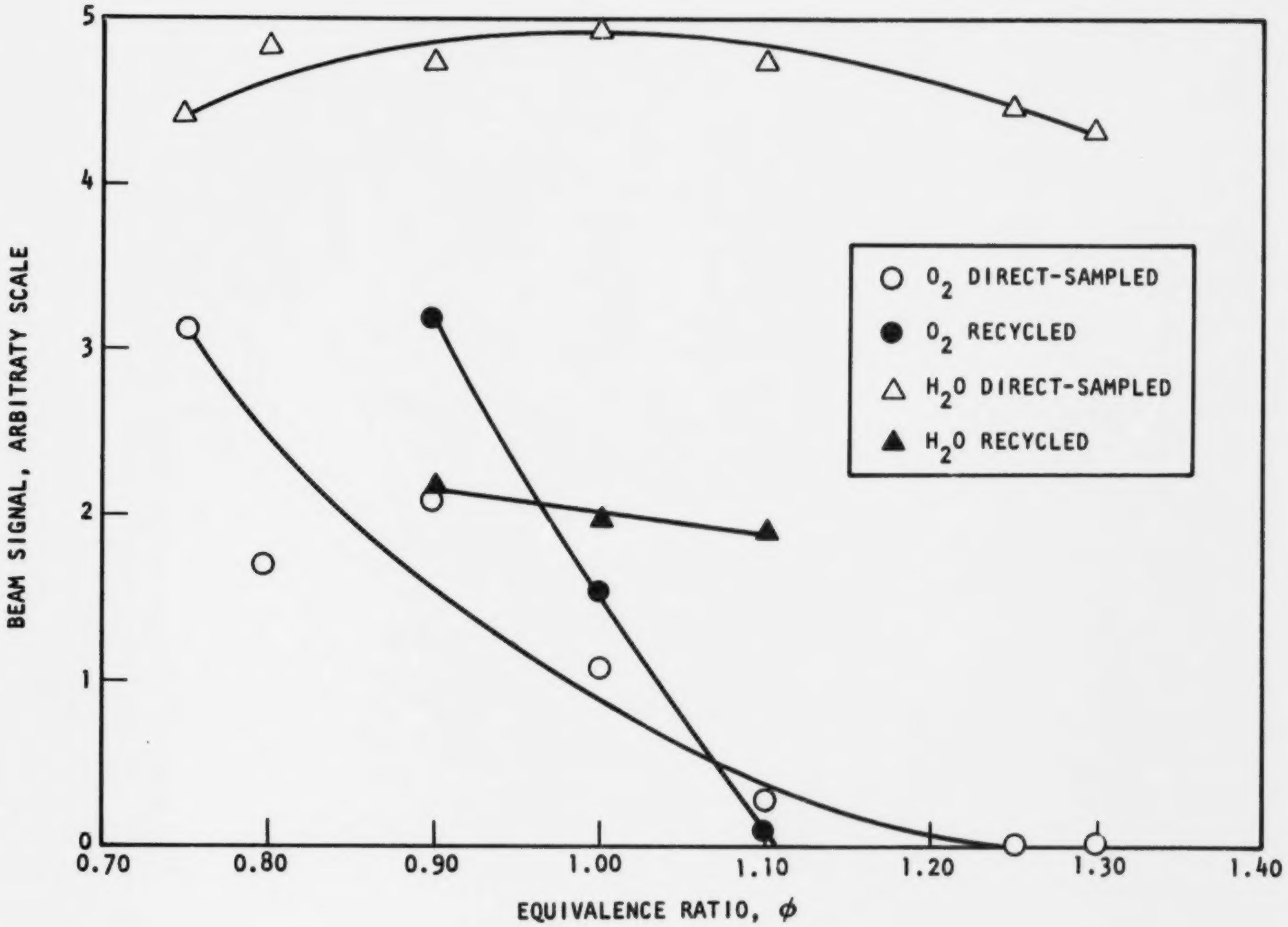

Figure 36. Beam signals for direct-sampled O_2 and H_2O and recycled O_2 and H_2O versus equivalence ratio for D = 2.00 inches

As the flame becomes fuel rich, the hydrogen atoms are consumed by

$$H + CH_4 \rightleftarrows H_2 + CH_3$$

Figure 33 shows that the H-atom signal increases as ϕ increases to 1.1 and then decreases as the flame becomes more fuel rich.

The presence of O atoms in the flame was deduced from the m/e = 16 signal. This signal represents, in general, both CH_4 and O atoms. Fristom (Ref. 16) concludes that CH_4 disappears within the first few millimeters of the reaction zone. The possible chemical reactions for this disappearance are:

$$CH_4 + OH \rightleftarrows CH_3 + H_2O$$

$$CH_4 + H \rightleftarrows CH_3 + H_2$$

$$CH_4 + O \rightleftarrows CH_3 + OH$$

$$CH_4 \rightleftarrows CH_3 + H$$

$$CH_4 + O_2 \rightleftarrows CH_3 + HO_2$$

$$CH_4 + HO_2 \rightleftarrows CH_3 + H_2O_2$$

In the present studies, the distance from the reaction zone to the sampling orifice was always equal to or greater than about 2 cm. Furthermore, no CH_2 or CH_3 (CH_4-fragment) signals were observed. (In heated-effusive-source calibrations for CH_4-N_2 at an ionizing electron energy of 20 ev, CH_3 and CH_2 fragments of CH_4 had been observed.) Therefore, the contribution of CH_4 to the m/e = 16 signal can be completely ignored and the beam signal in Fig. 33 for m/e = 16 represents only O atoms.

When CH_4 disappears in the flame, CH_3 radicals are formed. However, CH_3 was not observed in the samples. Perhaps the CH_3 was consumed by the reactions

$$CH_3 + O_2 \rightleftarrows H_2CO + OH$$

$$CH_3 + O \rightleftarrows H_2CO + H$$

The OH radical is very important in the methane flame. In order to isolate the OH signal from the m/e = 17 signal, the contribution caused by fragmentation of H_2O was established through a heated-effusive-source calibration. The resulting OH radical signal is shown also in Fig. 33. The OH is produced by means of

$$H + O_2 \rightleftarrows OH + O$$

$$O + H_2CO \rightleftarrows OH + HCO$$

$$O_2 + CH_3 \rightleftarrows OH + H_2CO$$

The measured mole fractions of CO and CO_2 versus equivalence ratio are displayed in Fig. 34. As expected, the mole fraction of CO increases, because of the incomplete combustion of the fuel, as ϕ increases. In methane-air flames, it is believed that the main sources of CO are

$$H_2CO + M \rightleftarrows CO + H_2 + M$$

$$H_2CO + OH \rightleftarrows HCO + H_2O$$

$$HCO + OH \rightleftarrows CO + H_2O$$

where M is an inert species. The mole fraction of CO_2 peaks in the neighborhood of $\phi = 1$. CO_2 is formed, and CO disappears, according to

$$CO + OH \rightleftarrows CO_2 + H$$

H_2 and NO mole fractions versus equivalence ratio are displayed in Fig. 35. H_2 appears, in fuel-rich flames, for $\phi > 1.10$. The concentration of NO increased from 80 ppm at $\phi = 0.75$ to 500 ppm at $\phi = 1.30$. NO is formed by the mechanism

$$N_2 + O \rightleftarrows NO + N$$

$$N + O_2 \rightleftarrows NO + O$$

Qualitative O_2 and H_2O signals versus equivalence ratio are given in Fig. 36. It is seen that the concentration of O_2 decreases as the flame becomes more fuel rich. The concentration of H_2O also peaks in the neighborhood of $\phi = 1$. The main source of H_2O is $CH_4 + OH \rightleftarrows CH_3 + H_2O$.

Temperature Measurements

Results from time-of-flight and thermocouple measurements of temperatures in methane-air flames are compared in Fig. 37. (See Appendix C for tabulated data.) TOF measurements were made at sampling to flame-holder distances of 1.00, 2.00, and 3.00 inches and thermocouple measurements were made at a sampling to flame-holder distance of 2.00 inches. As shown in Fig. 37, the flame temperature decreased as the flame holder to sampling orifice distance increased. The maximum temperature (2209 K) occurred at $\phi = 1.00$ and the minimum distance for which measurements were made, namely 1.00 inch. For the distance at which both TOF and thermocouple measurements were made (namely, D = 2.00 inches), the thermocouple measurements gave values about 400 to 500 K lower than the TOF measurements. This difference was attributed to the fact that the thermocouple had not been shielded against radiation losses to the surroundings.

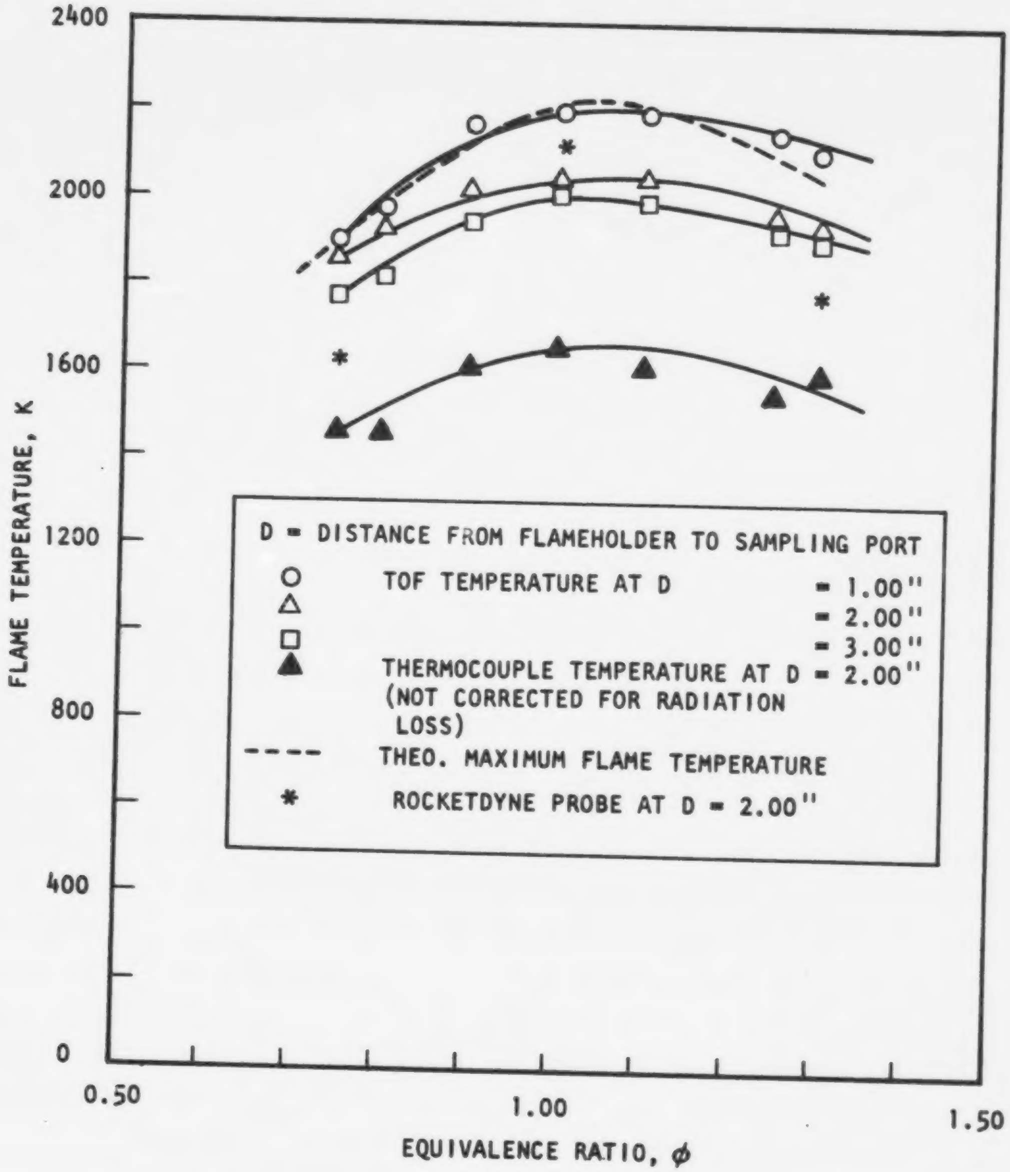

Figure 37. TOF and thermocouple measured flame temperatures versus equivalence ratio

H_2 and NO mole fractions versus equivalence ratio are displayed in Fig. 35. H_2 appears, in fuel-rich flames, for $\phi > 1.10$. The concentration of NO increased from 80 ppm at $\phi = 0.75$ to 500 ppm at $\phi = 1.30$. NO is formed by the mechanism

$$N_2 + O \rightleftarrows NO + N$$

$$N + O_2 \rightleftarrows NO + O$$

Qualitative O_2 and H_2O signals versus equivalence ratio are given in Fig. 36. It is seen that the concentration of O_2 decreases as the flame becomes more fuel rich. The concentration of H_2O also peaks in the neighborhood of $\phi = 1$. The main source of H_2O is $CH_4 + OH \rightleftarrows CH_3 + H_2O$.

Temperature Measurements

Results from time-of-flight and thermocouple measurements of temperatures in methane-air flames are compared in Fig. 37. (See Appendix C for tabulated data.) TOF measurements were made at sampling to flame-holder distances of 1.00, 2.00, and 3.00 inches and thermocouple measurements were made at a sampling to flame-holder distance of 2.00 inches. As shown in Fig. 37, the flame temperature decreased as the flame holder to sampling orifice distance increased. The maximum temperature (2209 K) occurred at $\phi = 1.00$ and the minimum distance for which measurements were made, namely 1.00 inch. For the distance at which both TOF and thermocouple measurements were made (namely, D = 2.00 inches), the thermocouple measurements gave values about 400 to 500 K lower than the TOF measurements. This difference was attributed to the fact that the thermocouple had not been shielded against radiation losses to the surroundings.

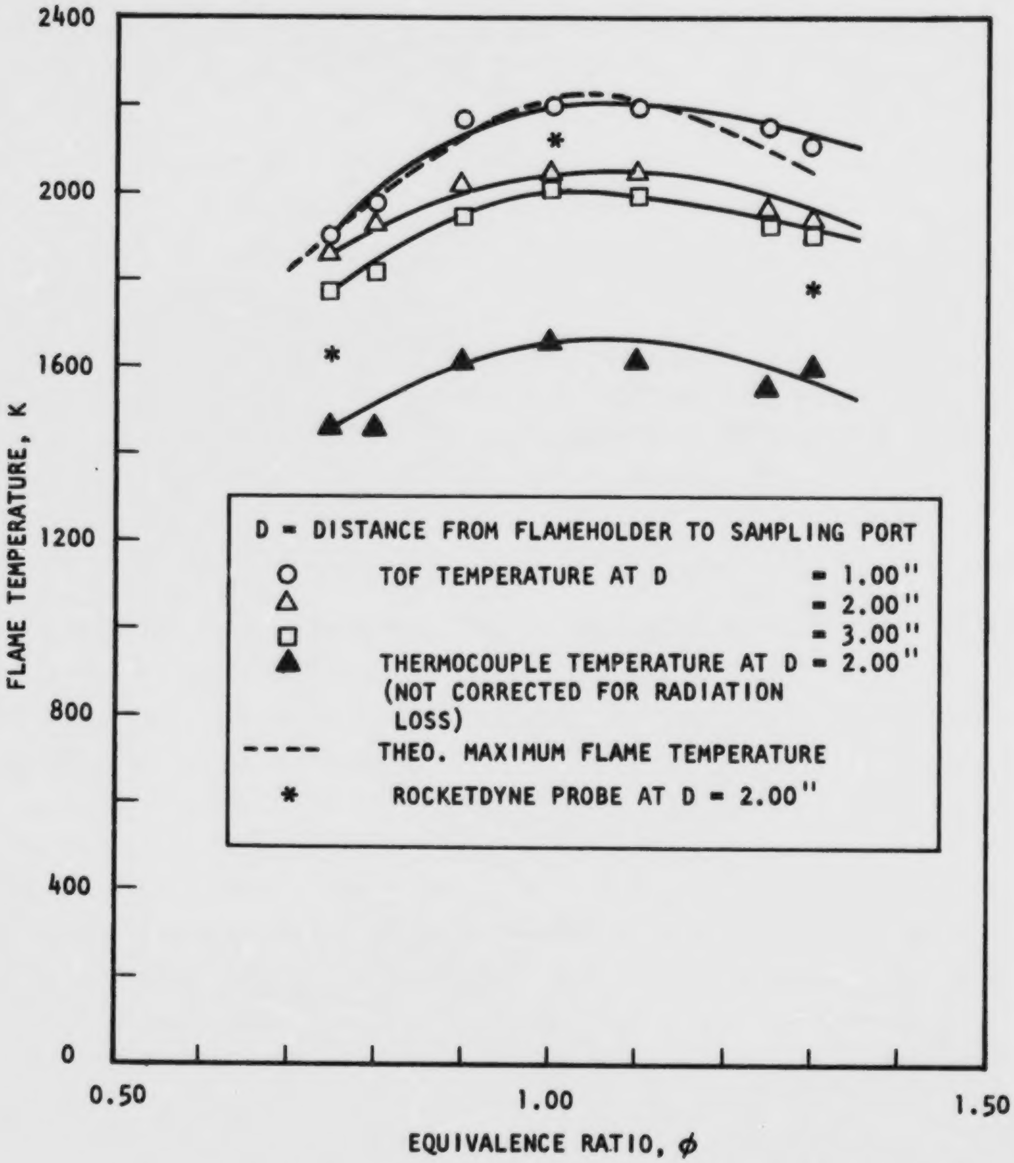

Figure 37. TOF and thermocouple measured flame temperatures versus equivalence ratio

VERIFICATION TESTING OF ROCKETDYNE PROBES

Both the temperature and species probes were taken to UCLA for comparative testing with the UCLA molecular beam/time-of-flight technique.

A short series of simultaneous flame temperature measurements at various equivalence ratios was made at UCLA with the Rocketdyne temperature probe and the UCLA technique. For these tests, a 4-foot-long quartz tube was used. The tube had a small hole on one side to permit insertion of the temperature probe (perpendicular to the flame and tube axis) and a larger hole to permit insertion of the conical quartz probe of the molecular-beam system directly opposite the probe. Measurements were made simultaneously at an axial distance of 2-inches with both measurement techniques. Data obtained using the molecular beam TOF technique resulted in the flame temperatures shown in Fig. 37. Data taken with the Rocketdyne temperature probe at equivalence ratios of 0.75, 1.0, and 1.3 resulted in flame temperatures denoted by the starred symbols in Fig. 37. Good agreement was obtained between the two techniques at $\phi = 1.0$, values of 2125 K and 2043 K being obtained with the Rocketdyne probe and the molecular-beam time-of-flight technique, respectively.* The agreement was not as good at off-stoichiometric conditions. The Rocketdyne probe resulted in flame temperatures of 1630 K and 1790 K at equivalence ratio of

---

*A theoretical maximum flame temperature of 2340 K is reported by Perry (Ref.17) who also reports an experimental determination of 2148 K obtained with the sodium line reversal technique. The theoretical flame temperature calculated as a function of equivalence ratio using the Rocketdyne n-element propellant performance program (See Appendix D) is also indicated in Fig. 37.

0.75* and 1.30, respectively, while the TOF technique resulted in temperatures of 1861 K and 1918 K at the corresponding equivalence ratios.

In addition, comparison tests were made with the species probe and the UCLA MBMS technique. These measurements were conducted consecutively, not simultaneously, because the UCLA mass spectrometer was used to analyze the composition of the samples obtained with both techniques. The UCLA MBMS technique was first used to obtain flame composition as a function of equivalence ratio. These direct sampling results are shown in Fig. 33 through 36 described previously. The methane/air gas burner was then repositioned to allow a gas sample to be withdrawn from the flame through the Rocketdyne species probe, cooled by passage through a cold trap (placed in an ice bath), and then passed directly into the pinhole at the end of the conical quartz probe of the MBMS system. The sample gas bypassing the MBMS system flowed into either a single pump for recycling or three other pumps for exhausting to the atmosphere (Fig. 28). Approximately 25-percent recycle was, therefore, used in this test series.

Species measurements, made earlier at Rocketdyne, involved the use of more sophisticated devices for removal of water from the combustion gas sample. Approximately 100 percent of the water contained in the combustion gas was removed in the previous tests at Rocketdyne. The less sophisticated water removal device installed temporarily at UCLA for verification testing of the species probe was apparently successful in removing (by condensation of the ice bath) only about 60 percent of the water from the combustion gas (Fig. 36).

Results from the spectrometer analysis of the gases withdrawn through the Rocketdyne species probe with internal recycle are shown in Fig. 34 through 36 for comparison with previous direct-sampling results. Caution should be used, however, in making direct comparisons between the "direct sampled" and "recycled" curves shown in Fig. 34 through 36. This is because, according to the H_2O curves in Fig. 36, the "recycled" curves represent combustion gas data in which 60 percent of the water has been removed. The "direct sampled" curces, on the other hand, represent data in which no water removal has taken place.

---

*It is recalled that previous preliminary testing of the temperature probe at Rocketdyne had yielded a temperature of 1626 K at ER = 0.75.

In Fig. 34, the CO_2 "direct-sampled" data agrees excellently with the theoretical results tabulated in Appendix D. The CO "direct-sampled" results, however, are significantly less than the theoretical results of Appendix D. This, perhaps, is indicative of the unattainment of thermal equilibrium in the flame at the sample distance (2 inches). If the "direct-sampled" measurements were reported on a water-free basis, the "direct-sampled" mole-fractions would be increased by approximately 20-percent. This would yield excellent agreement with the CO_2 "recycled" curve shown in Fig. 34, but a wide difference with the CO "recycled" curve would still exist. Calculations made on a 60-percent water-free basis would, of course, yield results in between the "direct-sampled" and 100-percent water-free results.

In Fig. 35, the "direct-sampled" data for NO and H_2 were approximately an order of magnitude and two orders of magnitude, respectively, below the theoretical concentrations found in Appendix D. The "recycled" data fell below the "direct-sampled" data, as shown in Fig. 35, on either an uncorrected or a water-free basis.

Comparison of the O_2 "direct-sampled" and the O_2 "recycled" data shown in Fig. 36 revealed that, if the direct-sampled data was converted to a 60-percent water-free basis, the amount of O_2 measured using the Rocketdyne probe was greater than that measured employing the MBMS technique over almost all of the 0.90 to 1.10 range of equivalence ratio.

Thus, in summation, passage of the sample gas through the Rocketdyne probe eliminated the radicals H, OH, O, and increased the measured concentrations of CO_2, CO, and O_2. The measured increases in the latter three species were not anticipated and merit further investigations. Less nitric oxide was observed in the "recycled" gases than in the direct-sampling gases. Possibly some of the NO was converted to O_2 and N_2 inside the probe. No H_2 was detected because comparisons were restricted to $\phi = 0.90$, 1.00 and 1.10.

CONCLUSIONS

Velocity, species and temperature probes for application in "dirty flame" environments have been designed and fabricated. These probes were designed based upon a review of the current literature and possess those characteristics believed to be necessary for successful application in dirty flames. This does not preclude, however, the likely need for periodic probe cleaning and/or maintenance.

The operation of these probes was evaluated in a premixed gas flame, and successful operation was indicated. The temperature and species probes were also evaluated relative to a known "standard" of the molecular beam technique, in a premixed gas flame. Again, successful operation was indicated, although some differences were observed.

The evaluation of the developed probes in a residual oil flame (or other "dirty flame" environment) is needed to verify their suitability. The results of such tests should be obtained before more advanced probe designs (such as combination probes) are undertaken.

Included in this report are relations necessary to estimate requirements, such as cooling water flow and allowable cooling water ΔP, which are needed for testing of the developed probes in other experimental situations.

REFERENCES

1. Beér, J. M., N. A. Chigier, G. Koopmans, and K. B. Lee. Measuring Instruments for the Study of Flame at Ijmuiden. International Flame Research Foundation Doc. nr. 72/a/9, Ijmuiden, Holland, May 1966.

2. Dickerson, R. A., A. S. Okuda, and C. L. Oberg. Design of an Optimum Oil Burner for Control of Pollutant Emissions. Report No. R-9465. Rocketdyne Division, Rockwell International, Canoga Park, California, February 1974.

3. Vizioz, J. P., and W. Leuckel. Méthodes et instruments utilisés à la Station Expérimentale de la F.R.I.F. pour des mesures dans les flammes de diffusion. (Instrumentation Methods Used at the F.R.I.F. Experimental Station for Diffusion Flame Measurements). Communication présentée à la Conférence "I Problem della Combustione - Bruciatori" de l'Associazone Termoteenica Italiana, Milan, 18 through 19 June 1969.

4. Chedaille, J., and Y. Braud. Industrial Flames, Vol. 1, Measurements in Flames. Crane, Russak & Co., Inc., New York, New York, 1972.

5. Heap, M. P. Private communication, December, 1972.

6. Temperature - Its Measurement and Control in Science and Industry. Vol. III, Part 2, Section IV, Articles 53-57, Reinhold Publ. Co., 1962.

7. Clark, J. A., and W. M. Rohsenow. A New Method for Determining the Static Temperature of High-Velocity Gas Streams. Trans. ASME. Feb. 1952, pp 219-228.

8. Godridge, A. M., R. Jackson and G. G. Thurlow. The Venturi Pneumatic Pyrometer. Journal of Scientific Instruments. Vol. 35, March 1958, pp. 81-88.

9. Holland, R. E., R. Jackson and G. G. Thurlow. The Behavior of the Venturi Pneumatic Pyrometer in Industrial Furnaces. Jour. of Institute of Fuel. April 1960, pp. 180 through 187.

10. Peacock, G. R. Land Instrument Co., Private Telephone Communication, December 11, 1972.

11. Milani, A., and W. Leuckel. Experimental Studies on the Venturi Pneumatic Pyrometer. International Flame Research Foundation Doc. nr. F72/a/14, Ijmuiden, Holland, March 1969.

12. Howard, J. B., and R. H. Essenhigh. Pyrolysis of Coal Particles in Pulverized Fuel Flames. IEC Process Design and Development, Vol. 6, p. 74, January 1967.

13. Young, W. S. An Arc-Heated Ar-He Binary Supersonic Molecular Beam with Energies Up to 21 ev. Report No. 69-39. Los Angeles: Department of Engineering, University of California, 1969.

14. Alcalay, J. A. and E. L. Knuth. Molecular-Beam Time-of-Flight Spectroscopy. Rev. Sci. Instr. 40:438, 1969.

15. England, C. Quantitative Evaluation of Reduction Techniques for Oxides of Nitrogen. Report No. 1200-37. Pasadena: Jet Propulsion Laboratory, California Institute of Technology, 1972.

16. Fristrom, R. M. and A. A. Westenberg. Flame Structure. New York: McGraw-Hill, 1965.

17. Chemical Engineers' Handbook. John H. Perry, Editor, Third Edition, McGraw Hill Book Co., 1950, p. 1589.

APPENDIX A.

FLAME MEASUREMENT TECHNIQUES APPEARING IN THE LITERATURE

LITERATURE SEARCH

In order to determine the measurement techniques most applicable to the characterization of "dirty" flame environments, a computer search of the combustion technique was made available at the program outset. The search included Rockwell International library holdings, as well as NASA and DDC searches. Among the available techniques for flame characterization reported in the literature are those summarized below.

TEMPERATURE MEASUREMENTS

Thermoelectric Thermometry

Potentially, the most simple temperature-sensing device is a thermocouple. A Pt/Pt-13 percent Rh thermocouple has been used to measure temperatures of 500 to 2100 K in swirling propane-air and butane-air flames (Ref. A-1). The thermoelectric sensor, however, must itself be in thermal equilibrium with the media being measured. This presents several problems. The thermocouple material must adequately withstand operation at the media temperature and cannot participate either directly or as a catalytic agent in chemical reactions with the surrounding high-temperature oxidizing or reducing gases. Thermocouple materials such as Ir/Ir-Rh or W/W-Re can participate directly in reduction or oxidation processes, respectively, while combinations such as Pt-4 percent Rh/Pt-20 percent Rh do not participate directly, but may act in a catalytic manner. Catalytic effects can have a notable influence on indicated temperature, particularly when there are nonequilibrium chemical species caused by nonequilibrium of reactions such as $N_2 + O_2 \rightarrow 2NO$ that could be catalyzed by metallic sensor surfaces. For example, at 20-percent excess air with No. 2 fuel oil, catalytically forcing completion of the NO formation reaction (endothermic) can reduce the flame temperature by almost 150 F. If a thermocouple surface were catalytic to the NO formation reaction, this reduction in flame temperature would be a localized phenomenon at the surface of the thermocouple, affecting the temperature indication, but not the bulk temperature of the combustor. Errors caused by catalytic effects can be minimized by coating the thermocouple with noncatalytic material and/or by increasing the rate of forced convection over the sensor. Coating with materials such as SiO_2 or Al_2O_3 reduces the likelihood of catalytic action. Conversely, very high rates of forced convection can saturate the catalytic-reaction-rate capability of the metallic surface, while enhancing heat transfer from the surface so that the heat transferred to the surface far overwhelms the endothermic effects of chemical reaction. This results in the sensor temperature closely approaching the bulk gas temperature in spite of endothermic reaction catalysis. A combination of coatings and high-convection rate taken together provides the best assurance that catalytic effects will be minimized. For the high temperatures found in flames, the usual SiO_2 coatings are not usable because of melting and higher temperature materials, such as Al_2O_3 or NBS ceramic coating A418, should be used.

An additional problem that arises when the sensor must reach thermal equilibrium with the high-temperature bulk gas is the loss of heat from the sensor by radiation to cool walls of the combustor. At temperatures above 2000 F, unshielded thermocouples can give temperature indications up to several hundred degrees too low, depending on the absolute temperature, geometry, temperature of the surrounding walls, opacity of the combustion gas, and local flow conditions. The usual method for reducing radiation losses from thermocouples is to surround the device with multiple radiation shields and to attempt to equilibrate the radiation shield and thermocouple temperatures to the bulk gas temperature by forced convection (Ref. A-2 and A-3). Corrections for radiation losses from the sensor head may also be made based on literature recommendation (Ref. A-4 and A-5).

In the noble metal suction pyrometer combustion gas is aspirated at high speed through a tube having a thermocouple on its axis, and surrounded by multiple concentric, ceramic radiation shields. Aspiration of gas through such a device tends to disturb the normal fluid dynamics of the combustion process, depending on the aspiration rate, however, it is helpful in maximizing heat transfer from the gas to the couple and minimizing catalytic reaction errors. Radiation shields are necessary to minimize radiative heat flow between the thermocouple and the walls of the combustion chamber or surroundings. According to Ref. A-6, a water-cooled suction pyrometer with a Pt/Pt-13 percent RH couple should be good for continuous use up to 1800 C (3280 F). An Ir-Ir/40 percent RH couple is more brittle, but could operate up to 2000 C (3630 F), while a W-W/26 percent Re couple could go up to 2800 C (5070 F) but only in a neutral or reducing atmosphere, all according to Ref. A-6 . Units of the Pt-Pt/13 percent Rh type are available commercially. The design of suction pyrometers is discussed in Ref. A-4. The suction pyrometer is used extensively in "dirty" flame environments at the International Flame Research Foundation in Ijmuiden, Holland (Ref. A-7).

Reference A-8 reports the application of a platinum resistance thermometer in an acetylene-oxygen flame at 2200 C (3990 F). It was necessary to make independent measurement of the emissivity of the platinum surface and take into account heat transfer and catalytic effects. Commercial resistance thermometers are said to be available in the range from 600 C (1110 F) up to 1400 C (2600 F), Ref. A-6 .

The compensated hot-wire method of flame temperature measurement is applicable to transparent flames in a region where burning is complete and involves compensation by electrical resistance heating of an immersed wire for radiation and conduction losses. The wire temperature is read by an optical pyrometer, corrected for wire emissivity, and a vacuum calibration is needed. This method has been in use for several decades (e.g., to measure flames at 1800 C (3270 F), Ref. A-9, and is applicable to transparent flames in a region where burning is complete, so that no chemical reactions take place on the wire.

The time response of thermocouple or resistance thermometer probes is dependent upon the geometrical size of the probe and the convective heat-transfer rate to the probe. Smaller probe size provides more heat-transfer surface area per unit thermal capacitance (mass), thus allowing the probe sensor to change temperature more rapidly in response to changes in flowfield temperature. Greater convection also increases the time response of the sensor to changes in flowfield temperature. In the case of radiation shielded temperature sensors, it is not only the mass and convective heat transfer to the sensor that is important, but also the size and convection heat transfer to the radiation shields. If the turbulent temperature fluctuations are large, it is necessary that the temperatures of the radiation shields also follow the fluctuating temperature of the flowfield, or else a fluctuating radiation error will be introduced into the temperature measurement. If the flowfield temperature fluctuates rapidly about some mean value and if the temperature sensor is small enough to follow the fluctuations, then the average indicated temperature will be nearly equal to the true average temperature, but the fluctuations will be reduced in amplitude because when the thermocouple is hotter than the sluggish radiation shields it will lose heat to the shields by radiation, and when the thermocouple is colder than the shields, it will be heated above the local gas temperature by radiation received from the shields. To obtain best response, it is therefore necessary to minimize size and maximize convection to both the temperature sensor and the associated radiation shields.

Other, less direct methods of flame temperature measurements such as pneumatic (choked flow), velocity of sound, optical probes, and molecular-beam mass spectrometry are available, which allow temperature determination without the necessity of having a sensor equilibrate to the same temperature as the gas being measured. Therefore, these methods avoid the materials problems and radiation corrections characteristic of the equilibrated devices.

Pneumatic Temperature Probes

A pneumatic probe depends on the application of the continuity equation to a continuously flowing sample of flame gas and provides an indication of temperature based on the maximum, choked-flow mass flux through a nozzle. Usually, two nozzles are used in series (Ref. A-10 and A-11). The flow entering the first nozzle is at the local flame temperature, and is not allowed to undergo any significant cooling during passage through the first nozzle. The gas flow is cooled in a heat exchanger between the two nozzle throats. The function of the second nozzle is to determine, from the easily measured cool stagnation temperature in the second throat, the product of flowrate and a function of gas molecular weight and specific heat ratio. The equation by which temperature is determined from pneumatic probe measurement is:

$$T_1 = \left[\frac{C_{w_1}^2 \; A_1^2 \frac{\gamma_1}{M_1} \left(\frac{2}{\gamma_1+1}\right)^{\frac{\gamma_1+1}{\gamma_1-1}}}{C_{w_2}^2 \, A_2^2 \frac{\gamma_2}{M_2} \left(\frac{2}{\gamma_2+1}\right)^{\frac{\gamma_2+1}{\gamma_2-1}}} \right] \frac{P_{01}^2}{P_{02}^2} \; T_2$$

or

$$T_1 = K \frac{P_{o_1}^{\;2}}{P_{o_2}^{\;2}} T_2$$

With

$$K = \left[\frac{C_{w_1}^2 \; A_1^2 \; \frac{\gamma_1}{M_1} \left(\frac{2}{\gamma_1+1} \right)^{\frac{\gamma_1+1}{\gamma_1-1}}}{C_{w_2}^2 \; A_1^2 \; \frac{\gamma_1}{M_2} \left(\frac{2}{\gamma_2+1} \right)^{\frac{\gamma_2+1}{\gamma_2-1}}} \right]$$

where T_1 = flame temperature

T_2 = cooled gas temperature, entering the second nozzle

P_o = stagnation pressure entering the nozzle

C_W = nozzle discharge coefficient

A = nozzle area

M = gas molecular weight

γ = gas specific heat area

1,2 = subscripts relating the specific parameter to either the first or the second nozzle

K = a collection of parameters frequently assumed to be constant

The calibration parameter, K, includes the influences of specific heat ratio, γ, and gas molecular weight, M. In the use of pneumatic probes for temperature measurement, it is usually assumed that the molecular weight does not change during the cooling process between the nozzles and, also, specific heat ratio is assumed constant. Under these assumptions, it is not practical to allow partial condensation of species such as water because this would have strong effect on the molecular weight (gas density). Similarly, for accurate temperature determination, all chemical reaction must stop on entry of the combustion gases into the first nozzle. If suspended solids are present, they must be considered. Generally, they add mass, but little volume to the gas in the continuity calculations.

The parameter K is frequently assumed to be, though not necessarily, a constant. The parameter K is usually determined by calibration in a flow of a known temperature, though it is possible to calculate K from knowledge of nozzle throat areas, discharge coefficients, and gas properties. The calibration is performed in position using room temperature air. When the pneumatic probe is calibrated in an inert gas that differs in temperature from the combustion gas to be ultimately measured, it becomes necessary, for small nozzles, to correct for Reynolds number effects on the nozzle discharge coefficients, C_w.

The pneumatic venturi pyrometer has been employed in "dirty" flame environments at the IFRF in IJmuiden, Holland (Ref. A-7).

The temperature-measuring time response of the pneumatic probe is dependent on the volume of the heat exchanger between the two nozzles of the probe, because it is the volume of this chamber that must be pressurized and depressurized to follow temperature fluctuations. The response time of a pneumatic probe is given approximately by the relationship:

$$t = \frac{v/A_{t_1}}{\left(\gamma RTg\right)^{1/2}}$$

where t = a time characterizing the response of the pneumatic probe

A_{t_1} = throat area of the probe entry nozzle

γ = specific heat ratio of combustion gas

R = universal gas constant

T = combustion gas temperature

g = gravitational constant

M = gas molecular weight

v = cooling chamber volume

For a 1-millisecond response time and typical combustion gas, the above equation requires the ratio of v/A_{t_1} to be approximately equal to 3 feet. If the cooling chamber were twice the diameter of the throat, the maximum allowable cooling chamber length would be approximately 8 inches to achieve the 1-millisecond response time. This does not include any effects of pressure transducer response time.

Velocity-of-Sound Method

It was suggested 100 years ago (Ref. A-12) that measurement of the velocity sound in a hot gas would be a way of finding the temperature of the gas if its thermocynamic properties are known. Measurement of sound velocity in combustion gases results in the determination of a value of $(\gamma T/M)^{1/2}$, where the ideal gas assumption is usually valid because of high temperature and 1 atmosphere pressure.

The ratio γ/M is nearly constant, and its estimation should result in less than 0.5- to 1.0-percent error on the final temperature determination. Velocity of sound measurements can be made either by noting the time of passage of a sound wave past two detectors, or by observation of the physical size of specially induced standing sound wave patterns. In both of these cases, on the order of 5 to 10 cm of sound wave path length is required to obtain a precise sound wave determination. This path length requirement infers very poor spatial resolution on the part of the sound velocity temperature measurement technique.

The velocity-of-sound method of temperature measurement has been applied to electric arc flames at 5500 K (Ref. A-13). Also, a method in which ultrasonic frequencies are used is described in Ref. A-14. It is, of course, essential to supply thermal protection to the sound source, typically an oscillating piezoelectric crystal.

Calorimetric Probes

These operate on the principle that the flame gas is aspirated through a sample tube located on the probe axis and in the process loses heat energy to the probe. Measurement of the transferred heat flux and of the exit temperature of the gas sample then gives the inlet temperature (really enthalpy) of the gas. In the steady-state version (Ref. A-15) all the heat transferred from the gas supply is absorbed by the coolant flowing through the probe body. A tare coolant temperature rise is measured with the probe immersed in the stream, but not aspirating a gas sample. This tare must be subtracted from the coolant temperature rise when a gas sample is normally aspirated. A "split-flow" probe (Ref. A-16) reduces the magnitude of the tare and claims higher accuracy. Another design (Ref. A-17) introduces an air gap between inner and outer coolant jackets to reduce probe heat losses. In the transient version (Ref. A-18) the walls of the sampling tube are insulated from the probe body, and the heat flux is obtained from transient temperature measurements along the sampling tube.

Optical Probes

Several optical techniques provide well-understood means for local temperature determinations without disturbing combustor physical processes. Methods of interferometry, pyrometry, radiometry, and absorption are all applicable to flame temperature measurement.

The simplest optical technique is pyrometry, in which essentially the flame brightness is measured by comparison with an object of known temperature, and related thereby to gas temperature. The absolute radiation pyrometer essentially finds the emissivity of the flame (and hence the temperature from the black-body radiation law) by viewing the flame against a mirror and also against a black background. Alternately, the apparatus may be calibrated against a standard tungsten lamp. References A-19 and A-20 are examples of this method, with photoelectric detection devices. This pyrometer is suitable for temperatures up to 2500 C (4570 F), according to Ref. A-6 . In the two-color pyrometer, the flame is observed in turn through two optical filters, each yielding a monochromatic color temperature. From the two observations, the flame temperature and absorptivity are determined.

A most obvious problem with pyrometry is the optical transparency of the flames at the visible wavelengths. For nearly transparent flames, pyrometric measurements must be made on volumes of gas large enough not to be "seen" through by the pyrometer to ensure that the temperature measurement turns out to be a gas temperature rather than a wall temperature for the opposite combustion chamber wall. The requirement for long optical paths essentially means that optical pyrometer techniques have poor spatial resolution of temperature. This poor spatial resolution can be improved by seeding the flame with material that reaches thermal equilibrium with the gas and emits strongly in the visible wavelengths. If solid particulate matter such as talcum powder (which emits as a gray or blackbody) is added, the flame becomes much less transparent and the usual flame pyrometer can be used directly with only a small correction for particulate size. If other materials (which vaporize and emit in spectra consisting of discrete lines) are added, and the brightness is measured only at a discrete line, then this pyrometric technique becomes known as the "line reversal" technique. In particular, if the additive is sodium ion, and the D line is selected, the method is a Na-D line reversal, the most commonly used line reversal method.

The sodium line reversal method has been in use for over 50 years (Ref. A-21). This method basically consists of introducing sodium onto the flame (e.g., by addition of small amounts of a sodium compound to the fuel) and shining a tungsten or xenon lamp through the flame and further onto the slit of a spectroscope. The electrical current to the lamp is adjusted until the sodium D doublet line seen through the spectroscope matches the brightness of the lamp background. Then the flame temperature is that of the lamp filament as read by an optical pyrometer. Numerous refinements have been devised, in some of which an interferometer takes the place of the spectrometer. This method is feasible for very hot flames, well above the 4500 F level. A temperature profile across a flame may be obtained by varying the optical depth.

Where additives must be used, line reversal is more desirable than addition of particulates because wideband or continuum emission from particulates can easily lead to significant cooling of the gas, which would not occur in the absence of the particles. Line reversal techniques, where energy is emitted only at a few specific wavelengths, do not drain as much thermal energy from the gas and, therefore, radiantly caused changes in temperature caused by the additive are not significant. Conversely, most line reversal method additives do not emit significantly below 2540 F and so the line reversal technique is not useful below this temperature.

Molecular Beam

Translational temperatures in gas flames can be determined directly from measurement of molecular speeds. This is accomplished by means of a molecular-beam sampling apparatus in conjunction with a time-of-flight mass spectrometer (Ref. A-22). The molecular-beam sampling apparatus causes gas withdrawn from a combustion process to undergo a very rapid expansion to supersonic velocities. The molecules that remain on or near the axis of this expanding flow are naturally those molecules whose velocity was directed in the axial direction at the end of transition from continuum to free molecular flow. The velocity of these molecules is statistically the same as the randomly directed molecular velocities of the gas when it was in the combustor, except that in the molecular beam, the velocity has been transformed so that it is essentially all in the axial direction. By intermittently chopping the molecular beam and measuring the time required for a chopped portion of the beam to arrive at the detector site in a time-of-flight mass spectrometer, it is possible to determine the average axial velocity of particular molecular species in the beam, and because this velocity is numerically equal to the randomly directed thermal velocities in the main combustion gas stream, the measured velocity is a direct indication of the mainstream temperature.

The molecular-beam method offers the advantage of temperature measurements without the need of blackbody or any other sort of temperature calibration. The calibration required is one of time (used in molecular-velocity determination), which can be performed very accurately. The molecular-beam technique also offers excellent response, well under one millisecond. However, the molecular-beam probe is generally associated with relatively large probes (90-degree cone typical), which might disturb flow patterns.

STABLE CHEMICAL SPECIES

The determination of stable-chemical species within a flame is generally conducted by either probe sampling or spectroscopic techniques.

Sampling Probes

Probe sampling techniques must make allowances for:

1. Continuous operation in a high-temperature environment
2. Minimizing physical disturbances to the combustor fluid dynamics and physical processes
3. Rapidly quenching the chemical reactions so that the composition of the gas analyzed is not influenced by reactions occurring within the probe.

Water-cooled sampling probes to measure flame composition are available as shelf and as specialty items from a number of suppliers. To approach sampling at a point, miniaturized probes are desirable. Miniaturization is expensive and also fraught with constructional difficulties in that it is hard to avoid coolant and gas leaks through joints of thin-walled metals exposed to relatively high temperature and often corrosive gases. This is particularly true of the probe tip, which is the least coolable part of the probe and the one that must assume special shapes.

Figure A-1shows three important probe tip design features. To get true samples at a point in a flame, the velocity of the sample through the probe should equal the stream velocity. This is especially important when solids are suspended in the sample. Such isokinetic sampling is ensured by matching probe inlet static pressure with stream static pressure by proper adjustment of the probe aspiration. In Fig. A-1, (a) shows that when this is done, the captured sample stream tube then equals the probe inlet size. When the sample must be quenched rapidly to freeze reactive consituents, a rapid-expansion inlet (b) and/or a diluent-quench inlet (c) can be used (Fig. A-1). In both cases, the temperature of the sample is reduced in microseconds to a level at which components of interest are fixed. The features discussed have been fabricated as part of specialty sampling probes.

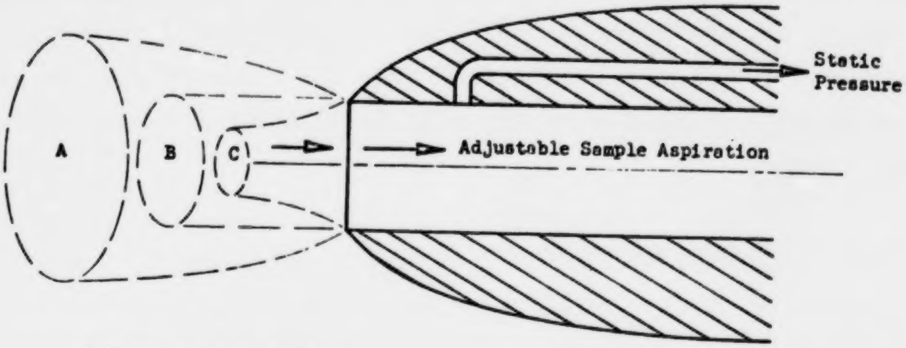
Static Pressure
A
B
C
Adjustable Sample Aspiration

(a) Isokinetic Sampling
(B is correct; A, C are incorrect)

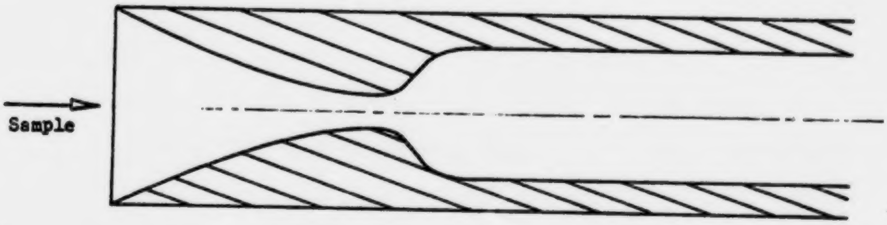

(b) Rapid Expansion Inlet

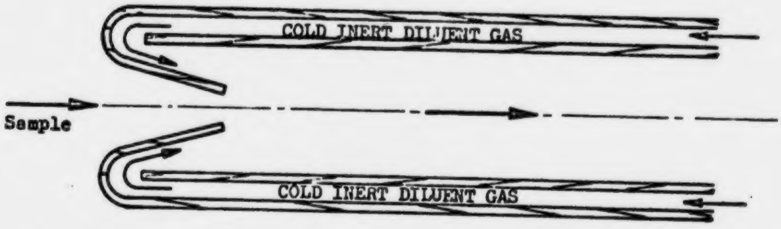
COLD INERT DILUENT GAS
Sample
COLD INERT DILUENT GAS

(c) Diluent Quench Inlet

Figure A-1. Features of composition sampling probes

An ordinary water-cooled probe (United Sensors) has been used successfully at Rocketdyne (Ref. A-23) to analyze the composition of typical distillate oil-burner flames. The results obtained are considered only near-quantitative in nature since the water-cooled probe does not offer the very short quench times required to absolutely ensure that the gas analysis corresponds exactly to the same concentrations as existed in the original flame.

Molecular Beam/Mass Spectrometer

Another method of rapidly quenching chemical reactions is to use a molecular-beam gas-sampling apparatus. As a sample removal technique, the molecular beam offers the most rapid possible quenching of chemical reactions. For a molecular-beam sample apparatus, gas is expanded from the zone of combustion through a small pinhole, as shown in Fig. A-2 into a high vacuum. This results in a Prandtl-Meyer expansion to supersonic speeds and low temperatures over a period of time as short as 0.1 microsecond. This aerodynamic expansion is continued until free molecular flow is achieved, and a portion of the expanded jet is skimmed and collimated to form a molecular beam for analysis by mass spectrometer. As described previously, this technique also is applicable for measurement of temperature, and it also is applicable to the determination of unstable species as described later.

Spectroscopy

Spectroscopic techniques offer additional methods for determination of chemical species in flame structures. Both emission and absorption characteristics can be used to identify various chemical elements within the flame. The infrared spectrum of the molecules in an air-oil flame are well known (Ref. A-24) at ambient conditions and recent work has made important contribution to the spectra at high temperatures. The spectrum of water will be dominant and carbon dioxide will also have some very strong bands. The band centers of the molecules of interest are listed in Table A-1.

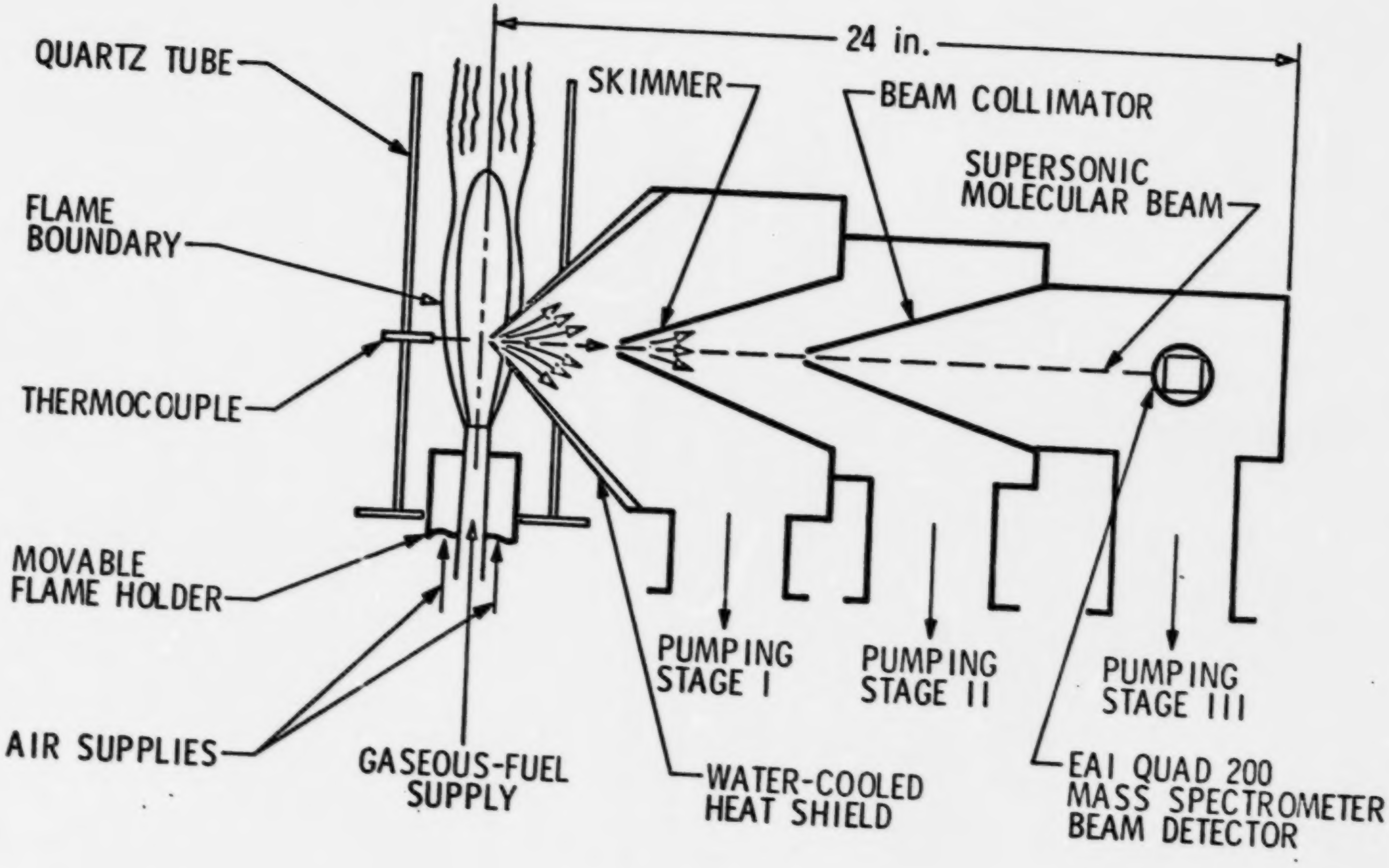
24 in.
QUARTZ TUBE
SKIMMER
BEAM COLLIMATOR
SUPERSONIC
MOLECULAR BEAM
FLAME
BOUNDARY
THERMOCOUPLE
MOVABLE
FLAME HOLDER
AIR SUPPLIES
GASEOUS-FUEL
SUPPLY
PUMPING
STAGE I
PUMPING
STAGE II
PUMPING
STAGE III
WATER-COOLED
HEAT SHIELD
EAI QUAD 200
MASS SPECTROMETER
BEAM DETECTOR

Figure A-2. Molecular-Beam Sampling System applied to flame studies

The species N_2, O_2, H_2 and Ar are not given because they are transparent.

Table A-1. SPECTRA OF SOME SPECIES IN AN OIL FLAME

H_2O	ν_1	3657 A°	ν_2	1593	ν_3	3756
CO_2	ν_1	[a]	ν_2	667	ν_3	2349
CO		2150				
SO_2	ν_1	1151	ν_2	519	ν_3	1361
NO_2	ν_1	1320	ν_2	648	ν_3	1621
NO		1890				

[a] Forbidden

The vibration-rotation bands of atmospheric pressure have a half-width of about 0.1 cm^{-1}. In low resolution spectra, the water and carbon dioxide would appear opaque throughout the middle infrared region (Ref. A-25) at temperatures over 2000 F. At high resolution, however, there would be very many small windows except near the water and carbon dioxide band centers (Ref. A-26). Use of high resolution is essential then to resolve the lines in emission. It is essential in absorption spectroscopy since the apparent intensity decreases rapidly when the resolution is less than line width. Achieving this resolution requires a monochromator with a focal length of at least one meter and an echelle grating at least 15 cm wide. Qualitative arguments indicate that, for instance, NO requires a pressure path length product of about 1 cm torr to be visible in absorption with a signal/noise ratio of 100. The limiting sensitivity then is better than 1 ppm for a burner 30 cm long.

Spectroscopic techniques offer the advantage of essentially zero interference with the physical and chemical processes occurring within the flame. However, to avoid such interference two alternatives are available:

1. Line of sight average path measurements with external optics
2. "Local" or "point" measurements with external optics

Average path measurements are not acceptable for nonuniform flowfields. For "local" or "point" measurements with external optics, a complex system is required and an entire matrix of data must be obtained.

UNSTABLE CHEMICAL SPECIES

Unstable species are, by their very nature, more difficult to determine than the stable species. The unstable species are very difficult to sample because their high reactivity leads to extremely short lifetime. Only two practical techniques for determination of the unstable species exist. These are molecular-beam sampling and spectroscopic methods.

Molecular Beam

Molecular-beam sampling offers very rapid transition of sampled material from the combustion zone to free molecular flow and is applicable to sampling of all of the unstable species of interest to the proposed program. Once the sample enters the free molecular flow regime, the molecules and radicals undergo no further reaction (other than perhaps spontaneous disintegration), because there are effectively no further collisions with other species before completion of mass spectrometric analysis of the sample.

Spectroscopy

Application of emission spectroscopy is difficult because emission depends not only on specie identity, but also on the mode and degree of excitation (temperature) of that specie. Since emission spectroscopy can be used only for vibrationally excited states, absorption techniques must also be employed to measure ground-state species that may dominate the distribution. However, because of limited available wavelengths for study of various species, the only radical specie that has been quantitatively studied in detail by this method is OH. For other radical species, there are no known convenient wavelengths at which detailed quantitative determination of species concentration are possible in the presence of the carbon continuum. Another problem arises from optical thickness and temperature gradients in thick-flame structures that tend to complicate the interpretation. The disadvantages of painstaking apparatus setup requirements and interpretation of experimental results are applicable to unstable species as well as stable species.

VELOCITY MAGNITUDE

Gas velocities can be measured by several techniques, depending on the particular environment of interest. Methods include pitot tube, hot-wire anemometry, mechanical anemometry, and pulsed tracer.

Modified Pitot Probes

Commercially available pitot probes can be used to obtain accurate velocity measurement in high-temperature gas streams. The pitot probe has an impact tap at the probe head and one or more taps located along the side of the probe. A measure of the local static pressure is obtained through the side tap. The dynamic pressure, which is a direct measure of the gas velocity, is then determined by use of a differential pressure measurement between the static pressure side tap and the impact probe tap.

Rocketdyne (Ref. A-23) has employed small pitot probes in dirty, but relatively low oil droplet density, combustion flames from domestic oil burners (distillate fuel oil). It was found that an 0.085-inch-ID, water-cooled pitot probe used in these dirty flames seldom plugs (mostly because no net flow passes through the probe), but occasionally suffers from the formation of oil meniscuses across the small diameter passages of the probe. To avoid errors caused by this effect, a purge system is installed to purge both the impact and the static pressure ports of the pitot probe before and after each measurement. This purging ensures that spurious pressures are not obtained as a result of pressure differences across the thin miniscuses.

In dense, two-phase (liquid-gas) flowfields the momentum of the liquid spray introduces errors in dynamic-pressure measurements that are used to infer gas velocities. Conventional gas-phase stagnation probes (pitot, etc.) are thus not applicable in dense two-phase sprayfields because of the interaction of the gas and liquid droplets near and within a conventional stagnation probe. A two-phase probe was developed at Rocketdyne (Ref. A-27) for measurement of local values of both liquid and gas mass fluxes in nonburning media. This probe is patterned after the Dussourd-Shapiro two-phase flow impact probe developed at MIT (Ref. A-28).

A schematic of the Rocketdyne probe, is presented in Fig. A-3. The probe was constructed of two concentric tubes (A and B) with a specially designed tip attached to tube B. The tip was designed to prevent the passage of liquid into the annulus formed by tubes A and B when the probe is used in high-mass-flow-ratio flowfields.

The operating principle for the determination of the gas-phase stagnation pressure by the concentric tube two-phase impact probe is illustrated in Fig. A-4. Basically, the intent is to decelerate the gas and measure the gas-phase stagnation pressure in a manner that minimizes momentum exchange from the condensed phase upstream of the measurement location. Droplets and gas (each at their own velocity) encounter the probe tip but the gas phase is stagnated at the probe tip where the pressure is approximately equal to the gas-phase stagnation pressure. Deviation from true gas-phase stagnation pressure is due to momentum exchange between the droplets and

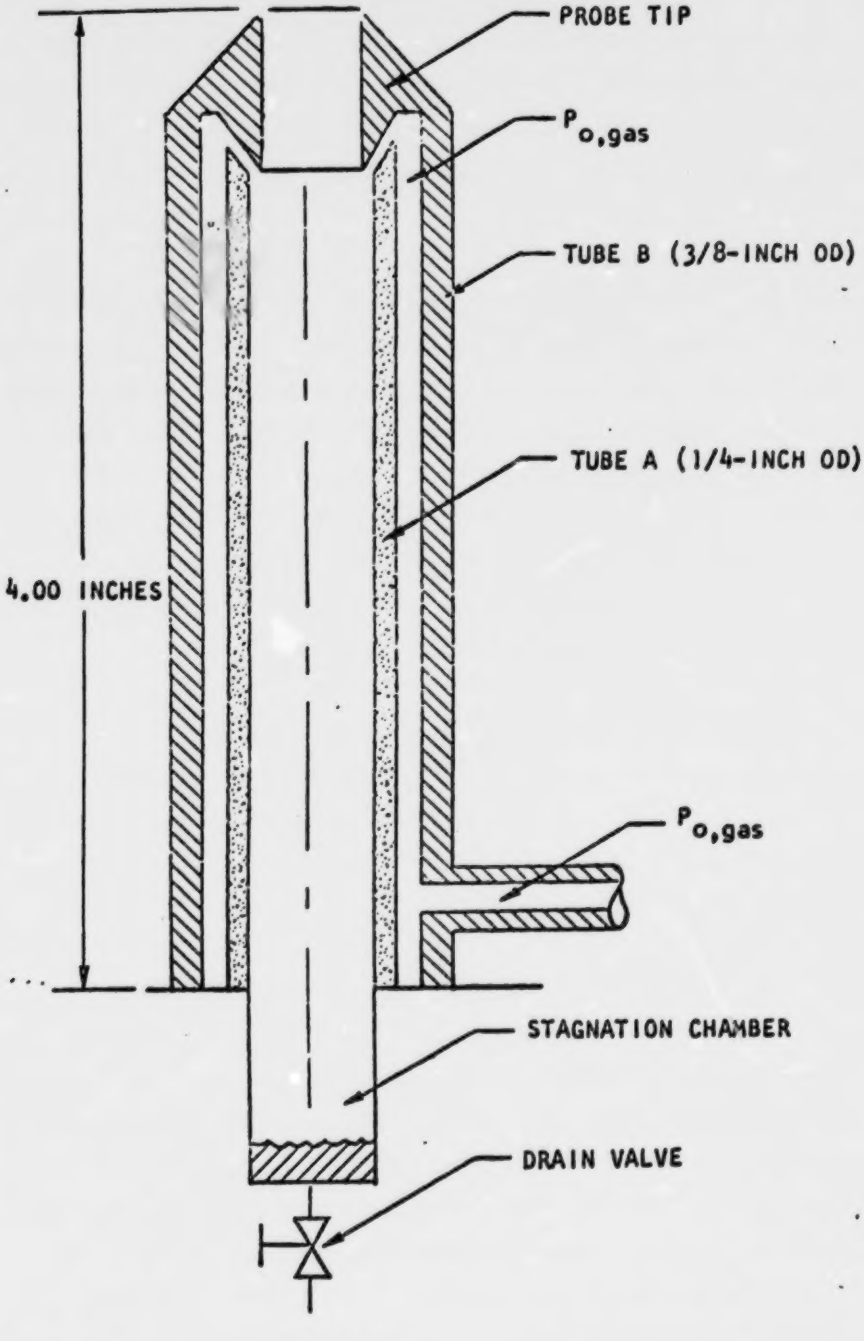
PROBE TIP
$P_{o,gas}$
TUBE B (3/8-INCH OD)
TUBE A (1/4-INCH OD)
4.00 INCHES
$P_{o,gas}$
STAGNATION CHAMBER
DRAIN VALVE

Figure A-3. Schematic of concentric tube two-phase impact probe

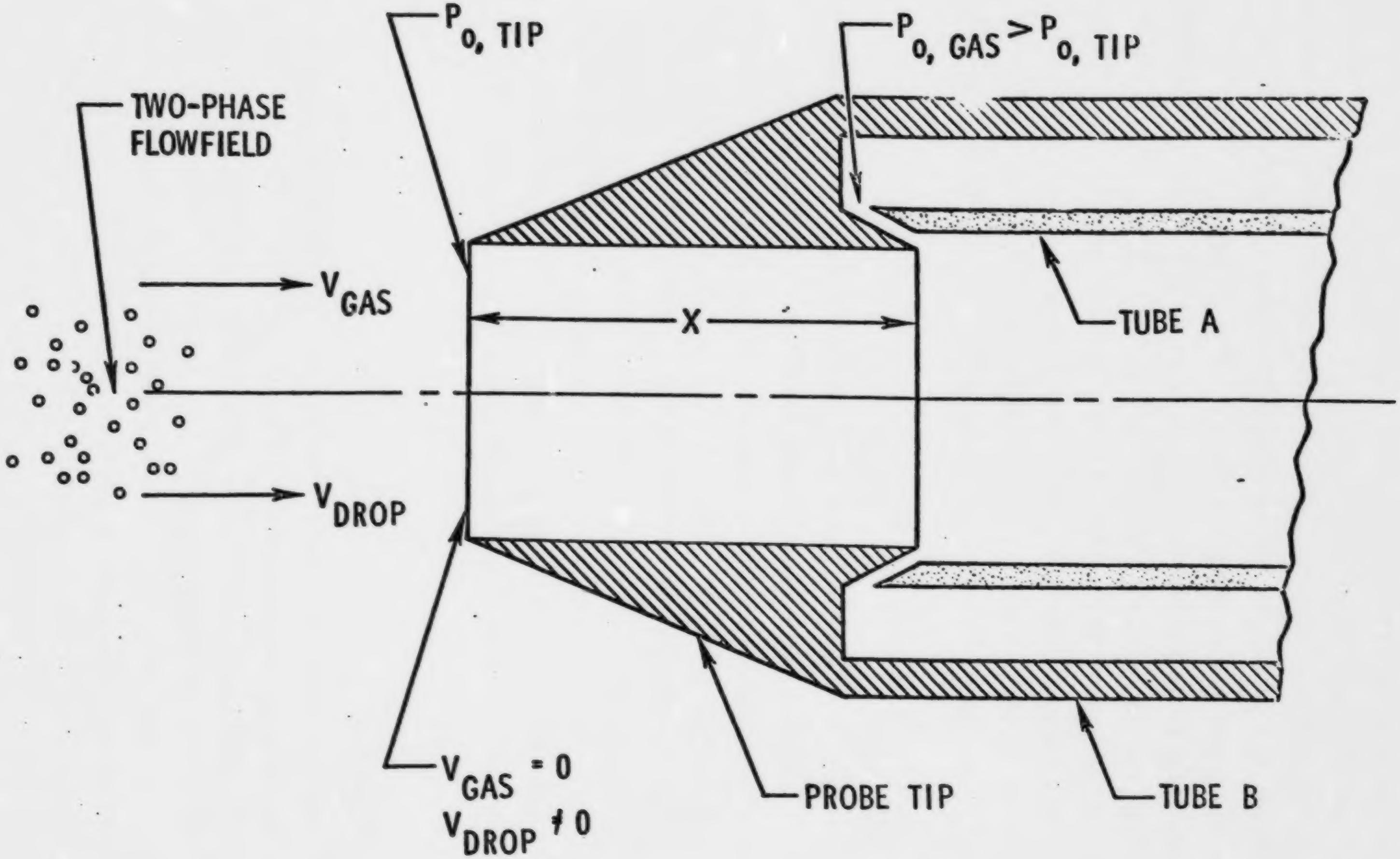
$P_{o,\ TIP}$
$P_{o,\ GAS} > P_{o,\ TIP}$
TWO-PHASE FLOWFIELD
V_{GAS}
X
TUBE A
V_{DROP}
$V_{GAS} = 0$
$V_{DROP} \neq 0$
PROBE TIP
TUBE B

Figure A-4. Principle of operation of two-phase probe the gas in the near flowfield of the probe tip (termed overpressure error). A droplet passes through the probe tip and is decelerated to zero velocity in the stagnation chamber formed by tube A. However, because of momentum exchange between the particles and the stagnated gas, the particles decelerate in the probe tip to some extent over the distance X (Fig. A-4). The gas-phase stagnation pressure, $P_{o,gas}$, as measured in the probe annulus is greater than the gas-phase stagnation pressure, $P_{o,tip}$. The difference between the two aforementioned pressures can be made small if the distance X is minimized. However, the total over-pressure error (caused by particle/gas momentum exchange both near and within the probe tip) can be determined by proper calibration of the probe in known two-phase flowfields.

Hot-Wire Anemometry

Hot-wire anemometry is another method for gas-velocity determination. For application to combustion processes, hot-wire anemometry is subject to considerable error because of flame temperatures and possible impingement of liquid droplets on the wire. The hot-wire techniques, therefore, are applicable only for nonspray cold-flow studies, or for use in zones of the combustion where ignition has not yet taken place and there are no liquid droplets or large, potentially wire-damaging particles in flight. The hot-wire technique offers excellent time resolution of velocities, so that it is readily feasible to study turbulence characteristics of the flow.

Mechanical Anemometry

Mechanical anemometry involves determination of velocities by the capability of the gas flow to cause movement of small, windmill-like structures. The most common application is in air-conditioning and heating-duct adjustment. For use with air, very sensitive mechanical anemometers are available at low cost from, for example, Anor Instrument Company, and are capable of measuring velocities as low as 1/3 ft/sec. Mechanical anemometers can be used with probes similar in design to an ordinary impact tube with air flow through a tube from the probe to the windmill indicating device. For use with combustion zones, mechanical anemometers require:

1. Calibration as a function of gas density
2. Parallel gas temperature and composition measurements
3. Accounting for gas temperature losses in the probe line to the windmill
4. Construction from corrosion-resistant materials
5. Capability for rapid and frequent cleaning to remove internal hydrocarbon and soot deposits.

Disadvantages of the mechanical anemometer are poor time resolution of velocity, typically a large probe size, and susceptibility of mechanical windmill bearings to the effects of dirt.

Pulsed Tracer

Pulsed-tracer techniques can be used to measure magnitude and/or direction of combustion gas velocity. An advantage of pulsed-tracer techniques is that velocity magnitude can be determined without knowledge of gas density. Therefore, it is not necessary to determine gas temperature and composition to obtain velocity. Also, pulsed-tracer techniques can easily be used in the dirty, sooty flames without unknown sacrifice of accuracy, because it is generally obvious when the apparatus is dirty enough to affect the velocity data.

Depending on the particular pulsed-tracer technique selected, care may be necessary to avoid unduly disturbing the flow patterns in the combustion process by the system for injecting the tracer, by the presence in the combustion process of the tracer itself, or by the downstream detector for the tracer. The pulsed-tracer technique involves injecting some easily detected disturbance into the combustion flow, and determining the time required for that disturbance to propagate to a position of known distance downstream. The pulsed tracer can consist of material such as a gas, which can be detected by thermal conductivity or density, or by thermal emission. The tracer can also consist of particulate material of small particle size selected so that the particle velocities closely follow the gas velocity. More commonly, the tracer is a nonmaterial quantity such as thermal energy or electrical energy. For example, electrical current can be pulsed through a thin wire to generate heat in the wire, which in turn is passed on to the gas. This thermal energy can then be detected downstream by a thermocouple or by a resistance thermometer, providing the amount of thermal energy is sufficient to allow detection over and above the random thermal fluctuations caused by the normal combustion processes. For combustion processes, a more appropriate nonmaterial tracer is ionization energy, supplied to the combustion gas in the form of an electrical spark. The high energy of an electrical spark ionizes many molecular species in the gas, and these ionized species flow with the gas past the spark source on downstream to a detection device. For detecting the pulse of ionized gas, simple detectors based on electrical capacitance or electrical conductance are applicable. A primary disadvantage of pulsed-tracer techniques is that it is necessary to know in advance, or to determine by trial and error, the direction of the gas flow before the tracer technique can be used to determine velocity magnitude. This is not true, of course, if the tracers are followed photographically. In which case, the optical problems become almost as difficult as the trial and error determination of gas flow direction. In general, the tracer techniques are not affected by the presence or absence of solid or liquid particulates in the gas flow.

VELOCITY DIRECTION

There are several techniques applicable to the determination of velocity direction in a gas flow. These techniques include tracer methods, multipleport impact probes, and multiple crossed hot-wire anemometers.

Tracers

The use of tracer techniques in combination processes has already been discussed with respect to velocity magnitude determinations, but this method also is applicable to velocity direction determination. Gas ionization, added gas, added particles, or thermal energy as the tracer are all applicable to velocity direction determination. The trial and error process of direction determination by tracers can, in some cases, be simplified by visual observations of the dirty-gas flow or by visual observation of injected tracer. For velocity direction, the added tracer does not need to be added in a pulsed manner and, therefore, with continuous tracer addition at one point, it is possible to trace or follow the streamline for a significant distance before random turbulence totally disintegrates the streamer of tracer. Disadvantages noted previously, such as flow disturbances caused by the tracer addition mechanism, the tracer detector, and the tracer itself are also of concern for both velocity-magnitude and velocity-direction measurements.

Multiple-Port Impact

Multiple-port impact probes are one of the more generally applicable and reliable methods for determination of flow direction. These probes made use of the fact that the reading obtained with an impact probe changes most rapidly with angle when the probe axis is at 45 degrees to the direction of gas flow. For velocity known to be in a single plane, the direction can be obtained by balancing the impact-pressure readings from two probes having their axes intersect at 90 degrees to each other in the plane of the velocity. The balance is obtained by maneuvering the orientation of the combined probes. For velocities not known to be in the same plane, two such pairs of impact tubes can be used. For this four-tube probe, the pressure readings are balanced for one pair at a time by maneuvering the orientation of the probe in the plane of the pair being balanced. Consecutive balancing of the two pairs of probes will quickly result in obtaining the compound angle of the flow velocity in a three-dimensional field. Because of the high sensitivity of the impact probe when at 45 degrees to the flow direction and because of the difficulty in making individual probes of a pair exactly identical, multiple-impact probes require calibration by a gas velocity stream of known direction. At velocities in excess of about 50 feet per second, the multiple-impact tube probe is capable of indicating gas velocity to within less than a 1-degree angle, but at velocities of the order of 5 ft/sec, when the flow is relatively turbulent, the resultant lower impact pressures makes it difficult to resolve velocity direction to much better than about ±2- or ±3-degree angle. To achieve velocity direction measurements with the multiple-impact tube probe requires that the probe be mounted on a gimbaling apparatus capable of rotating the probe through compound angles in each of the planes corresponding to the two pairs of impact probes. The gimbaling apparatus must be such that the tip of the multitube probe remains stationary while the orientation angles are changed. An advantage of this multiple-impact tube probe is that it requires only the indication of a null differenct between the impact pressures indicated by opposing tubes and, therefore, it is necessary to have only a highly sensitive pressure indicator and not a highly accurate, highly sensitive indicator.

The use of a gimbaling apparatus can be avoided if a spherically or hemispherically-shaped multiple-port pitot probe is employed (Ref. A-29). Consider, for example, the case of a spherical body suspended in a gas flow, in a fixed orientation, for which the distribution of pressure over the sphere surface as a function of distance from the forward impact stagnation point is well known. By measuring the pressure at four locations on the spherical surface, it is possible to locate the stagnation point and, therefore, the direction from which the gas flow is coming at the sphere as well as its magnitude. The same principle applies to multiple-port impact probes of any tip geometry, but it is generally necessary to use empirical calibration curves previously obtained for the particular probe to account for imperfections in symmetry and theoretically difficult-to-handle geometries. Use of this nongimbaled technique does have the advantage of not requiring the somewhat difficult-to-construct gimbaling apparatus, but it has the disadvantage of requiring quantitative impact-pressure measurements at several ports. Obtaining these impact-pressure measurements with sufficient accuracy to interrelate the multiple readings, and thereby determine velocity magnitude and direction, is generally not difficult with high-velocity flows (~50 ft/sec), but it becomes difficult at lower velocities (~10 ft/sec), particularly if the flow is somewhat turbulent, as is usually the case in combustion devices.

A five-hole hemispherical pitot probe is used by the IFRF for the determination of velocity magnitude and direction in "dirty" flame environments (Ref. A-7).

Multiple Crossed Hot-Wire Anemometers

Multiple crossed hot-wire anemometers offer an additional method for the determinations of velocity directions. Determination of direction with hot-wire anemometers is based on the different magnitude of heat conduction from the wire to the gas depending on whether the wire is located perpendicular or parallel to the direction of flow. Heat transfer away from the wire tends to be maximized when the wire is perpendicular to the flow direction. Therefore, maximizing the heat transfer from two nonparallel wires will define the plane that is perpendicular to the gas-flow direction. Such multiple hot-wire anemometers work well in noncombustion environments; however, for application in hot, turbulent, dirty combustion environments, they are generally not acceptable.

REFERENCES

A-1. Chervinsky, A., et al. TAE-56 Experimental Investigation of Turbulent Swirling Flames. September 1966.

A-2. Landenburg, R. W., B. Lewis, R. N. Pease, and H. S. Taylor (ed.). Physical Measurements in Gas Dynamics and Combustion, Vol. IX. Princeton Series on High Speed Aerodynamics and Jet Propulsion. Princeton University Press, 1954.

A-3. International Combustion Symposia (III (1948) through XIII (1970)), organized by the Combustion Institute. Pittsburgh, Pennsylvania.

A-4. Laud, T., and R. Barber. The Design of Suction Pyrometers. Trans. Soc. Tust. Tech. (London). 6, No. 3, 112-130, September 1954.

A-5. Fristrom, R. M. Experimental Techniques for Study of Flame Structure. Report No. 300. Applied Physics Lab, Johns Hopkins University. January 1963.

A-6. Barber, R. Review of High Temperature Measurement Methods. The Chemical Engineer (London). April 1967.

A-7. Chedaille, J., and Y. Braud. Industrial Flames. Vol. 1: Measurements in Flames. New York, Crane, Russak & Co., Inc., 1972.

A-8. Gilbert, M., and J. H. Lobdell. Resistance-Thermometer Measurements in Low-Pressure-Flame. Presented at the Fourth Symposium of the International Combustion Institute, IV, 285 (1952).

A-9. Griffiths, E., and J. H. Awbery. Proc. Roy. Soc. 123, 401 (1929).

A-10. Holland, R. E., R. Jackson, and G. G. Thurlow. The Behavior of the Venturi Pneumatic Pyrometer in Industrial Furnaces. J. Inst. Fuel. 180-7, April 1960.

A-11. Grey, J. Thermodynamic Methods of High-Temperature Measurements. Trans. Inst. Soc. of America. 4, 102-15, 1965.

A-12. Mayer, A. M. Phil. Map. 45, 18, 1873.

A-13. Suits, C. G. J. App. Phys. 6, 190, 315, 1935.

A-14. Marlow, D. G., C. R. Nisewanger, and W. M. Cady. J. App. Phys. 20, 771, 1949.

A-15. Grey, J., P. F. Jacobs, and M. P. Silverman. Calorimetric Probe for Measurement of Extremely High Temperature. Rev. Sci. Inst. 33, 738-41, July 1962.

A-16. O'Connor ,T. J. A Split-Flow Enthalpy Probe for Measurement of Enthalpy in Highly Heated Subsonic Streams. Inst. Soc. of America Papd. 68-539, Annual Meeting, New York, October 1968.

A-17. Grossman, R. D., and Associates. Cooled Aspirating Calorimetric Probes. Canoga Park, California, 1971.

A-18. Vassiallo, F. A. Miniature Enthalpy Probes for High Temperature Gas Streams. Report No. ARL 66-0115. USAF, June 1966.

A-19. Hett, J. H., and J. B. Gilstein. J. Opt. Soc. Am. 39, 909, 1949.

A-20. Bundy, F. P., and H. M. Strong. Phys. Review, 76, 457, 1949.

A-21. Kohn, H. Annelen der Physik. 44, 749, 1914.

A-22. Alcalay, J. A., and E. L. Knuth. Molecular-Beam Time-of-Flight Spectroscopy. Rev. Sci. Instr. 40:438, 1969.

A-23. Dickerson, R. A., A. S. Okuda, and C. L. Oberg. Design of an Optimum Oil Burner for Control of Pollutant Emissions. Report No. R-9465. Rocketdyne Division, Rockwell International, Canoga Park, California, February, 1974.

A-24. Herzberg, G. N. Molecular Spectra and Molecular Structure, II: Infrared and Raman Spectra of Polyatomic Molecules. D. Van Nostrand Co., Inc., New York, 1945, I. Spectra of Diatomic Molecule, 2nd Ed. 1950.

A-25. Study on Exhaust Plume Radiation Predictions, Final Report, under Contract NAS8-11363, General Dynamics. GDC-DBE66-017. December 1966.

A-26. Herget, W. F., J. S. Muirhead, and S. A. Golden. Band Model Parameters for H_2O. Rocketdyne Division, Rockwell International, under Contract NAS8-20397, R-6916. Canoga Park, California. January 1967.

A-27. Burick, R. J., C. H. Scheuerman, and A. Y. Falk. Determination of Local Values of Gas and Liquid Mass Flux in Highly Loaded Two-Phase Flow. Symposium on Flow--Its Measurement and Control in Science and Industry, Pennsylvania (to be published in symposium proceedings). Paper No. 1-5-21.

A-28. Dussourd, F. L., and A. H. Shapiro. A Deceleration Probe for Measuring Stagnation Pressure and Velocity of a Particle-Laden Gas Stream. Jet Propulsion. January 1958. p. 24-34.

A-29. Lee, J. E., and J. E. Ash. A Three-Dimensional Spherical Pitot Probe. Trans. ASME. Vol. 78: April 1956. p. 603-608.

APPENDIX B

REVIEW OF
SELECTED LITERATURE ON FLAME CHARACTERIZATION
BY MOLECULAR-BEAM SAMPLING

Prepared by K. Gorji

Molecular-Beam Laboratory
Energy and Kinetics Department
School of Engineering and Applied Science
University of California
Los Angeles, California 90024

Prepared for Environmental Protection Agency Under Contract No. 68-02-0628

I. INTRODUCTION

The desire to observe reactive species in flames has been one of the chief motivations for developing molecular-beam-sampling techniques. It is the objective of this paper to review the existing technology for measurements of reactive-species concentrations in flames using the molecular-beam sampling technique, and for measurements of flame temperature employing the time-of-flight technique. Composition measurements are reviewed first, and temperature measurements last.

II. COMPOSITION MEASUREMENTS

MECHANISM OF BEAM FORMATION

For the past few years, molecular beams for sampling from steady sources have been studied extensively, both analytically and experimentally. As shown in Fig. B-1, a typical molecular-beam mass-spectrometer sampling system consists mainly of a source, source orifice, source chamber, skimmer, collimating chamber, and a detection chamber which contains the beam detector. The sampling gas is accelerated from the source, at pressures up to several atmospheres and temperatures up to several thousand K, via the sampling orifice into a highly evacuated source chamber at pressures from 10^{-1} to 10^{-3} torr. The core of the supersonic jet is then transferred, via the skimmer and collimating orifices, to the detector.

In theoretical treatments of the molecular beam obtained from a nozzle source, it is usually assumed that the flow between the source orifice and the skimmer orifice is continuum flow with isentropic expansion of the gas through the source orifice. It is also assumed that the specific-heat ratio γ is constant during the expansion, the flow into the skimmer orifice is supersonic, the flow is undisturbed by the presence of the skimmer, molecular collisions occurring after the skimmer orifice are negligible, and the gas composition is the same in the detector and the

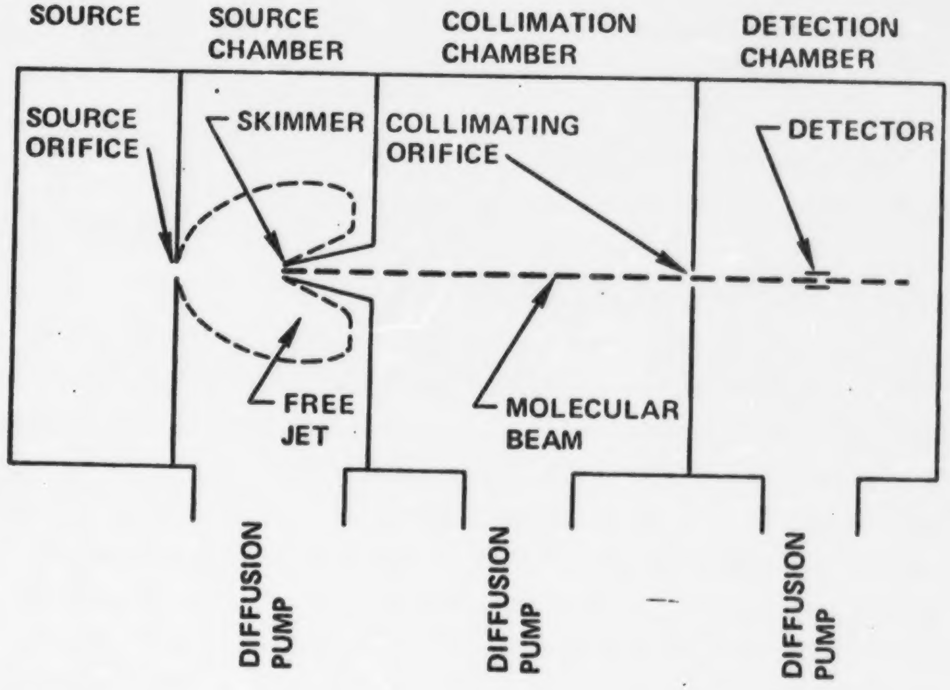
SOURCE
SOURCE CHAMBER
COLLIMATION CHAMBER
DETECTION CHAMBER
SOURCE ORIFICE
SKIMMER
COLLIMATING ORIFICE
DETECTOR
FREE JET
MOLECULAR BEAM
DIFFUSION PUMP
DIFFUSION PUMP
DIFFUSION PUMP

Figure B-1. Schematic Diagram of Molecular-Beam Sampling System source. When designing and using sampling systems for high-pressure and high-temperature sources, various departures from the above assumptions must be considered. The principal causes of these departures are:

1. Nonequilibrium processes and shock waves
2. Skimmer interference
3. Mass separations
4. Nucleation
5. Background scattering
6. Molecule fragmentations in the detector

Nonequilibrium Processes and Shock Waves

When a gas sample expands through the nozzle, simplifications are realized if the expansion time is short in comparison with the reaction times for the unstable or reactive species. Hence, information on the temperature and pressure histories for the expansion is required. This information can be obtained from subsonic and supersonic calculations. In studying 1-atmosphere flames, Greene (Ref. B-1) found that, for a monatomic gas at 2000 K and at 1 atmosphere expanding through a 0.125 mm orifice, the pressure drops to 10^{-5} atmosphere and the temperature to less than 100 K within 1.5 microseconds after the first significant pressure and temperature changes.

In the expansion process, the gas obtains high Mach numbers, usually above 10. The expansion continues until its density becomes less than the surrounding gas; a "barrel shock" around the jet and a "Mach disk" shock perpendicular to the direction of flow is generated. If the sampling gas is allowed to pass through this shock, its composition will be altered due to the change of its density and temperature. Therefore, it is necessary to place the skimmer upstream of the Mach disk.

It is generally accepted that the expansion downstream of the sampling orifice within the "barrel shock" is isentropic. Sherman (Ref. B-2) has

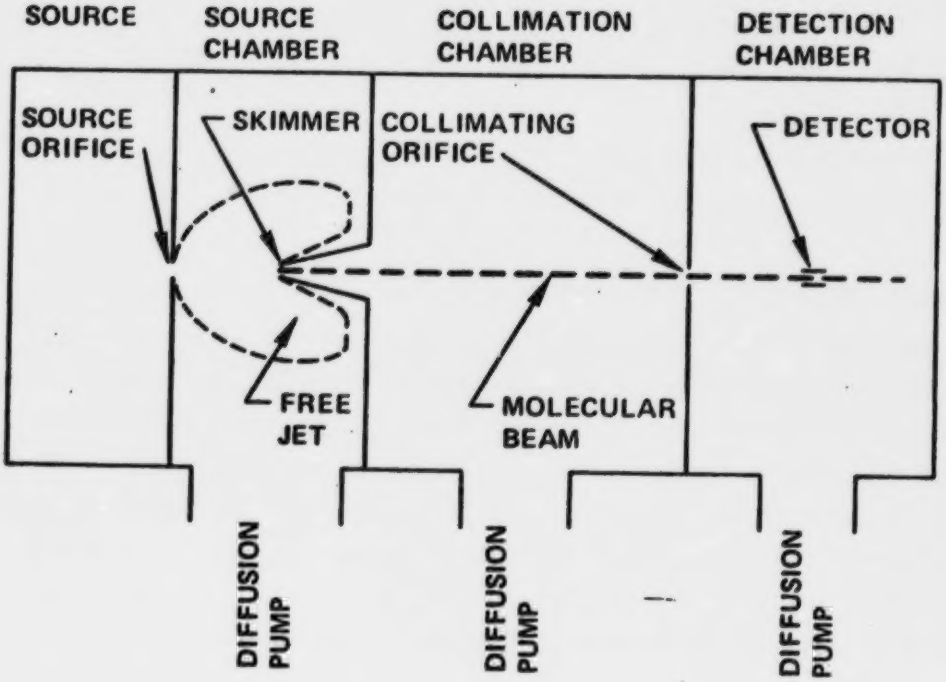
SOURCE
SOURCE CHAMBER
COLLIMATION CHAMBER
DETECTION CHAMBER
SOURCE ORIFICE
SKIMMER
COLLIMATING ORIFICE
DETECTOR
FREE JET
MOLECULAR BEAM
DIFFUSION PUMP
DIFFUSION PUMP
DIFFUSION PUMP

Figure B-1. Schematic Diagram of Molecular-Beam Sampling System source. When designing and using sampling systems for high-pressure and high-temperature sources, various departures from the above assumptions must be considered. The principal causes of these departures are:

1. Nonequilibrium processes and shock waves
2. Skimmer interference
3. Mass separations
4. Nucleation
5. Background scattering
6. Molecule fragmentations in the detector

Nonequilibrium Processes and Shock Waves

When a gas sample expands through the nozzle, simplifications are realized if the expansion time is short in comparison with the reaction times for the unstable or reactive species. Hence, information on the temperature and pressure histories for the expansion is required. This information can be obtained from subsonic and supersonic calculations. In studying 1-atmosphere flames, Greene (Ref. B-1) found that, for a monatomic gas at 2000 K and at 1 atmosphere expanding through a 0.125 mm orifice, the pressure drops to 10^{-5} atmosphere and the temperature to less than 100 K within 1.5 microseconds after the first significant pressure and temperature changes.

In the expansion process, the gas obtains high Mach numbers, usually above 10. The expansion continues until its density becomes less than the surrounding gas; a "barrel shock" around the jet and a "Mach disk" shock perpendicular to the direction of flow is generated. If the sampling gas is allowed to pass through this shock, its composition will be altered due to the change of its density and temperature. Therefore, it is necessary to place the skimmer upstream of the Mach disk.

It is generally accepted that the expansion downstream of the sampling orifice within the "barrel shock" is isentropic. Sherman (Ref. B-2) has calculated values of the Mach number as a function of location in the jet for three different values of γ.

In a typical free-jet expansion of a gas from 1 atmosphere, an individual molecule undergoes several hundred collisions. If the vibrational, rotational, and translational degrees of freedom are all active initially, the number of collisions required for relaxation is greatest for vibration, least for translation. Therefore, as the gas expands in the jet, the vibrational degrees of freedom freeze first, the translational degrees of freedom last. Possible effects of chemical relaxations in the free jet have been studied by Knuth (Ref. B-3).

Skimmer Interference

The skimmer may interfere with the properties of a molecular beam formed from a sampling kit. This interference may result in

1. A decreased beam density
2. An increased velocity distribution width
3. A decreased mean velocity
4. Distortion of the beam composition.

The first three effects have been studied by several investigators, e.g., Anderson et al. (Ref. B-4). Composition distortions due to skimmer interference have been reported by Reis and Fenn (Ref. B-5) and Young et al. (Ref. B-6). The skimmer interference may arise from the Mach disk, shock detachment, the stand-off shock, small internal skimmer angles, a blunt leading edge, and a large skimmer orifice. Knuth (Ref. B-3) has reviewed criteria for minimizing this skimmer interference.

Mass Separations

Several investigators have observed that when a mixture of gases is expanded to form a supersonic jet, the composition of the gas taken from the core of the jet is depleted in the lighter component. This mass separation has been investigated by several investigators, e.g., Becker et al. (Ref. B-7), Waterman et al. (Ref. B-8 and B-9), Abuaf et al. (Ref. B-10), Milne and Greene (Ref. B-11). Young et al. (Ref. B-12) have studied the most important possible separations, namely mass separations due to pressure diffusion, skimmer induced separation, Mach-number focusing, and background invasion by varying (1) the source pressure, (2) the orifice-skimmer distance and (3) the background pressure. Criteria for either avoiding or minimizing distortion of gas composition during the sampling process are available.

Nucleation

When the temperature and pressure drop during a free jet expansion, condensation of one or more species may occur. Hence studies of nucleation in supersonic molecular beams are highly motivated.

Studies in free-jet nucleation have mostly involved observations of the final extent of nucleation, or cluster growth, after the collisions have ceased. It would be better if one could probe through the continuum flowfield with the skimmer, having demonstrated that collisions effectively cease at the skimmer, and thus follow the growth of clusters as a function of time.

Greene and Milne (Ref. B-13) noticed that, when argon at atmospheric pressure was passed over water at 4 C and expanded through a 0.004-inch-diameter sampling orifice, the majority of the water in the free jet was nucleated to form dimeric and higher species. They suggest that the correction for nucleation could be made by extrapolating a plot of intensity versus orifice diameter to zero orifice diameter. (The rate of expansion is inversely proportional to the orifice diameter.) Other investigators have studied nucleation of Ne, Ar, CO_2, O_2, N_2O, N_2, NH_3, H_2O (Ref. B-14), Ar, CO_2, N_2, O_2, H_2O (Ref. B-15), Hg, CsCl, CH_3OH (Ref. B-16), and NO, N_2, O_2, Ar, CO_2 (Ref. B-17).

Background Scattering

In sampling studies, the scattering of beam molecules by background molecules can become a problem. Anderson and Fenn (Ref. B-18) investigated the interaction of background gases and supersonic free jets from sonic nozzles and found out that, at sufficiently low jet densities, the background gases freely invade the jet flowfield. Attenuation of the molecular beam results. Knuth (Ref. B-3) states that the scattering of beam molecules is a problem if the background molecules either attenuate the beam density appreciably or alter greatly the relative densities of the several beam species. He presents criteria for avoiding both problems.

Molecule Fragmentation in the Detector

The problem of molecular-beam sampling of unstable and reactive species is complicated by possible confusions of these species with fragment ions of other molecules. Furthermore, in sampling of gases at different temperatures, the variations of their fragment patterns with temperature must be taken into account. The fragment pattern is dependent on the vibrational energy of the molecule. For example, the measurements of Greene and Milne (Ref. B-1) on flames show that the fragmentation of CO_2 to CO varies at least from 12 percent at room temperature to 17 percent at 2000 K. On the other hand, Homann et al. (Ref. B-18) could not find any change in the mass spectrum of acetylene sampled from burned gases at 1700 K compared with the spectrum obtained at room temperature. The problems of vibrational relaxation in free jets, and the dependence on the vibrational state of fragmentation patterns, must be studied for a variety of molecules of interest in high-temperature sampling situations.

Applications

The development of the molecular-beam mass-spectrometer sampling technique has been motivated partly by the desire to observe reactive and unstable species in flames. In 1953, Foner and Hudson (Ref. B-19) employed a molecular-beam mass-spectrometer system to sample and detect atoms and radicals of chemical reactions and flames. In their sampling system, which was especially designed for the study of reactive free radicals, the gas being sampled entered the system through a small circular aperture in a glass or quartz cone and was collimated by two additional slits. The three sections of the molecular-beam sampling system were separately evacuated by high speed diffusion pumps, the pressure typically being 10^{-3} torr in the source chamber, 10^{-5} torr in the collimation chamber, and 10^{-7} torr in the ion source chamber. The molecular beam traversed 10 cm from the entrance aperture to the center of the ion source. This distance corresponded to a transit time of about 230 μsec for an oxygen molecule at room temperature. The molecular beam was mechanically interrupted at 170 cps by a vibrating reed beam chopper in the source chamber to discriminate against background signals. The several species were identified and monitored by a 90-degree sector magnetic mass analyzer. A movable burner assembly was used to position the flame at various distances from the sampling pinhole. Hydrogen-oxygen and methane-oxygen flames were studied. The hydrogen-oxygen flame clearly showed the presence of the stable species H_2, O_2, and H_2O and the unstable species H, O, and OH in sufficient abundances to permit mapping of intensities as functions of burner distance from the pinhole. The atom and radical intensity measurements were made at sufficiently low ionizing-electron energies to eliminate contributions from dissociative ionizations of the stable components. In the absence of absolute calibrations for the radicals, reasonable estimates were made of their ionization cross sections. Taking into account that low electron energies were used in the radical measurements, they suggest multiplying the adjusted ion intensities in the lower half of their figure (Ref. B-10) by a factor of about 10 to put the concentrations of the stable components and radicals on a common basis. The maximum radical concentrations were thus estimated to be of the order of 1 percent of the composition profiles. Although the measurements were reproducible, their interpretations were complicated by diffusion effects, turbulent mixing, and changes in the flame configuration as the burner was moved with respect to the diaphragm.

The mass spectra obtained for the methane-oxygen flame were of unanticipated complexity. The stable products that were readily identified were H_2, H_2O, C_2H_2, CO, CO_2, and C_4H_2. Other stable components were obviously present, but only tentative identifications could be made for some of these, such as C_2H_4 at mass 28, C_2H_6 or HCHO at mass 30, and CH_3OH at mass 31. Evidence suggested also the presence of C_3H_4, C_3H_6, and C_3H_8. The only radical that was positively identified was CH_3.

In these experiments, the detection and positive identification of HO_2 radicals as an intermediate was the principal objective. Careful experiments were performed varying the burner position and the hydrogen-oxygen ratio without obtaining conclusive evidence for existence of the HO_2 radical. Due to (1) the complexity of the methane-oxygen reaction, (2) the inability to identify all the stable components present, and (3) the possibility that some of the molecules could have been in excited states, and therefore had different fragmentation patterns than unexcited molecules, it was felt that identifications of radicals other than methyl would be somewhat speculative. Several years later, Foner and Hudson (Ref. B-20) used the same system with a number of modifications to study the production, identification, and determination of the thermochemical energy of HO_2. The modifications were made to improve the sensitivity and precision of measurement. Phase-sensitive detection was replaced by ion counting. The output of the electron multiplier detector consisted of about 10^{-3} Coulomb per ion. The pulses were amplified and sent through a gated amplifier and an electronic switch which was synchronized with the beam chopper so that one of the ion counters recorded ions only when the beam chopper was open, the other only when the beam chopper was closed. The difference between the two ion counts represented the ion intensity contributed by the molecular beam, while the square root of the sum of the two ion counts was approximately equal to the standard deviation of the measurement and served as a useful indicator of the quality of the data.

In this experiment, the reactions found to produce HO_2 radicals, and examined in some detail, were (1) reaction of H atoms with O_2, (2) reaction of H atoms with H_2O_2, (3) reaction of O atoms with H_2O_2, (4) reaction of OH radicals with H_2O_2, (5) photolysis of H_2O_2, and (6) low-power electrical discharge in H_2O_2. Of the various reactions investigated, the low-power electrodeless electrical discharge in a rapidly flowing system of H_2O_2 was found to be a fairly intense and convenient source of HO_2 radicals. A maximum concentration of about 0.4 percent HO_2 was obtained at 15 percent H_2O_2 decomposition in a typical experiment. The production of HO_2 in the various reactions involving H_2O_2 was predominantly by OH radicals, generated in assorted primary steps, reacting in the fast reaction

$$OH + H_2O_2 \rightarrow H_2O + HO_2$$

From 1964 to 1966, other investigators attempted to study flame reactions using similar sampling techniques. For example, Vriens et al (Ref. B-21) employed a molecular beam in sampling 1-torr to 1-atmosphere gases (Ar or H_2) for three sampling-orifice diameters. Their apparatus was somewhat similar to the previously mentioned apparatus. The sampling orifice was a pinhole in a gold foil of 0.02 mm thickness. The diameters chosen for the experiments were about 0.20, 0.035, and 0.07 mm. The distance between the sampling orifice and the second orifice was 10 mm, and the distance between the second and the third orifices was 240 mm. The diameters of the second and third orifices were 0.18 and 3.5 mm, respectively. At normal operating conditions, the background pressures in the first and second chambers were 5×10^{-5} to 3×10^{-3} torr (dependent on sampling orifice diameter) and 10^{-6} torr, respectively. The molecular beam was modulated using a mechanical 50 cps chopper. This modulation facilitated the measurement of the scattering of the molecular beam.

The 1-atmosphere flame was replaced by a gas container filled with argon or hydrogen of variable pressure, and for three diameters of the sampling orifice the dependence of the mass spectrometer ion current on gas pressure was measured. The dependence of the background pressure in the first chamber on gas pressure and sampling-orifice diameter was also determined.

From the measurements, it was concluded that for sampling-orifice diameters of 0.035 and 0.07 mm, and for a gas pressure of 1-atmosphere, the density in the beam between the sampling orifice and the second orifice was large. The numerous collisions between beam molecules in this region result in conversion of much of the translational energy, and internal energy in the case of molecules, into directed motion of the beam. Therefore, the static temperature decreases and a shift of composition of the flame gas is possible during expansion. Predicting the amount of this composition change is difficult. It is simpler perhaps to use a smaller sampling orifice diameter, e.g., 0.02 mm, in order to decrease the number of collisions appreciably. Fortunately, since the flame has a higher temperature, the gas density in the flame is less than the gas density of room-temperature Ar or H_2. Therefore, the number of collisions between beam particles is less for the flame gas.

Quantitative studies of mass spectrometric sampling of sources at and above 1 atmosphere and temperatures up to 3000 K have been carried out by Greene and Milne (Ref. B-22 & B-1). The sampling system, similar to previously mentioned systems, included three differentially pumped stages between the sampling orifice and the ion source of a Bendix time-of-flight mass spectrometer. The beam was modulated at 10 cps, which facilitated the detection of beam signals, even when the ratio of background density to beam density was greater than 100. In subsequent studies, the beam chopper and the phase-sensitive detection system were replaced by a magnetically driven vibrating reed, and lock-in amplifiers. Modulation at 10 and 50 cps gave identical results, indicating that effects of modulation of the background gas were negligible.

Several flames (H_2-O_2-N_2, CH_4-O_2-Ar, CO-O_2) were analyzed, both for stable reaction products and reactive species. In the CH_4-O_2-Ar flame, the sampling of the stable products H_2, H_2O, CO, O_2, and CO_2 was very simple. Equilibrium concentrations of these species were maintained by fast bimolecular free-radical reactions.

The temperature dependence of the fragmentation of the molecules in the ionizer complicated the stable-product measurements. In order to determine the magnitude of this temperature effect, CO_2 was added to a lean H_2O_2 flame which burned at 1950 K. Fragmentation of CO_2 to CO^+ increased from 12 percent at room temperature to 17 percent at 2000 K. The effect of temperature on fragmentation of HCl was studied by sampling HCl from a series of rich H_2-O_2-N_2 flames.

Although spatial resolution for sampling from the main reaction zone was only fair (the sampling orifice diameter was 0.24 mm), the authors did measure quantitatively Cl, H, O, and OH concentration profiles in the recombination zones of the flames. Experimental values agreed within the limits of experimental error with those calculated for chemical equilibria between stable species and radicals at the adiabatic flame temperature. Other species such as S, SH, SO, HBO_2, and F were readily detected in the reaction zones of 1-atmosphere flames; excess radical concentrations were observed. It was predicted that the extremely rapid cooling achieved in free-jet direct sampling would allow almost any non-condensible chemical species to be quantitatively measured from systems at pressures of several atmospheres and temperatures as high as 3000 to 5000 K.

Molecular beam sampling also has been used in flame studies by Wagner et al. (Ref. B-18, B-23, & B-25). The apparatus used in these experiments was similar to previously mentioned apparatuses. A quartz cone, used as the sampling probe, was attached to an intermediate vacuum chamber, which was maintained at pressures from 10^{-3} to 10^{-4} torr. The apex angle of the skimmer was so chosen that the particles inside the cone did not undergo collisions with the inner wall of the cone. The objective of the investigation was to study the formation of solid carbon and to observe the intermediates formed in this process. Various rich hydrocarbon oxygen flames were examined for such hydrocarbon radicals as CH_3, C_2H, C_4H_3, acetylenic polymers C_4H_2 to $C_{12}H_2$, and for very reactive cyclic hydrocarbon species in the 60 to 100 amu range. The profiles of some highly reactive hydrocarbon intermediates were quantitatively related to the increase in solid carbon concentration. In hydrogen-oxygen flames concentration profiles of O, H, OH, and H_2O_2 were measured. Evidence for the presence of the HO_2 radical in rich H_2-O_2 flames was obtained. In the same manner, hydrazine decomposition flames were investigated for NH_2 and N_2H_2 intermediates (Ref. B-25).

The same apparatus was used (Ref. B-26) to sample reacting gases in an isothermal flow reactor. Rapid flow around the probe tip favored the removal of the gas that had hit the wall around the orifice at the probe tip, and diminished the thermal influence of the probe on the reacting gases. (This influence cannot be totally excluded when sampling the reaction zone of flames.) In this way, the mechanism of the oxidation of CS_2 by O_2, strongly diluted with argon, was investigated at temperatures up to 1400 K. CS_2 was injected into the hot argon stream already containing oxygen. The concentration profiles of all stable species and radicals were measured by changing the distance between the mixing point and the sampling probe in the stationary reaction system. SO_2 and CO were the main reaction products, with little CO_2 being formed after the CS_2 had been consumed completely. In addition to the comparatively stable intermediate COS, radicals such as SO, S, O, CS, and S_2O were measured. In subsequent experiments, the rates of individual steps in this complex reaction were studies in a low pressure fast flowing system (Ref. B-27, B-28, B-29. A molecular-beam system combined with a Bendix time offlight mass spectrometer was used. A suitable electron energy for ionizing was found to be 25 eV. At this energy, dissociation of the ions into sub-particles were relatively small.

The elementary step O + COS → CO + SO, by which the COS is oxidized, was distinguished completely from consecutive reactions of SO to SO_2. The reaction O + CS_2 → CS + SO also was followed separately. The reaction rates for O + H_2, O + C_2H_2, O + NH_3 and other reactions were measured. By following quantitatively the concentrations of each participant in the reactions, primary reaction steps were distinguished from combined reaction steps.

The reactions of oxygen atoms with nitric oxide and nitrogen dioxide have been studied by Klein and Herron (Ref. B-30). The calibration for oxygen atoms at an electron energy of 20 eV was obtained by determining the atom concentration independently by titration with nitrogen dioxide. Young et al. (Ref. B-31) sampled reactive gases from engine cylinders using molecular beam techniques and determined densities of N_2, O_2, C_3H_8, H_2O, CO_2, HO, and CO.

Molecular beams have been employed also by several investigators to study ions in high pressure flames. DeJaegere et al. (Ref. B-32) have identified the most abundant ions in methane-oxygen, acetylene-oxygen, and CH_2-NH_3-O_2-N_2 flames. Ions produced in halogen-containing flames and the most abundant ions in nitrogen-oxide-producing flames were also studied. Hayhurst and Telford (Ref. B-33) studied the charge exchange reaction of the H_3O^+ ion with metal in atmospheric flames of H_2-O_2-N_2 at temperatures from 1815 to 2445 K. The metals CS, Rb, K, Na, Li, Tl, Cr, Pb, Mn, Cu, Fe, and Cd were used.

Shock tubes combined with molecular-beam sampling systems also can be used to study reactive gases. Skinner (Ref. B-34) pioneered in sampling from shock tubes; his objective was a neutral beam with energy above 1 eV. Penn and Liquornik (Ref. B-35) used an O-He mixture in a shock tube to generate an O beam with energy of 3 eV. Jones and Byrne (Ref. B-36) also developed such a system to study the production of a metastable argon beam and its interaction with a copper surface.

More recently, Solomon et al (Ref. B-37) used a nozzle-beam mass spectrometer system to study 1 atmosphere flames. An ionization energy of 20 eV was used in the mass spectrometer in order to reduce fragmentation of the molecules. Output signals were recorded on a high-speed oscillograph. The scan rate for the mass range m/e from 1 to 60 was 250 milliseconds. Use of 2000 Hz galvanometers in the recording oscillograph permitted recording at this scan rate without peak clipping. The premixed-gas flame was slowly traversed toward the sampling orifice, starting approximately 10 mm above the reducing portion. Probing through the reaction zone resulted only in qualitative profiles since the reaction zone was very thin. Measurements from 1 to 5 mm above the inner reducing cone tip were most suitable for calculations of equilibrium constants. Beyond 5 mm, heat loss shifted the reaction equilibrium. No corrections for heat loss were made. Flames of CH_4-O_2-Ar with four different mole fractions and four different temperatures from 2444 to 2877 K were samples. The concentrations of H_2, O_2, OH, H_2O, CO, Ar, and CO_2 were determined. These flames showed similar behavior to previously studied flames, such as H_2-O_2, and CH_4-air flames. The investigators concluded that their molecular beam system was capable of quantitatively sampling high-pressure, high-temperature flames, and that the data agreed well with the equilibrium properties of methane-oxygen flames. No particular problems were encountered in sampling atoms and radicals.

III. TEMPERATURE MEASUREMENTS

High temperature sources have been studied using the time-of-flight technique. Applications of this basic technique can be divided into two general types: those in which the beam intensity as a function of time is measured directly, and those in which the flight time is determined as a phase shift by means of a phase-sensitive detector. The direct measurement technique is older and provides more detailed information. When a molecular beam is pulsed on for a short time interval, at time between t and t + dt the number of molecules n(t) arriving at the detector will have velocities between L/t and L/t + dt, where L is the distance from the beam pulser to the detector. If the total number of molecules is N, then n(t)/N will be the fraction of molecules with velocity between v, and v + dv add the velocity distribution can be determined by measuring n(t) as a function of t.

In order to use the time-of-flight technique to determine the stagnation temperature of the source, it is necessary to determine the velocities of the molecules in a beam extracted from the source. This method was used, e.g., by Anderson and Fenn (Ref. B-38) in their studies of supersonic jets of hydrogen or helium containing small concentrations of heavier molecules. The beam was chopped into short segments by a rotating shutter and the flight times to a downstream detector were measured. Velocities were obtained for 1 mole percent of solute in hydrogen or helium. If a pure gas expands isentropically in a free jet, then the average kinetic energy of the molecules is

$$1/2\ mV^2 = \int_T^{T_o} C_p dT$$

where V = hydrodynamic velocity
m = molecular mass
C_p = molecular specific heat at constant pressure
T_o = stagnation or source pressure
T = static temperature in the jet

At Mach numbers above 5, the static temperature becomes negligible. Hence, in expansions to high Mach numbers, the kinetic energy of the heavy species is given by:

$$1/2\ m_h V^2 = \frac{m_h}{m_m} \int_0^T C_{p_m} dT$$

where subscript m indicates the mean value for the mixture and h indicates the heavy species.

Alcalay and Knuth (Ref. B-39) developed a moment method to extract from the measured TOF signal the beam density, temperature and energy. Algebraic relations between the moments of the measured time-of-flight signal, the speed distribution function, the modulator gate function, and the dynamic function of the detector and its electronics were derived. The simplest gate functions are the triangular, trapezoidal, step, rectangular, and impulse gate functions. This technique was applied to time-of-flight measurements of an arc-heated supersonic molecular beam; values of the temperature and mean beam energy were calculated using $T = m\Upsilon^2/2k$ and $E = m\Upsilon^2 n_2\{f_2(s)\}/2$, respectively. Here Υ is the most probable random speed of the beam, m is the molecular mass, k is Boltzman's constant, and $n_2\{f_n(s)\}$ is the second moment of the speed distribution function. Values of the stagnation temperature were calculated relating the energy of the beam to the enthalpy at the source conditions.

Young (Ref. B-40) has overcome the problems in determining the dynamic function of the detector and its electronics, the gate function, and the zero-time reference by using a dual-disk TOF chopper. Each disk consists of four small slits and four large slits. The depth of the small slit (angular width = α) was greater than the large slit (angular width = θ) in order to facilitate use of a photocell in conjunction with the small slits to trigger the oscilloscope. The two disks were mounted on a shaft with angular orientation such that the centers of α on one disk were offset relative to the centers of θ on the other disk, with a phase angle of

$$\theta = \frac{2\pi}{2N_\alpha} = \frac{\pi}{N_\alpha}$$

where N_α was the number of α slits in one disk.

General moment relations for the dual-disk TOF signals were developed. These relations included expressions for extracting values of the static temperature and energy of the beam.

IV. CONCLUSIONS

The feasibility of using a molecular-beam mass-spectrometer system to measure the concentrations of most stable species and free radicals in high-temperature 1-atmosphere flames has been demonstrated. Possible adverse effects which must be either avoided or handled quantitatively include certain nonequilibrium processes, shock waves, skimmer interference, mass separations, nucleation, background scattering, and molecule fragmentations. Of these several effects, nucleation is perhaps the least well understood. Fortunately, available experimental results indicate that all of these effects, excepting mass separations and molecule fragmentations, can be avoided, and that these two exceptions can be handled quantitatively. Additional data are required in order to extend criteria and methods obtained for given systems to other systems.

The measurement of flame temperatures by the time-of-flight technique has unique advantages over other methods. The use of a dual-disk chopper simplifies this measurement significantly by avoiding the uncertainties in the zero-time reference point, the gate function, and the dynamic function of the detector and its electronics.

REFERENCES

B-1. Milne, T. A. and F. T. Greene, "Mass Spectrometric Studies of Reactions in Flames," *J. Chem. Phys.*, 44:2444, 1966.

B-2. Sherman, F.S., "Hydrodynamical Theory of Diffusive Separation of Mixtures in a Free Jet," *Physics of Fluids*, 8:773, 1965.

B-3. Knuth, E. L., "Direct-Sampling Studies of Combustion Processes," to be published in *Engine Emissions* (G. S. Springer and D. Patterson, eds.), Plenum Publishing Co.

B-4. Anderson, J. B., R. P. Andres, J. B. Fenn, and G. Maise, "Studies of Low Density Supersonic Jets," *Rarefied Gas Dynamics*, II:106, 1966.

B-5. Reis, V. H., and J. B. Fenn, "Separation of Gas Mixtures in Supersonic Jets," *J. Chem. Phys.*, 39:3240, 1963.

B-6. Young, W. S., W. E. Rodgers, C. A. Cullian, and E. L. Knuth, "Molecular Beam Sampling of Gas Mixtures in Cycling-Pressure Sources," Proceedings of the *Seventh International Symposium on Rarefied Gas Dynamics* held at Pisa, Italy, June 29-July 3, 1970.

B-7. Becker, E. W., K. Bier, and H. Burghoff, "Die Trennduse," *Z. fur Naturforschung*, 10a:565, 1955.

B-8. Waterman, P. C. and S. A. Stern, "Separation of Gas Mixtures in a Supersonic Jet," *J. Chem. Phys.*, 31:405, 1959.

B-9. Stern, S. A., P. C. Waterman, and T. F. Sinclair, "Separation of Gas Mixtures in a Supersonic Jet. II. Behavior of Helium-Argon Mixtures and Evidence of Shock Separation," *J. Chem. Phys.*, 33:805, 1960.

B-10. Abuaf, N., J. B. Anderson, R. P. Andres, J. B. Fenn, and D. R. Miller, "Studies of Low Density Supersonic Jets," *Rarefied Gas Dynamics*, II:1317, Academic Press, New York, 1967.

B-11. Greene, F. T., J. Brewer, and T. A. Milne, "Mass Spectrometric Studies of Reactions in Flames," *J. Chem. Phys*., 40:1488, 1964.

B-12. Young, W. S., Y. G. Wang, P. K. Sharma, W. E. Rodgers, E. L. Knuth, "Molecular-Beam Sampling of Continuum Gas Mixtures," presented at the *Eighth International Symposium on Rarefied Gas Dynamics* held at Palo Alto, California, 10-14 July 1972.

B-13. Greene, F. T. and T. A. Milne, "Molecular Beam Sampling of High Temperature Systems," *AIAA Paper No. 67-37*, 1967.

B-14. Greene, F. T. and T. A. Milne, "Mass Spectrometric Detection of Polymers in Supersonic Molecular Beams," *J. Chem. Phys*., 39:3150, 1963.

B-15. Milne, T. A. and F. T. Greene, "Mass Spectrometric Observations of Argon Clusters in Nozzle Beams. I. General Behavior and Equilibrium Dimer Concentrations," *J. Chem. Phys*., 47:4094, 1967.

B-16. Milne, T. A. and F. T. Greene, "Mass Spectrometric Study of Metal-Containing Flames," *Final Tech. Summ. Rept*., 1961-67, Contract NONR-3599100. Kansas City: Midwest Research Institute, 30 January 1968.

B-17. Milne, T. A. and F. T. Greene, "Mass Spectrometric Detection of Dimers of Nitric Oxide and Other Polyatomic Molecules," *J. Chem. Phys*., 47:3668, 1967.

B-18. Homann, K. H. and H. G. Wagner, *Ber. Bunsengesellschaft Physik. Chem*., 69:20, 1965.

B-19. Foner, S. N. and R. L. Hudson, "The Detection of Atoms and Free Radicals in Flames by Mass Spectrometric Techniques," *J. Chem. Phys*., 21:1374, 1953.

B-20. Foner, S. N. and R. L. Hudson, "Mass Spectrometry of the HO_2 Free Radical," *J. Chem. Phys*., 36:2681, 1962.

B-21. Vriens, L., A. L. Boers, and J. A. Smit, "Measurement on a Moleccular Beam Apparatus for Mass Spectrometric Study of Reactions in Flames," *App. Sci. Research* (Sec. B), 12:65, 1965-66.

B-22. Greene, F. T., J. Brewer, and T. A. Milne, "Mass Spectrometric Sampling of 1 Atm. Flame," *Tenth Int. Symp. on Combustion*, p. 153. Pittsburgh: The Combustion Inst., 1965.

B-23. Bonne, U., K. H. Homann, and H. G. Wagner, "Carbon Formation in Premixed Flames," *Tenth Int. Symp. on Combustion*, p. 503. Pittsburgh: The Combustion Inst., 1965.

B-24. Homann, K. H. and H. G. Wagner, "Some New Aspects of the Mechanism of Carbon Formation in Premixed Flames," *Eleventh Int. Symp. on Combustion*, p. 371. Pittsburgh: The Combustion Inst., 1966.

B-25. Homann, K. H., D. I. MacLean, and H. G. Wagner, *Naturwissenschaften* 52:12, 1965.

B-26. Krome, G., "Massenspektrometrische Untersuchungen des Reaktionsablaufes der Schwefelkohlenstoff-Oxidation bei Hohen Temperaturen," *Diplomarbeit*. Göttingen: Universität Göttingen, April 1965.

B-27. Wagner, H. G. and J. Wolfrum, "Bestimmung der Geschwindigkeit der Reaktion O + COS → CO + SO," *Ber. Bunsengesellschaft Phys. Chem*. 71: 603: 1967.

B-28. Homann, K. H., K. H. Hoyermann, and J. Wolfrum, "Versuche sur Vollständigen Bestimmung der Geschwindigkeiten Bimoleklarer Reaktionen," Kurznachrichten Nr. 2, Akademie der Wissenschaften, II. Math. Phys. Klasse. Göttingen, 1967.

B-29. Homann, K. H., G. Krome, and H. G. Wagner, "Schwefelkohlenstoff-Oxydation Geschwindigkeit von Elementarreaktionen," *Ber. Bunsengesellschaft Physik. Chem*. 72:998, 1968.

B-30. Klein, F. S. and J. T. Herron, "Mass Spectrometric Study of the Reactions of O Atoms with NO and NO_2," *J. Chem. Phys*. 41:1285: 1964.

B-31. Young, W. S., Y. G. Wang, W. E. Rodgers, and E. L. Knuth, "Molecular Beam Sampling of Gases in Engine Cylinders," Technology Utilization Ideas for the 70's and Beyond, 281-289. Tarzana: American Astronautical Society, 1971.

B-32. De Jaegere, S., J. Deckers, and A. Tiggelen, "Identity of the Most Abundant Ions in Some Flames," Eighth Int. Symp. on Combustion, p. 155. Baltimore: Williams and Wilkins, 1962.

B-33. Hayhurst, A. N. and N. R. Telford, "Charge Exchange Reactions of H_3O^+ with Metals in Flames," Trans. Faraday Soc. 66: 2784, 1970.

B-34. Skinner, G. T., "Scattering at a Solid Surface and Observations of Radiation Accompanying the Beam," Rarefied Gas Dynamics, II: 1325, Academic Press, New York, 1969.

B-35. Peng, T. C. and D. L. Liquornik, "Shock Tube Molecular Beam for 0 to 3 eV," Rev. Sci. Instr. 38:989, 1967.

B-36. Jones, T. V. and M. A. Byrne, "The Production of a Metastable Argon Beam with Kinetic Energy up to 3 eV and its Interaction with a Copper Surface," Rarefied Gas Dynamics II:1311, Academic Press, New York, 1969.

B-37. Solomon, W. C. and B. B. Goshgarian, "Nozzle Beam-Mass Spectrometer Systems for Studying One-Atmosphere Flames," Tech. Rept. AFRPL-TR-27-30. Edwards: Air Force Rocket Propulsion Laboratory, April 1972.

B-38. Abuaf, N., J. B. Anderson, R. P. Andres, J. B. Fenn, and D.G.H. Marsden, "Molecular Beams with Energies Above One Electron Volt," Science 155:997, 1967.

B-39. Alcalay, J. A. and E. L. Knuth, "Molecular-Beam Time-of-Flight Spectroscopy," Rev. Sci. Instr. 40:438, 1969.

B-40. Young, W. S., "An Arc-Heated Ar-He Binary Supersonic Molecular Beam with Energies up to 21 eV," Report No. 69-39, Los Angeles: Department of Engineering, University of California, 1969.

APPENDIX C

TABULATION OF DATA OBTAINED WITH UCLA MOLECULAR-BEAM MASS-SPECTROMETER SAMPLING SYSTEM

Table C-1. MOLE FRACTION OF CO_2 AT VARIOUS SAMPLING ORIFICE-TO-FLAME HOLDER DISTANCES AND VARIOUS EQUIVALENCE RATIOS

$$[CO_2] = \frac{S_{CO_2}}{S_{N_2}} \times \frac{1}{R \cdot E \cdot I} [N_2]$$

Distance, inches → / Equivalence Ratio ↓	0.75	1.00	1.25	1.50	1.75	2.00	2.25	2.50	2.75	3.00
ϕ = 0.75	0.065	0.067	0.065	0.065	0.067	0.065	0.067	0.067	0.073	0.067
ϕ = 0.80	0.071	0.070	0.071	0.070	0.071	0.071	0.071	0.077	0.077	0.077
ϕ = 0.90	0.082	0.083	0.085	0.084	0.084	0.084	0.084	0.084	0.080	0.081
ϕ = 1.00	0.082	0.084	0.085	0.082	0.082	0.082	0.082	0.084	0.083	0.085
ϕ = 1.10	0.063	0.065	0.064	0.067	0.067	0.067	0.067	0.067	0.069	0.069
ϕ = 1.25	0.069	0.068	0.066	0.065	0.065	0.068	0.067	0.066	0.068	0.066
ϕ = 1.30	0.050	0.051	0.049	0.049	0.051	0.048	0.049	0.05	0.053	0.049

Table C-2. MOLE FRACTION OF ARGON AT VARIOUS SAMPLING ORIFICE-TO-FLAME HOLDER DISTANCES AND VARIOUS EQUIVALENCE RATIOS

$$[Ar] = \frac{S_{Ar}}{S_{N_2}} \times \frac{1}{R \cdot E \cdot I} [N_2] \times 10^2$$

Distance, inches → / Equivalence Ratio ↓	0.75	1.00	1.25	1.50	1.75	2.00	2.25	2.50	2.75	3.00
ϕ = 0.75	1.34	1.36	1.34	1.26	1.24	1.19	1.27	1.24	1.26	1.29
ϕ = 0.80	1.21	1.21	1.22	1.24	1.22	1.19	1.25	1.15	1.11	1.18
ϕ = 0.90	1.33	1.33	1.32	1.24	1.22	1.22	1.20	1.22	1.21	1.26
ϕ = 1.00	1.15	1.18	1.19	1.24	1.23	1.20	1.23	1.25	1.25	1.28
ϕ = 1.10	1.32	1.34	1.38	1.41	1.40	1.39	1.36	1.38	1.39	1.39
ϕ = 1.25	1.24	1.25	1.26	1.27	1.21	1.28	1.30	1.27	1.28	1.29
ϕ = 1.30	1.13	1.07	1.08	1.05	1.06	1.06	1.08	1.08	1.08	1.10

Table C-3. VALUES OF $\frac{(O_2 \text{ SIGNAL})}{(N_2 \text{ SIGNAL})}$ (N_2 MOLE FRACTION) AT VARIOUS SAMPLING ORIFICE-TO-FLAME HOLDER DISTANCES AND VARIOUS EQUIVALENCE RATIOS

$$\frac{S_{O_2}}{S_{N_2}} [N_2] \times 10^2 .$$

Distance, inches → Equivalence Ratio ↓	0.75	1.00	1.25	1.50	1.75	2.00	2.25	2.50	2.75	3.00
ϕ = 0.75	4.67	4.27	4.00	4.04	3.41	3.26	3.34	3.37	3.46	3.10
ϕ = 0.80	2.52	2.44	2.42	2.23	2.11	1.86	1.98	2.62	2.67	2.91
ϕ = 0.90	1.87	1.95	1.83	2.01	1.87	2.12	2.07	2.12	2.12	2.40
ϕ = 1.00	1.30	1.27	1.38	1.11	1.11	1.06	1.01	1.58	1.68	1.90
ϕ = 1.10	0.24	0.30	0.18	0.33	0.34	0.29	0.16	0.21	0.21	0.21
ϕ = 1.25	0.069	0.058	0.029	0.025	0.0	0.023	0.023	0.013	0.017	0.014
ϕ = 1.30	0	0	0	0	0	0	0	0	0	0

Table C-4. MOLE FRACTION OF NO AT VARIOUS SAMPLING ORIFICE-TO-FLAME HOLDER DISTANCES AND VARIOUS EQUIVALENCE RATIOS

$$[NO] = \frac{S_{NO}}{S_{N_2}} \times \frac{1}{R \cdot E \cdot I} [N_2] \times 10^4$$

Distance, inches → / Equivalence Ratio ↓	0.75	1.00	1.25	1.50	1.75	2.00	2.25	2.50	2.75	3.00
ϕ = 0.75	0.87	0.85	0.94	0.85	0.88	0.87	0.91	0.89	0.92	0.92
ϕ = 0.80	1.50	1.52	1.50	1.55	1.59	1.57	1.59	1.56	1.56	1.52
ϕ = 0.90	2.42	2.37	2.47	2.47	2.43	2.54	2.50	2.46	2.54	2.41
ϕ = 1.00	3.06	2.85	2.91	2.98	3.13	3.03	2.89	2.90	3.25	3.28
ϕ = 1.10	3.25	2.94	3.68	3.06	3.44	3.45	3.57	3.52	3.39	3.39
ϕ = 1.25	4.41	4.54	4.42	4.42	4.37	4.66	4.59	4.50	4.60	4.52
ϕ = 1.30	4.96	4.97	4.72	4.96	5.04	4.88	5.0	5.0	4.96	4.96

Table C-5. VALUES OF $\frac{\text{(MOLE = 29 SIGNAL)}}{(N_2 \text{ SIGNAL})}$ (N_2 MOLE FRACTION) AT VARIOUS SAMPLING-ORIFICE TO FLAME-HOLDER DISTANCES AND VARIOUS EQUIVALENCE RATIOS

$$\frac{S_{29}}{S_{N_2}} \quad [N_2] \times 10^3$$

Distance, inches → / Equivalence Ratio ↓	0.75	1.00	1.25	1.50	1.75	2.00	2.25	2.50	2.75	3.00
ϕ = 0.75	5.92	6.11	6.13	6.35	6.34	6.38	6.27	6.22	6.02	6.15
ϕ = 0.80	6	5.29	5.83	5.82	5.68	5.77	5.94	5.94	5.73	5.83
ϕ = 0.90	5.88	5.89	5.75	6.06	6.23	6.34	6.06	6.16	6.11	5.96
ϕ = 1.00	6.06	5.62	5.48	5.78	5.76	5.99	5.75	5.71	5.71	5.77
ϕ = 1.10	5.98	6.15	6.23	6.23	6.30	6.19	6.12	6.08	6.17	6.17
ϕ = 1.25	6.14	6.10	6.05	6.13	5.79	6.34	6.15	6.13	6	6
ϕ = 1.30	5.78	5.83	5.56	5.53	5.78	5.74	5.78	5.78	5.82	5.76

Table C-6. MOLE FRACTION OF CO AT D = 2.00 INCHES AS FUNCTION OF EQUIVALENCE RATIO

AT D = 2.00 INCHES $[CO] = \frac{S_{CO}}{S_{N_2}} \times \frac{1}{R \cdot E \cdot I} [N_2] \times 10^3$

$\phi = 0.75$	$\phi = 0.80$	$\phi = 0.90$	$\phi = 1.00$	$\phi = 1.10$	$\phi = 1.25$	$\phi = 1.30$
0	1.62	4.95	48.02	43.45	76.87	143.66

Table C-7. VALUES OF $\frac{(H_2O \text{ SIGNAL})}{(N_2 \text{ SIGNAL})}$ (N_2 MOLE FRACTION) AT VARIOUS SAMPLING-ORIFICE TO FLAME-HOLDER DISTANCES AND VARIOUS EQUIVALENCE RATIOS

$$\frac{S_{H_2O}}{S_{N_2}} \; [N_2] \times 10^2$$

Distance, inches → Equivalence Ratio ↓	1.75	1.00	1.25	1.50	1.75	2.00	2.25	2.50	2.75	3.00
φ = 0.75	4.76	4.76	4.72	4.37	4.75	4.48	4.75	4.63	4.69	4.79
φ = 0.80	4.86	4.65	4.84	4.97	4.97	4.85	4.86	4.82	4.82	4.82
φ = 0.90	5.23	5.15	5.12	5.07	4.77	4.78	4.64	4.86	4.78	4.97
φ = 1.00	5.30	5.14	4.73	5.12	5.11	4.95	5.04	5.24	5.10	5.03
φ = 1.10	4.58	4.68	4.67	4.79	4.75	4.75	4.74	4.69	4.69	4.69
φ = 1.25	4.53	4.58	4.50	4.65	4.11	4.54	4.43	4.62	4.53	4.57
φ = 1.30	4.41	4.41	4.43	4.22	4.41	4.36	4.49	4.39	4.47	4.52

Table C-8. VALUES OF $\frac{\text{(OH SIGNAL)}}{(\text{N}_2\text{ SIGNAL)}}$ (N_2 MOLE FRACTION) AT VARIOUS SAMPLING-ORIFICE TO FLAME-HOLDER DISTANCES AND VARIOUS EQUIVALENCE RATIOS

$$\frac{S_{OH}}{S_{N_2}} \; [N_2] \times 10^4$$

Distance, inches → / Equivalence Ratio ↓	0.75	1.00	1.25	1.50	1.75	2.00	2.25	2.50	2.75	3.00
ϕ = 0.75	2.13	2.50	2.47	2.31	2.12	1.95	2.35	2.11	2.30	2.12
ϕ = 0.80	3.48	3.76	3.12	3.79	3.33	3.25	3.65	3.71	3.68	3.79
ϕ = 0.90	4.87	4.73	5.00	5.23	4.97	5.15	4.79	4.94	5.85	5.92
ϕ = 1.00	4.21	4.09	4.62	4.90	4.92	4.75	4.55	4.73	4.91	4.78
ϕ = 1.10	1.40	1.65	1.57	1.50	1.40	1.65	1.62	1.75	1.43	1.43
ϕ = 1.25	0.75	0.79	0.77	0.76	0.72	0.65	0.74	0.65	0.69	0.75
ϕ = 1.30	0.1	0.28	0	0.29	0.24	0.17	0	0	0	0.21

Table C-9. VALUES OF $\frac{(\mathrm{O\ SIGNAL})}{(\mathrm{N_2\ SIGNAL})}$ (N_2 MOLE FRACTION) AT VARIOUS-ORIFICE-SAMPLING TO FLAME-HOLDER DISTANCES AND VARIOUS EQUIVALENCE RATIOS

$$\frac{S_{(O)}}{S_{N_2}} [N_2] \times 10^4$$

Distance, inches → Equivalence Ratio ↓	0.75	1.00	1.25	1.50	1.75	2.00	2.25	2.50	2.75	3.00
ϕ = 0.75	15.77	15.70	15.60	16.05	16.15	15.72	15.52	15.36	15.96	16.06
ϕ = 0.80	15.37	15.70	15.44	15.44	15.04	15.05	15.44	15.00	15.20	15.50
ϕ = 0.90	14.93	14.92	15.22	15.18	14.62	14.44	15.35	14.85	15.48	15.24
ϕ = 1.00	14.37	14.44	14.77	14.64	14.90	14.34	14.47	14.80	14.15	14.00
ϕ = 1.10	12.68	13.15	12.56	13.38	13.20	13.23	13.04	13.42	13.23	13.29
ϕ = 1.25	10.49	10.80	10.09	9.85	9.34	10.28	10.35	10.29	10.12	10.59
ϕ = 1.30	9.56	9.64	9.86	9.84	9.76	9.56	9.47	9.44	9.76	10.56

Table C-10. VALUES OF $\left(\frac{m/e = 15\ \text{SIGNAL}}{N_2\ \text{SIGNAL}}\right)$ (N_2 MOLE FRACTION) AT VARIOUS SAMPLING-ORIFICE TO FLAME-HOLDER DISTANCES AND VARIOUS EQUIVALENCE RATIOS

$$\frac{S_{15}}{SN_2}\ [N_2]$$

Distance, Inches→ Equivalence Ratio ↓	0.75	1.00	1.25	1.50	1.75	2.00	2.25	2.50	2.75	3.00
ϕ = 0.75	0	0	0	0	0	0	0	0	0	0
ϕ = 0.80	0	0	0	0	0	0	0	0	0	0
ϕ = 0.90	0	0	0	0	0	0	0	0	0	0
ϕ = 1.00	0	0	0	0	0	0	0	0	0	0
ϕ = 1.10	0	0	0	0	0	0	0	0	0	0
ϕ = 1.25	0	0	0	0	0	0	0	0	0	0
ϕ = 1.30	0	0	0	0	0	0	0	0	0	0

Table C-11. VALUES OF $\left(\frac{m/e = 14 \text{ SIGNAL}}{N_2 \text{ SIGNAL}}\right)$ (N_2 MOLE FRACTION) AT VARIOUS SAMPLING-ORIFICE TO FLAME-HOLDER DISTANCES AND VARIOUS EQUIVALENCE RATIOS

$$\frac{S_{14}}{S_{N_2}} [N_2]$$

Distance, inches → Equivalence Ratio ↓	0.75	1.00	1.25	1.50	1.75	2.00	2.25	2.50	2.75	3.00
ϕ = 0.75	0	0	0	0	0	0	0	0	0	0
ϕ = 0.80	0	0	0	0	0	0	0	0	0	0
ϕ = 0.90	0	0	0	0	0	0	0	0	0	0
ϕ = 1.00	0	0	0	0	0	0	0	0	0	0
ϕ = 1.10	0	0	0	0	0	0	0	0	0	0
ϕ = 1.25	0	0	0	0	0	0	0	0	0	0
ϕ = 1.30	0	0	0	0	0	0	0	0	0	0

Table C-12. MOLE FRACTION OF H_2 AT VARIOUS SAMPLING-ORIFICE TO FLAME HOLDER DISTANCES AND VARIOUS EQUIVALENCE RATIOS

$$[H_2] = \frac{S_{H_2}}{S_{O_2}} \quad x \quad \frac{1}{R \cdot E.I} \quad [N_2] \times 10^4$$

Distance, inches → Equivalence Ratio ↓	0.75	1.00	1.25	1.50	1.75	2.00	2.25	2.50	2.75	3.00
ϕ = 0.75	0	0	0	0	0	0	0	0	0	0
ϕ = 0.80	0	0	0	0	0	0	0	0	0	0
ϕ = 0.90	0	0	0	0	0	0	0	0	0	0
ϕ = 1.00	0.33	0.29	0	0.380	0.29	0.324	0.29	0	0.359	0.25
ϕ = 1.10	0.578	0.54	0.561	0.638	0.656	0.731	0.560	0.610	0.527	0.527
ϕ = 1.25	3.125	2.953	3.191	2.779	2.655	2.326	2.705	2.528	3.198	2.833
ϕ = 1.30	5.814	6.240	5.635	6.694	5.814	5.990	5.814	4.933	6.166	4.688

Table C-13. VALUES OF $\frac{(H_2 \text{ SIGNAL})}{(N_2 \text{ SIGNAL})}$ (N_2 MOLE FRACTION) AT VARIOUS SAMPLING-ORIFICE TO FLAME-HOLDER DISTANCES AND VARIOUS EQUIVALENCE RATIOS

$$\frac{S_H}{S_{N_2}} \; [N_2] \times 10^5$$

Distance, inches → / Equivalence Ratio ↓	0.75	1.00	1.25	1.50	1.75	2.00	2.25	2.50	2.75	3.00
ϕ = 0.75	0	0	0	0	0	0	0	0	0	0
ϕ = 0.80	3.03	3.39	3.80	3.30	2.80	2.90	2.99	2.79	2.68	2.50
ϕ = 0.90	4.00	4.16	3.98	3.52	4.36	4.52	4.42	4.96	4.37	4.32
ϕ = 1.00	5.09	5.19	5.32	5.00	5.51	5.00	5.60	5.21	5.67	5.27
ϕ = 1.10	7.34	6.65	6.61	6.18	7.18	7.30	7.58	7.16	6.76	6.69
ϕ = 1.25	3.51	3.22	3.32	3.59	3.60	3.38	3.00	3.08	3.00	3.14
ϕ = 1.30	2.16	2.05	2.01	2.40	2.48	2.64	2.27	2.22	2.75	2.00

Table C-14. RECYCLED-GAS DATA TAKEN AT D = 2.00 INCHES AND FOR THREE DIFFERENT EQUIVALENT RATIOS

Equivalence Ratio	$\frac{S_H}{S_{N_2}}[N_2]$	$[H_2] = \frac{S_{H_2}}{S_{N_2}} \times \frac{1}{R \cdot E \cdot T}[N_2]$	$\frac{S_{14}}{S_{N_2}}[N_2]$	$\frac{S_{15}}{S_{N_2}}[N_2]$	$\frac{S_O}{S_{N_2}}[N_2]$	$\frac{S_{OH}}{S_{N_2}}[N_2]$	$\frac{S_{H_2O}}{S_{N_2}}[N_2]$	$\frac{S_{29}}{S_{N_2}}[N_2]$	$[NO] = \frac{S_{NO}}{S_{N_2}} \times \frac{1}{R \cdot E \cdot T}[N_2]$	$\frac{S_{O_2}}{S_{N_2}}[N_2]$	$[Ar] = \frac{S_{Ar}}{S_{N_2}} \times \frac{1}{R \cdot E \cdot T}[N_2]$	$[CO_2] = \frac{S_{CO_2}}{S_{N_2}} \times \frac{1}{R \cdot E \cdot T}[N_2]$	$[CO] = \frac{S_{CO}}{S_{N_2}} \times \frac{1}{R \cdot E \cdot T}[N_2]$
$\phi = 0.90$	0	0	0	0	0	0	2.15×10^{-2}	5.54×10^{-3}	1.40×10^{-4}	3.18×10^{-2}	1.35×10^{-2}	0.108	0.0373
$\phi = 1.00$	0	0	0	0	0	0	1.97×10^{-2}	5.31×10^{-3}	2.21×10^{-4}	1.54×10^{-2}	1.28×10^{-2}	0.103	0.061
$\phi = 1.10$	0	0	0	0	0	0	1.92×10^{-2}	5.34×10^{-3}	3.28×10^{-4}	0.013×10^{-2}	1.32×10^{-2}	0.098	0.074

Table C-15. TIME-OF-FLIGHT TEMPERATURE MEASUREMENTS, K

Distance, inches → Equivalence Ratio ↓	1.00	2.00	3.00
$\phi = 0.75$	1896	1861	1785
$\phi = 0.80$	1968	1934	1805
$\phi = 0.90$	2163	2011	1933
$\phi = 1.00$	2209	2043	2000
$\phi = 1.10$	2192	2033	1985
$\phi = 1.25$	2148	1950	1920
$\phi = 1.30$	2109	1918	1907

Table C-16. THERMOCOUPLE-TEMPERATURE MEASUREMENTS, K

Distance, inches → Equivalence Ratio ↓	1.00	2.00	3.00
$\phi = 0.75$	1506	1453	1282
$\phi = 0.80$	1552	1465	1299
$\phi = 0.90$	1649	1621	1383
$\phi = 1.00$	1711	1659	1498
$\phi = 1.10$	1627	1602	1453
$\phi = 1.25$	1571	1556	1391
$\phi = 1.30$	1613	1598	1413

NOTE: The temperature increase as ϕ increases from 1.25 to 1.30 might be related to the relatively unstable flame observed at $\phi = 1.30$.

APPENDIX D

THEORETICAL[a] MAXIMUM FLAME TEMPERATURE AND SPECIES COMPOSITION OF METHANE - AIR MIXTURES[b] AT VARIOUS EQUIVALENCE RATIOS[c]

COMPOSITION - MOLE PERCENT

Equivalence Ratio → Species ↓	0.70	0.75	0.80	0.90	1.00	1.10	1.25	1.30
H	0.00033	0.00095	0.00245	0.01203	0.03990	0.06781	0.05838	0.05078
O	0.00420	0.00773	0.01273	0.02419	0.02190	0.00555	0.00043	0.00019
Ar	0.83817	0.83389	0.82954	0.82022	0.80839	0.79052	0.75992	0.75003
O_H	0.07220	0.11165	0.16075	0.26714	0.28650	0.14471	0.03607	0.02305
H_2	0.00443	0.01047	0.02301	0.09557	0.36763	1.25004	3.53288	4.41979
H_2O	13.64600	14.52675	15.38109	16.98793	18.33098	18.93414	18.58275	18.29323
CO	0.00872	0.02224	0.05204	0.23536	0.90434	2.60837	5.32788	6.06929
CO_2	6.83462	7.27452	7.69081	8.37618	8.52657	7.53686	5.75355	5.30369
NO	0.25436	0.29556	0.32562	0.32458	0.19930	0.05299	0.00659	0.00353
NO_2	0.00030	0.00027	0.00023	0.00013	0.00000	0.00000	0.00000	0.00000
N_2	72.60706	72.21524	71.82288	71.01418	70.05022	68.57321	65.94055	65.08405
O_2	5.72961	4.70070	3.69883	1.84246	0.46421	0.03576	0.00098	0.00035

Equivalence Ratio	Flame Temperature, K
0.70	1840
0.75	1922
0.80	2000
0.90	2137
1.00	2229
1.10	2214
1.25	2100
1.30	2061

---

[a] Based on Rocketdyne n-element propellant performance computer program

[b] Accounts for establishment of definite equilibrium conditions between products and reactants

[c] Equivalence Ratio = $(CH_4/Air) \big/ (CH_4/Air)_{Stoichiometric}$

APPENDIX E

FACTORS FOR THE CONVERSION OF UNITS TO THE METRIC SYSTEM

Physical Quantity	To Convert From	To	Multiply by
Length	inch	meter	0.0254
	foot	meter	0.3048
Mass	pound	kilogram	0.45359
Pressure	atmosphere	pascal	101325.
	inch of water	pascal	248.84
	psi	pascal	6894.8
	torr	pascal	133.32
	newton/meter^2	pascal	1.0000
Speed	foot/second	meter/second	0.3048
Temperature	Celsius (C)	Kelvin (K)	$K = C + 273$
	Fahrenheit (F)	Kelvin (K)	$K = (F + 460)/1.8$
	Fahrenheit (F)	Celsius (C)	$C = (F - 32)/1.8$
	Rankine (R)	Kelvin (K)	$K = R/1.8$
Time	hour	second	3600.
Volume	gallon (U.S. liquid)	meter^3	0.0037854